UNIVERSITY OF UDINE

PhD COURSE IN
BIOMEDICAL AND BIOTECHNOLOGICAL SCIENCES

XXV CYCLE

PhD THESIS

DEFINING THE ROLE OF YAP1 IN 11q22-AMPLIFIED CANCER CELL LINES

PhD student: Erica Lorenzetto

Supervisors: Dr.Roberta Maestro
Prof. Claudio Brancolini

Co-Supervisor: Dr.Piergiorgio Modena

ACADEMIC YEAR 2012-2013

TABLE OF CONTENTS

ABSTRACT

The recently described Salvador-Warts-Hippo pathway (SWH) is involved in organs size regulation.

Salvador-Warts-Hippo pathway consists of several negative growth regulators acting in a kinase cascade that ultimately inactivates Yorkie in *Drosophila*, or YAP1 (Yes-associated protein 1) in mammalian; these two effector proteins are both transcriptional coactivators that positively regulate cell growth, survival and proliferation.

Literature data report apparently conflicting results on YAP1 role in carcinogenesis. In fact, YAP1 has been reported to exhibit both oncogenic properties and tumor-suppressive functions in distinct *in vitro* or *in vivo* models. In specific cancer cell line models YAP1 induces a pro-apoptotic pathway mediated by TP73. On the contrary, in human nontransformed mammary epithelial cells, ectopic overexpression of YAP1 induced an increase of tumorigenic proprieties *in vitro*. In addition, in conditional tissue-specific transgenic mouse model, YAP1 induced hyperproliferation of liver and, when it is maintained continuously, frank neoplasia. On the other hand, genomic amplification events at locus 11q22 comprising YAP1 gene have been detected in a small fraction of different tumor types. Due to the magnitude of the amplicons, multiple genes, in addition to YAP1, are contained and there is no direct evidence about the oncogenic role of endogenous YAP1 in tumors carrying the 11q22 amplification event.

Therefore the aim of my thesis is to study whether YAP1 is an oncogenic target of 11q22 amplicons.

In order to reach this goal, I analyzed a panel of established cancer cell lines and identified genomic amplification and overexpression of YAP1 in Ca-Ski (Cervical squamous cell carcinoma), EKVX (Non small cell lung-adenocarcinoma) and RO82 (Follicular thyroid carcinoma) cell lines, that were used as model systems in my experiments. I managed to efficiently silence YAP1 expression using RNA interference strategies (both short hairpin lentivirus and siRNAs) and I studied the effects of downregulation of endogenous YAP1 on tumorigenic properties in these cell lines. I found that YAP1 silencing induced a moderate reduction in cell proliferation without evidence of apoptosis induction. Anchorage-independent growth was significantly affected by YAP1 silencing in all three cell lines. Sphere-forming capacity (which is a typical stemness feature) was reduced in the two cell lines that are capable to grow as spheres in suspension.

Moreover I detected that YAP1 silenced cells migrated less respect to control cells. In Ca-Ski cell line only, YAP1 silenced cells were significantly more sensitive to pharmacological genotoxic stress. In addition, by *in vivo* experiments, I have established that YAP1 silencing limited xenograft tumor growth in nude mice.

Furthermore, since YAP1 is a transcriptional coactivator, I identified its target genes in 11q22-amplified cancer cell lines by gene expression profiling experiments. Using class comparison analysis, I compared YAP1 proficient cells versus YAP1-silenced cells and I identified 707 statistically significantly modulated genes that were functionally annotated. The majority of target genes identified were mainly annotated for cell proliferation, cell signaling and cellular movement ontologies.

I selected 16 genes as particularly promising targets of YAP1 and performed a validation of microarray data by qPCR. The analysis confirmed that 14 of these genes are also modulated in all cell lines in agreement with microarray data. In addition gene expression analysis suggested that YAP1 exerts a feedback loop function into the signaling pathway contributing to its homeostasis.

Finally, I investigated the frequency of YAP1 amplification in a panel of human tumor samples from different cancer types and I detected the amplification event in 3-23% of the cases, depending on the tumor type. These results confirmed the relevance of such genetic aberration in carcinogenesis in different tumor types.

In conclusion, my results demonstrate that in the YAP1-amplified cancer cell lines under study the YAP1 gene effectively sustains multiple transformed traits and that YAP1 amplification is actually present in a fraction of carcinoma subtypes.

INTRODUCTION

1. THE YAP1 GENE AND ISOFORMS

In 1994 Marius Sudol identified, characterized and cloned the cDNA of a novel chicken protein that binds the SH3 (Src homology domain 3) domain of the Yes proto-oncogene product. The protein has a molecular mass of 65 kDa and was initially named YAP65 (Yes associated protein of 65 KDa) (Sudol 1994). In 1995 Sudol and collaborators characterized and cloned the cDNA of the human and mouse orthologues of the chicken gene and he found that it is localized in 11q22 human genomic region (Sudol et al. 1995).
Subsequently the HUGO Gene Nomenclature Committee established the official name of the gene as YAP1 (Yes-associated protein 1) and it represents a critical downstream regulatory target of the Salvador-Warts-Hippo pathway in mammal.

YAP1 protein contains one or two WW domains, which are domains highly conserved along evolution and composed by two Tryptophan (W) residues, separated by 20-22 aminoacids. The WW domain binds the proline-rich peptides with the PPxY consensus motif, where P is proline, x is any aminoacid and Y is tyrosine (Chen and Sudol 1995). In addition to the WW domains, YAP1 protein also contains a N-terminal proline-rich domain, while the C-terminus of the protein regulates the transcription activation.
The structure of human YAP1 gene comprises 9 exons (Figure 1). Interestingly the presence of one or two WW domains relies on alternative splicing isoforms of YAP1 gene. The first WW domain resides within exons 2 and 3 and the second WW domain is located within exon 4. The YAP1-1 isoform contains only the first WW domain and therefore lacks of the exon 4, while YAP1-2 isoform includes two WW domains. Depending on additional alternative splicing events, both YAP1-1 and YAP1-2 include 4 isoforms which are indicated α, β, γ, δ. The α isoform lacks exon 6, the β isoform lacks exon 6 but contains a short extension (4 aminoacids) of the exon 5, the γ isoform contains the exon 6 but does not have the extension of the exon 5 and the δ isoform includes both the exon 6 and the extension of the exon 5 (Gaffney et al. 2012).
Analyses performed on different human tissues have shown that YAP1 gene is ubiquitously expressed in the majority of normal human tissues. High expression of YAP1 protein was found in placenta, prostate, testis, ovary and small intestine, and lower expression was

found in brain, liver and spleen, while no expression was found in peripheral blood leukocytes (Sudol et al. 1995).

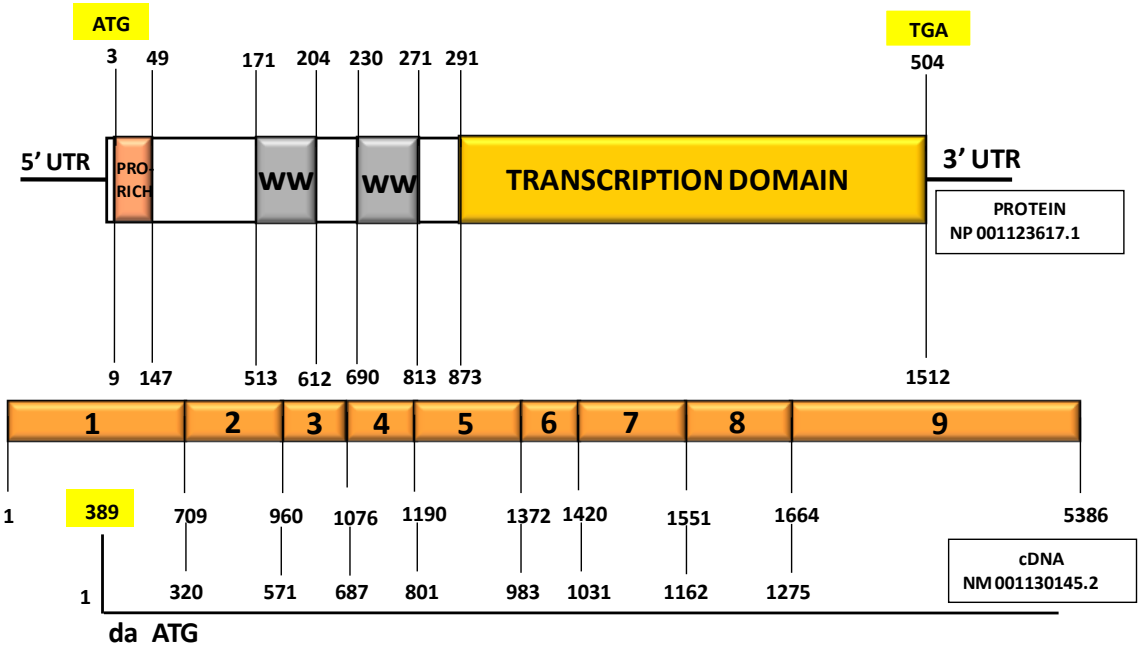

Figure 1. Structure of YAP1 protein and cDNA. The schematization of YAP1 protein (isoform YAP1-2 γ) domains (prolin rich domain, WW domains and transcription domain) and the corresponding 9 exons of the YAP1 cDNA.

In 2005 Pan and collaborators identified Yorkie (Yki) (Huang et al. 2005), which is the homologue of YAP1 in *Drosophila* and in 2000 Kanai and collaborators described TAZ gene as a paralogue of YAP1 (Kanai et al. 2000). About 50% of TAZ sequence is identical to YAP1 sequence and it contains only one WW domain.

In the recent years, Yki in *Drosophia*, and YAP1 and TAZ in mammals, have been described as transcription co-factors of Hippo pathway representing the critical final effectors of this signaling cascade involved in the control of organ growth and size (Pan 2010).

2. YAP1 IS A COMPONENT OF SALVADOR-WARTS-HIPPO SIGNALING PATHWAY

Salvador-Warts-Hippo pathway (SWH or Hippo pathway) has been recently involved in the regulation of organs size. Studies performed in the fruit fly *Drosophila melanogaster* have allowed deciphering this pathway which limits cell proliferation (Edgar 2006).

In *Drosophila* adult organs, such as eyes, wings, legs and genitalia, are derived from epithelial precursor tissue known as imaginal discs, which mature during larval and pupal development. SWH pathway is involved to limit imaginal discs size, therefore imaginal discs that loss of SWH activity are abnormally large due to excessive cell proliferation (Harvey and Tapon 2007). Deregulation of this pathway leads to dramatic increase in organ size suggesting that the Hippo pathway is a key regulator of organ growth and tissue size.

The Hippo pathway is composed of several components acting in a kinase cascade that is regulated by multiple upstream components and has many transcriptional outputs. The *Drosophila* Hippo pathway is highly conserved throughout evolution, in fact most components have a direct homologue (orthologs) in mammal (Halder and Johnson 2011) (Figure 2).

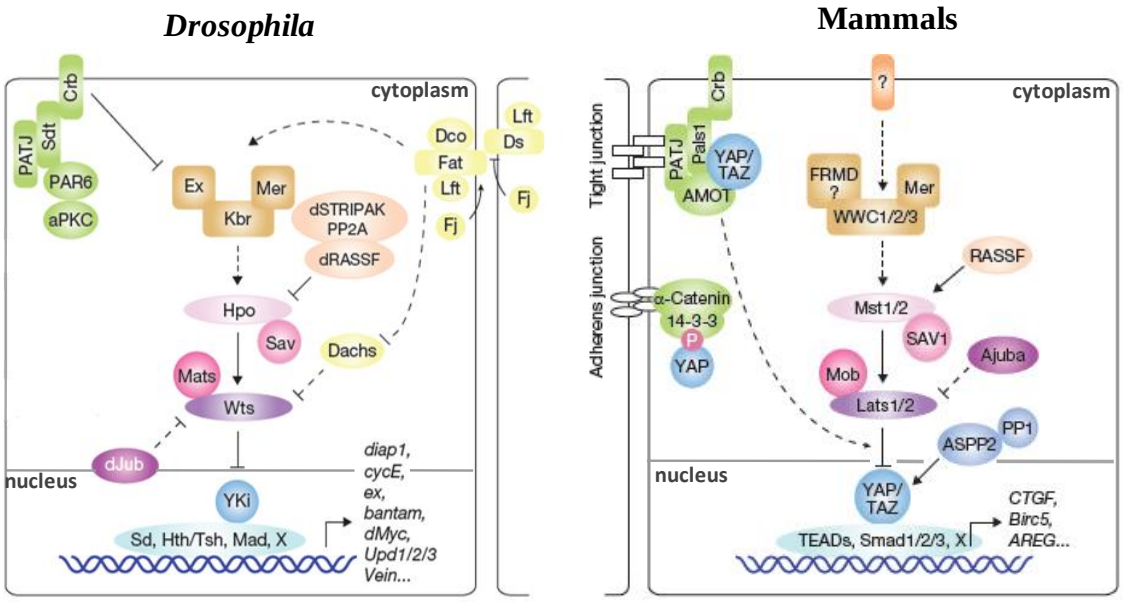

Figure 2. Hippo pathway in *Drosophila* and mammals. Description of the Hippo signaling pathway in *Drosophila* (on left) and in mammalian (on right). The corresponding proteins of the two different models are indicated by the same color. Arrowed or blunted ends indicate activation or inhibition, respectively. Dashed lines describe unknown mechanisms. *Modified by Zhao et al. 2011b.*

The Hippo components (Figure 2 and Table 1) in mammals include Mst1/2 (Hpo homologue in *Drosophila*) (Creasy and Chernoff 1995a; Creasy and Chernoff 1995b), WW45 also called Sav1 (Sav homolog in *Drosophila*) (Tapon et al. 2002), Lats1/2 (Wts homolog in *Drosophila*) (Tao et al. 1999; Yabuta et al. 2000), MOBKL1A and MOBKL1B often collectively referred as Mob1 (Mats homolog in *Drosophila*) (Stavridi et al. 2003) YAP1 and its paralogue TAZ (Yki homologues in *Drosophila*) (Kanai et al. 2000; Sudol 1994) (Figure 3).

Table 1. Hippo pathway components in *Drosophila* and in mammalian reported so far.

DROSOPHILA	**MAMMALIAN**	**PROTEIN FUNCTIONS**
Core components		
Hippo (Hpo)	Mst1, Mst2	Ste20 family Ser/Thr kinase
Salvador (Sav)	Sav1/WW45	WW-domain adaptor protein
Warts (Wts)	Lats1, Lats2	NDR family Ser/Thr kinase
Mats	Mob1A, Mob1B	Wts co-factor
Yorkie (Yki)	Yap, Taz	WW-domain transcriptional co-activator
Upstream components		
Expanded (Ex)	FRMD6/Ex1; FRMD1/Ex2	FERM-domain adaptor protein
Merlin (Mer)	Merlin/Nf2	FERM-domain adaptor protein
Kibra	Kibra/ WWC1,WWC2	WW-domain adaptor protein
Fat	Fat4	Transmembrane cadherin
Dachsous (Ds)	Dchs1, Dchs2	Transmembrane cadherin
Four-jointed (Fj)	Fjx1	Golgi resident Ser/Thr kinase
Lowfat (Lft)	Lix1, Lix1	Adaptor, unknown function
Dachs (D)	?	Unconventional myosin
Downstream components		
Scalloped (Sd)	TEAD1-4	TEA-domain transcription factor
Teashirt (Tsh)	Tshz1-3	Zn-finger transcription factor
Homothorax (Hth)	Meis1-3, Prep1-2	Homeodomain transcription factor
Other modulators		
Rassf	Rassf1-6	RA-domain adaptor
dJub	Ajuba, LIMD1, WTIP	LIM-domain adaptor protein
dSTRIPAK PP2A	dSTRIPAK PP2A	PP2A Ser/Thr phosphatese complex

Signal transduction in mammalian pathway components is analogous to *Drosophila* (Figure 2 and Table 1). At the core of the signaling cascade there are the Sterile 20-like kinases Mst1/2 and the regulatory protein Sav1 (also known as WW45), which interact and form an activated complex. Mst1/2 can directly phosphorylate the tumor suppressor kinases

Lats1/2, which are regulated by Mob1. Mob1 is also phosphorylated by Mst1/2 in order to enhance the binding in the Lats1/2-Mob1 complexes (Praskova et al. 2008). In response to different cellular conditions, Lats1/2 phosphorylate the WW domain of the transcription factor YAP1 at serine 127 and of TAZ at serine 89 inducing their cytoplasmic retention and inactivation, thus preventing the transcription of the target genes (Hao et al. 2008; Lei et al. 2008; Zhang J. et al. 2008; Zhao et al. 2007). During development or in response to growth signals or stimuli, Hippo pathway is inhibited therefore Mst1/2 and Lats1/2 remain inactive, allowing YAP1 and TAZ translocation into the nucleus in order to bind transcription factors that mediate the transcription of target genes involved in regulation of cell survival and proliferation (Liu et al. 2012) (Figure 3). Up to now, some of these DNA-binding proteins that mediate the transcription of target genes have been identified (Table 2).

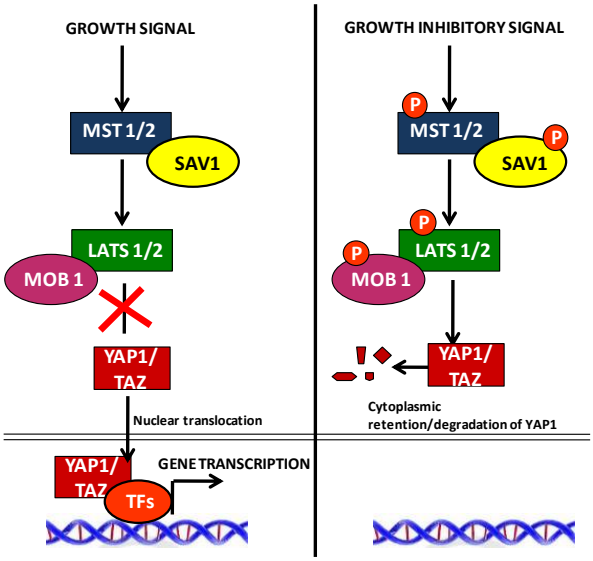

Figure 3. Hippo pathway signaling transduction in response to growth signals. Core components of the signaling cascade in mammalian. Left panel: during development or under growth signals YAP1 and TAZ translocate into the nucleus to activate a set of genes which regulate cell survival and proliferation. Right panel: in response to growth inhibition signals phosphorylation of YAP1 at Ser127 and of TAZ at Ser89 induces their retained into the cytoplasm and later their degradation. *Modified by Liu et al. 2012.*

Table 2. Transcription factors binding to Yorkie in *Drosophila* and YAP1 and TAZ in mammals.

TRANSCRIPTION FACTOR	
Yorkie	**REFERENCE**
Scalloped	Zhang L. et al. 2008
Homothorax	Peng et al. 2009
Teashirt	Peng et al. 2009

TRANSCRIPTION FACTOR	
YAP1	**REFERENCE**
TEAD1-4	Zhao et al. 2008
SMAD7	Ferrigno et al. 2002
SMAD1-2-3	Alarcon et al. 2009
RUNX	Levy et al. 2008
TP73	Strano et al. 2001
CTNNB1	Heallen et al. 2011
Tbx5	Rosenbluh et al. 2012
Meis1-3	Halder and Johnson 2011
Tshz1-3	Halder and Johnson 2011

TRANSCRIPTION FACTOR	
TAZ	**REFERENCE**
TEAD1-4	Zhang L. et al. 2009
SMAD2-3-4	Varelas et al. 2010b
PAX3	Murakami et al. 2006
RUNX2	Hong et al. 2005
TTF1	Park et al. 2004
Tbx5	Murakami et al. 2006
PPARG	Wang et al. 2009
Meis1-3	Halder and Johnson 2011
Tshz1-3	Halder and Johnson 2011

The main transcription factor of YAP1 and TAZ, which mediated the transcription of several target genes, is TEA-domain family member (TEAD), (Zhang H. et al. 2009; Zhao et al. 2008) (Table 2). The TEAD transcription factors are widely express in most tissues and organs. However YAP1 and TAZ bind numerous other transcription factors (Kaneko and DePamphilis 1998) (Table 2).

In *Drosophila* the homologous of TEAD is Scalloped (Table 2) (Wu et al. 2008; Zhang L. et al. 2008). In addition to Scalloped other transcription factors are known to be able to bind Yorkie to induce the transcription of target genes (Table 2).

Upon interaction between YAP1, TAZ and Yorkie with these transcription factors, the transcription of specific target genes is induced. Until now, some of these target genes have been defined (Tables 3, 4, 5).

Table 3. Yorkie target genes in *Drosophila* reported so far.

Yorkie TARGET GENES		
TARGET GENE	**FUNCTION**	**REFERENCE**
Diap1	Inhibitor of apoptosis	Wu et al. 2003
Myc	Regulator of cell growth	Ziosi et al. 2010
CycE	Regulator of cell cycle	Silva et al. 2006
E2F1	Regulator of cell cycle	Goulev et al. 2008
Ex	Hippo pathway component	Hamaratoglu et al. 2006
Mer	Hippo pathway component	Hamaratoglu et al. 2006
Kibra	Hippo pathway component	Genevet et al. 2010
Cr	Hippo pathway component	Genevet et al. 2009
Fj	Hippo pathway component	Cho et al. 2006
Batam microRNA	Regulator of cell survival and cell proliferation	Nolo et al. 2006
Vein	EGFR ligand	Zhang J. et al. 2009
Karen	EGFR ligand	Zhang J. et al. 2009
Spritz	EGFR ligand	Zhang J. et al. 2009
Unpaired 1/2/3	Jak-Stat pathway ligands	Ren et al. 2010

Table 4. YAP1 target genes in mammals reported so far.

YAP1 TARGET GENES		
TARGET GENE	**FUNCTION**	**REFERENCES**
CTGF	Regulator of cell proliferation	Zhao et al. 2008
Gli2	Downstream effector of Sonic Hedgehog pathway	Li et al. 2012
CYR61	Regulator of cell proliferation	Lai et al. 2011
SNAI2	Wnt pathway target gene	Heallen et al. 2011
TP53AIP1	Pro-apoptotic effect	Strano et al. 2005
BBC3/Puma	Pro-apoptotic effect	Matallanas et al. 2007
Bax	Pro-apoptotic effect	Strano et al. 2005
BCL2L1	Pro-apoptotic effect	Rosenbluh et al. 2012
Oct3/4	Stemness gene	Lian et al. 2010
Nanog	Stemness gene	Lian et al. 2010
Sox2	Stemness gene	Lian et al. 2010
AREG	EGF family member	Zhang J. et al. 2009
BIRC5	Inhibitor of apoptosis	Hao et al. 2008
BIRC2	Inhibitor of apoptosis	Dong et al. 2007

Table 5. TAZ target genes in mammals reported so far.

TAZ TARGET GENES		
TARGET GENE	**FUNCTION**	**REFERENCE**
CTGF	Regulator of cell proliferation	Zhao et al. 2008
Gli2	Downstream effector Sonic hedgehog pathway	Li et al. 2012
Cyr61	Regulator of cell proliferation	Lai et al. 2011
Oct3/4	Stemness gene	Lian et al. 2010
Nanog	Stemness gene	Lian et al. 2010
Sox2	Stemness gene	Lian et al. 2010
AREG	EGF family member	Zhang J. et al. 2009

The Yorkie target genes in *Drosophila* and the YAP1 and TAZ target genes in mammals are mainly involved in proliferation and in apoptosis regulation (Tables 3, 4, 5). In addition, some target genes in mammalian are involved in stemness, in fact Hippo pathway participates in regulation of pluripotency in mammalian embryonic stem cells (Tables 4, 5).

Upstream components of the Hippo pathway have been only partially identified. In *Drosophila*, two apical cytoskeleton-binding proteins, Merlin (Mer) and Expanded (Ex) (Hamaratoglu et al. 2006) and their interacting protein Kibra (Krb) (Yu et al. 2010), activate the Hippo pathway (Figure 2, Table 1). The Fat protocadherin, a cell-surface molecule, is also identified as an upstream regulator of the Hippo pathway (Silva et al. 2006). Fat activity is regulated by binding to another protocadherin, Dachsous (Ds) (Matakatsu and Blair 2006) and it is modulated by binding to other proteins, such as the casein kinase Discs overgrowth (Dco) (Sopko et al. 2009), the Golgi resident kinase Four-jointed (Fj) (Smith et al. 2000) and Fat/Ds-interacting protein Lowfat (Lft) (Mao et al. 2009). Fat may also inhibit a nonconventional myosin Dachs, which represses Wst protein level (Cho et al. 2006) or activates Ex with a unknown mechanism (Bennett and Harvey 2006; Silva et al. 2006). Mer and Ex activate the Hippo pathway (Hamaratoglu et al. 2006) forming a complex with Hpo and Sav. Kybra interacts with both Mer and Ex and participates to the complex (Yu et al. 2010). Hpo kinase interacts with Sav and induces a kinase cascade that ultimately phosphorylates and inactivates Yki (Figure 2, Table 1).

In mammals, functional significance of Fat and Ex homologues is not clear. The mammalian homologues for upstream regulators of the Hippo pathway include Kibra/WWC1/2/3 (Kibra homologues), FRMD6/Ex1 and FRMD1/Ex2 (Ex homologues) and NF2/Mer (Mer homologues). Mer forms complexes with WWC1/2/3 and FRMD, leading to pathway activation. RASSF, a group of Ras effector proteins, may also act as activators of the pathway by binding Mst1/2 (Oh et al. 2006). On the contrary, RASSF exerts an inhibitory effect on Hpo in *Drosophila* (Polesello et al. 2006) through competing with Sav for Hpo binding and through recruitment of the dSTRIPAK-PP2A (Ribeiro et al. 2010) (Figure 2, Table 1).

As previously described, the activation of the Hippo pathway induces phosphorylation and inhibition of YAP1, TAZ and Yki transcription cofactors (Figure 4a). YAP1 and TAZ are phosphorylated by Lats1/2, YAP1 at serin 127, TAZ at serine 89 and Yki is phosphorylated by Wts at serine 168. This phospholylation event induces the binding of YAP1, TAZ and Yki with the 14-3-3 protein and subsequent cytoplasmatic sequestration

and inactivation (Hao et al. 2008; Lei et al. 2008; Oh and Irvine 2008; Zhao et al. 2007) (Figure 4a). There is another mechanism that induces the inhibition of YAP1, TAZ and Yki. This system is based on protein-protein interaction that results in cytoplasm sequestration of these proteins (Figure 4b). Yki contains two WW domains that can interact with PPXY motifs present in Mob, Ex, Wts and Hpo (Oh et al. 2009; Zhao et al. 2011a). YAP1 and TAZ bind AMOT family of proteins, and this interaction sequesters YAP1 and TAZ in the cytoplasm (Chan et al. 2011; Zhao et al. 2011a) (Figure 4b). Moreover literature data report that phosphorylation of YAP1 can also induce its degradation (Figure 4c). Lats1/2 phosphorylates YAP1 at serine 381 which primes YAP1 for a subsequent phosphorylation by another kinase, probably casein kinase 1 (CK1δ/ε) which induces interaction with SCFβ-TRCP leading to polyubiquitylation and degradation of YAP1 (Zhao et al. 2010) (Figure 4c).

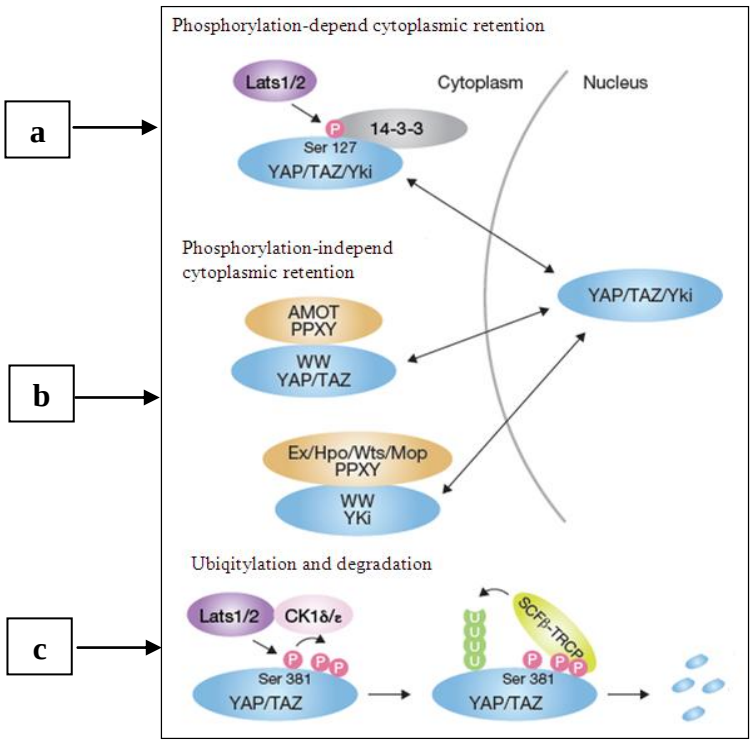

Figure 4. Elucidation of the mechanisms of YAP1/TAZ and Yki inhibition. a) Phosphorylation-dependent cytoplasmic retention. YAP1 is phosphorylated on Ser 127 by Lats1/2 leading to 14-3-3 binding and cytoplasmic retention. The mechanism is the same also for TAZ and Yki. **b)** Phosphorylation-independent cytoplasmic retention. Through interactions between WW domain and PPXY motif, Yki binds to Mop, Ex, Hpo and Wts, and YAP1/TAZ binds to AMOT protein. These interactions physically sequester Yki and YAP1/TAZ in the cytoplasm. **c)** Phosphorylation-induced ubiquitylation and degradation. YAP1 is phosphorylated at Ser 381 by Lats1/2 trigged further phosphorylation of YAP1 by CK1δ/ε, which determines interaction with SCFβ–TRCP and finally induces to YAP1 ubiquitylation and degradation. This mechanism is conserved in TAZ. *Modified by Zhao et al. 2011b.*

Recent evidences have been shown that the actin cytoskeleton is involved in regulation of the cell proliferation through the Hippo pathway both in *Drosophila* and in mammals. In mammalian tissue culture, YAP1 activity and subcellular localization is influenced by changes in cell morphology and in the actin cytoskeleton (Dupont et al. 2011; Oh et al. 2009; Wada et al. 2011).

Literature data report that in mammalian, the YAP1 subcellular localization is dependent on cell density. In sparsely growing cells condition, YAP1 is mainly contained into the nucleus where it functions as a transcriptional cofactor. On the contrary, in confluence cell condition, characterized by cell-cell contact, YAP1 is accumulated into the cytoplasm (Zhao et al. 2007). The cytoplasmic sequestration of YAP1 in response to cell density correlates with an increase in YAP1 phosphorylation (Ota and Sasaki 2008).

In addition, the intercellular junctions have been shown to play a critical role in cell signaling events. In fact, recent studies, regarding the mechanisms of YAP1/TAZ regulation by cell-cell contact, demonstrate that the tight-junction protein complex is capable to sequester YAP1/TAZ to the tight-junction (Chan et al. 2011; Zhao et al. 2011b) (Figure 2). In addition, in the presence of adherens-junction, α-catenin is able to interact with YAP1, probably through 14-3-3 protein, in a phosphorylation-dependent manner (Schlegelmilch et al. 2011; Silvis et al. 2011) (Figure 2).

Furthermore, recent evidences suggest that Hippo signaling pathway is involved not only in organ size control (paragraph 4, Introduction) but also in the maintenance of pluripotency in mammalian embryonic stem cells in culture (Lian et al. 2010). YAP1 is activated in induced pluripotent stem cells while simultaneously it inhibited the differentiation of mouse ES cells when ectopically overexpressed (Lian et al. 2010). The YAP1-TEAD complex binds and promotes the transcription of important stemness genes (*Oct3/4, Sox2* and *Nanog*) (Lian et al. 2010). In addition, Hippo pathway also regulates tissue specific progenitor cells. YAP1 expression is restricted to the progenitor cells in normal mouse intestines (Karpowicz et al. 2010) and it expands basal epidermal progenitors in mouse skin inhibiting their terminal differentiation (Zhang H. et al. 2011). There are also evidences of YAP1 role in tissue regeneration program. Indeed, it was demonstrated that YAP1 protein levels are increased during rat liver regeneration (Wang et al. 2012) and also in intestinal crypts regeneration in mice (Cai et al. 2010).

Based on these evidences, YAP1 may represent a great promise as a target in cancer therapy and in regenerative medicine and proper elucidation of the multiple YAP1 functions in different cellular contexts is required.

3. CROSSTALK OF YAP1 WITH MULTIPLE SIGNALING PATHWAYS

Recent studies have revealed a complex network of interactions that connected YAP1 and Hippo pathway with other key signaling pathways suggesting that YAP1 may influence a multitude of cellular processes.

Sonic Hedgehog pathway. Sonic Hedgehog pathway activity has been linked to YAP1 oncogenic potential in human medulloblastomas (Fernandez-L et al. 2009). Sonic Hedgehog pathway sustains the proliferation of cerebellar granule neuron precursors (CGNPs), the cells that primarily contributing to the genesis of medulloblastoma. YAP1 mRNA and protein result upregulated and localized into the nucleus in medulloblastomas, inducing hyper-proliferation of cerebellar granule neuron precursor in combination with TEAD transcription factors (Fernandez-L et al. 2009). Moreover, literature data described that the expression of YAP1 induced the activation of Sonic Hedgehog signaling pathway during neuronal differentiation (Lin et al. 2012). These observations suggest Hippo pathway activity may in fact bolster Sonic Hedgehog signaling.

TGF-β/BMP pathway. Over the past several years, studies reported that the Hippo pathway has an important role in regulating of TGF-β/BMP signaling. The highly conserved core of the canonical TGF-β/BMP signaling is a cascade that involves the TGF-β/BMP ligands, two types of receptors and the signal transducers, SMADs. On activation, the receptor complex phosphorylates the receptor-regulated SMAD proteins (R-Smads), including SMAD1, 5 and 8 for BMP signaling and SMAD2 and 3 for TGF-β signaling. Activated R-SMADs interact with the common partner SMAD4 and the SMAD complex directly binds defined elements on the DNA and regulates target genes expression (Guo and Wang 2009).

Initial evidences reported an association between the BMP and the Hippo signaling pathway by the WW domain of YAP1. YAP1 was identified as a SMAD7-binding partner with the potential to inhibit TGF-β/SMAD signaling (Ferrigno et al. 2002). Later, Varelas and collaborators demonstrated that TAZ binds SMAD2/3/4 complexes in the presence of TGF-β (Varelas et al. 2008). In addition, a subsequent study showed that YAP1 interacts with SMAD1/5 in a BMP-dependent manner. This study also reveals the phosphorylation at CDK8 and CDK9 in the linker domain of SMAD1. The linker phosphorylation regulates SMAD1 protein stability and also stimulates the interaction with YAP1, which functions to promote BMP-mediated transcriptional signals (Alarcon et al. 2009).

Although YAP1 and TAZ are linked to both TGF-β and BMP mediated SMAD signaling, TAZ was found to only weakly interact with BMP-activated SMAD1, suggesting that TAZ may have a limited role in regulation of BMP signaling with respect to YAP1. Moreover Hippo pathway participates to the control of SMAD subcellular localization. In fact it was described that YAP1 is involved in SMAD2/3 nuclear accumulation (Varelas et al. 2010).
In addition, the interaction between Hippo pathway and TGF-β pathway may stimulate the oncogenic role of TAZ and YAP1, including the induction of the metastatic cellular properties. TGF-β and SMAD signaling pathway represent mediators of epithelial-mesenchymal transition (Thiery et al. 2009) and therefore the increase of YAP1 and TAZ in nuclear localization would sensitize the cells to TGF-β facilitating tumor development.

WNT pathway. Recent studies have reported that Hippo pathway has a key role also in the regulation of Wnt signaling pathway. The Wnt signaling pathway consists of several proteins that transducts the signals from receptors present on the surface into the nucleus leading to target genes expression. Wnts ligands bind to Frizzled and LRP cell surface receptors inducing β-catenin which transduces the signal into the nucleus (Nusse 2005).
Analysis of the Wnt pathway highlights that TAZ is a potential regulator of Wnt signaling (Miller et al. 2009). TAZ/YAP1 functions both as inhibitors and activators of Wnt/β-catenin signaling depending on Hippo pathway activity. When the Hippo pathway is active, Wnt signaling is inhibited by cytoplasmic TAZ/YAP1 indeed TAZ acts on a ubiquitin ligase complex that promotes the ubiquitination of β-catenin (Tian et al. 2007). On the contrary, in the absence of Hippo pathway signaling, TAZ/YAP1 localize into the nucleus where they can induce Wnt/β-catenin signals. Recent evidences reveal a key role for β-catenin in regulation of TAZ stability. Azzolin and collaborators showed that the TAZ binding with GSK3 β-phosphorylated β-catenin is required for its ubiqitination and destruction. Therefore the TAZ degradation is directly dependent on β-catenin (Azzolin et al. 2012). Another study classified β-catenin activity in several cancer cell lines and Rosenbluh and co-workers found that β-catenin active cancers are dependent on Hippo pathway involving the transcriptional regulator YAP1. In these cell models they detected that YAP1 and the transcription factor TBX5 forms a complex with β-catenin. The YAP1 phosphorylation leads to the localization of this complex to the promoters of the pro-apoptotic genes, including *BCL2L1* and *BIRC5*. Therefore, these observations define a β-catenin-YAP1-TBX5 complex crucial to cell transformation in β-catenin-driven cancers (Rosenbluh et al. 2012).

4. DEFINITION OF YAP1 ROLE IN CANCER

Several reports describe the involvement of YAP1 in cancerogenesis. Initially, convincing data classified YAP1 as a tumor suppressor gene (or at least as helper of tumor suppressors). In fact, it was reported that YAP1 increases the ability of TP73 to induce apoptosis as a consequence of DNA damage. On the contrary, recent discoveries suggest that YAP1 may function as an oncogene by promoting increase in organ size and cancer development.

Here below I report multiple evidences regarding YAP1 as a tumor suppressor and, on the other hand, other studies which describe the importance of YAP1 as a proto-oncogene.

4.1 YAP1 AS A TUMOR SUPPRESSOR GENE

The shuttle of YAP1 between nucleus and cytoplasm exerts an important means for regulating the activity of the protein. Indeed, in response to different stimuli, such as DNA damage, the subcellular localization of YAP1 is critical for the induction of different mechanisms including apoptosis. In unstressed cells, YAP1 is retained into the cytoplasm, it is phosphorylated by Akt at serine 127, leading to 14-3-3 protein binding and preventing nuclear import (Basu et al. 2003).

As previously described, YAP1 interacts with DNA binding protein TP73. In 2001 Blandino and collaborators identified the binding between WW domain of YAP1 and PY motifs on the C-terminal region of TP73 (Strano et al. 2001).

The TP73 is a member of TP53 family of transcription factors and, similarly to TP53, induces arrest of the cell cycle or apoptosis hence it is considered a tumor suppressor gene. TP73 is mutated or deleted in few human cancers and the activity of the protein is altered in the presence of a mutated form of TP53. In these conditions, mutated TP53 binds to TP73 preventing its capability to activate pro-apoptotic genes (Di Como et al. 1999; Strano et al. 2001).

Basu and collaborators proposed a model in which, in response to different stimuli, such as DNA damage, YAP1 dissociates from the cytoplasmatic multiprotein complex formed with the protein kinase Akt and 14-3-3 protein and moves into the nucleus, where it functions as a coactivator of transcriptional cofactors including TP73, therefore inducing the transcription of the pro-apoptotic

genes (Basu et al. 2003). In the nucleus YAP1 appears to bind and stabilize TP73 protein by competing with the ITCH E3-ligase for binding to TP73 (Levy et al. 2007).

Moreover a further work of Blandino group found that, following DNA damage, YAP1 was released from the cytoplasmatic multiprotein complex with 14-3-3 and Akt and translocated into the nucleus where it promotes TP73-dependent apoptosis through the specific and selective coactivation of apoptotic TP73 target genes and potentiation of p300-mediated acetylation of TP73 (Strano et al. 2005). The transcriptionally active complex thus assembled induced the transcription of target genes such as *p53AIP1* and *Bax* (Strano et al. 2005). Then, it was described that PML is a direct transcriptional target of TP73/YAP1. PML contributes to the TP73-dependent apoptotic response by regulating YAP1 stability. PML and YAP1 physically interact causing YAP1 stabilization upon DNA damage treatment (Lapi et al. 2008). In addition, Shaul and collaborators defined an additional mechanism involved in activation of pro-apoptotic genes. In fact, they demonstrated that DNA damage induces ABL1-mediated YAP1 phosphorylation at position Y357, resulting in more stable protein that displays higher affinity to TP73 and selectively co-activates TP73 pro-apoptotic target genes (Levy et al. 2008).

RASSF1 is a tumor suppressor gene that is inactivated in multiple types of carcinomas. RASSF1 gene presents different isoforms resulting by alternative splicing. RASSF1A isoform is frequently lost in cancer cells though promoter methylation. Matallanas and collaborators defined that, in mammalian cells, RASSF1A stimulates apoptosis by inducing the activation of Mst2, once dissociation of the inhibitory complex formed by Mts2 and Raf1 is occurred. Raf1 is a proto-oncogene, which binds to Mst2 preventing its activation. Apoptotic stimuli, such as Fas receptor activation, which induces the Hippo pathway, promote the release of Mts2 from Raf1. Under these conditions, RASSF1A activates Mts2 and stimulates the interaction with its substrate Lats1. This in turn induces the phosphorylation and following release of YAP1 from Lats1. YAP1 moves into the nucleus where it interacts with the transcription factor TP73 and stimulates the transcription of the pro-apoptotic *BBC3/puma* gene. Silencing of RASSF1A removes its capability to activate the pro-apoptotic pathway via Mts2 (Matallanas et al. 2007).

A study reports YAP1 as a tumor suppressor in breast, demonstrating that the 11q22 genomic region, encompassing YAP1 gene, is a site of frequent LOH in this tumor type. Moreover, the authors suggest that loss of YAP1 protein correlates with the deletion of the YAP1 gene locus (Yuan et al. 2008).

4.2 YAP1 AS AN ONCOGENE

In addition to the oncosuppressor role of YAP1, recent evidences describe it as an oncogene connected its activity with an increase in organ size that can lead to tumor development.

The YAP1 gene, contained in 11q22 genomic region, was found amplified in a small percentage of several human tumors (Table 5, paragraph 5 of Introduction). In addition, elevated YAP1 expression levels and nuclear localization have been also observed in several types of human cancers such as liver cancer (Xu et al. 2009; Zhao et al. 2007), prostate cancer (Zhao et al. 2007), colon cancer (Steinhardt et al. 2008), lung cancer (Steinhardt et al. 2008), ovary cancer (Steinhardt et al. 2008; Zhang X. et al. 2011) and gastric cancer (Song et al. 2012).

Furthermore, independent studies identified YAP1 as a candidate oncogene in human HCC (Hepato Cellular Carcinoma) (Zender et al. 2006) and in breast cancer (Overholtzer et al. 2006; Cordenonsi et al. 2011).

Scott Lowe and collaborators induced cancer development in the liver of mice by transplantation of modified mouse embryonic liver progenitor cells. These cells were modified *in vitro* by removing TP53 alleles and introducing active oncogenes (*Myc*, *Akt* or *Ras*), and were seeded into the host mouse liver, thus inducing HCC. Analysis of induced HCC by genome wide screening revealed a recurrent amplification of locus 9qA1, containing cIAP apoptosis inhibitor and YAP1 transcription factor. Notably, they also verify the occurrence of an amplification event in human hepatocellular carcinomas in the syntenic region of human 11q22. The authors established that cIAP and YAP1, in the genetic context of their amplification, exert a synergistic effect when overexpressed and both these two adjacent genes can cooperate to promote tumorigenesis (Zender et al. 2006).

Haber and collaborators demonstrated that the overexpression of YAP1 in nontransformed human MCF10A mammary epithelial cells induces a transformed phenotype characterized by epithelial-mesenchymal transition, suppression of

apoptosis, growth factor-independent proliferation, anchorage-independent growth in soft agar and activation of Akt and ERK. Therefore the authors concluded that YAP1, in this cell context, contributes to malignant transformation (Overholtzer et al. 2006).

Furthermore, contrary to the tumor suppressive role suggested by Yuan and co-workers (Yuan et al. 2008), a recent report identified that increased TAZ and YAP1 activity correlates with high histological grade and with metastasis in breast cancer (Cordenonsi et al. 2011).

In addition, two independent groups reported that the overexpression of YAP1 in transgenic mice produced a significant overgrowth of liver organ size, demonstrating how variations in YAP1 expression levels can overcome organ size control (Dong et al. 2007; Camargo et al. 2007).

Using a conditional, Doxo-inducible YAP1 transgenic mouse model, Pan and co-workers induced an increase of YAP1 expression in liver and they showed that YAP1 induction caused massive epatomegaly. The increase in liver mass was detectable as early as 3 days after induction and reached 25% (in normal condition liver represents 5% of the body weight) of total body weight after 4 weeks of Doxo feeding. The overexpression of YAP1 for a short period of time stimulated an increase in liver size and the effect was reversible, in fact the enlargement of the liver can revert to almost normal condition after Dox withdrawal for an adequate period of time. The increase in liver mass was determined by an increase in cells number (hyperplasia) not by an increase in cells size (hypertrophy). Sustained YAP1 overexpression for longer period of times induced the growth of carcinomas (Dong et al. 2007).

These data are in accordance with the work conducted by Camargo and collaborators which have generated transgenic mice in which YAP1 can be activated in inducible manner. They used a mutated version of YAP1 which contained a S127A mutation. The ablation of this phosphorylation site increases the nuclear localization of YAP1 because it escapes 14-3-3-mediated inhibition. The activation of YAP1 for 35 days induced a more than 4-fold increase in liver size and the expanded liver size is due to increase in cells number. The increase in liver mass is completely reversible, as the interruption of YAP1 overexpression for 5 weeks induces a normally sized liver without any gross abnormalities. Moreover they found that overexpression of YAP1 in the intestine of the transgenic mouse

correlates with increased intestinal dysplasia and loss of cell differentiation through the apical region of the microvilli epithelium. Overexpression of activated YAP1 in the mouse small intestine leads to Notch-dependent hyperplasia and loss of terminally differentiated cell types, but does not cause appreciably increasing in overall size of the organ (Camargo et al. 2007).

As previously reported in paragraph 3, Fernandez and collaborators (Fernandez-L et al. 2009) demonstrated that YAP1 and TEAD1 are overexpressed in Sonic Hedgehog (Shh)-driven medulloblastoma in both mouse models and human and they also detected amplification of YAP1 in a subset of human medulloblastomas, mainly Shh-associated ones (Fernandez-L et al. 2009).

Finally, Pan and collaborators showed that Yki, the ortolog of YAP1 in *Drosophila,* has similar biological activity when overexpressed in *Drosophila*. In fact, the overexpression of Yki induces a phenotype characterized by an increased proliferation, in tissue overgrowth and in apoptosis inhibition (Huang et al. 2005). These data suggest that Yki-YAP1 proproliferative biologic functions are largely conserved throughout evolution.

5. 11q22 GENOMIC LOCUS AMPLIFICATION

11q22 genomic region includes YAP1 gene and, as already described, was found amplified in individual cases from several human tumors (Table 5).

Table 5. Tumors types in which 11q22 genomic region, encompassing YAP1 gene, is reported to be amplified.

TUMOR TYPE	N° CASES	N° (%) 11q22 AMPL	N° DIRECT EVIDENCE OF YAP1 AMPL	REFERENCE
Medulloblastoma	27	1 (4%)	Not available	Reardon et al. 1997
Medulloblastoma	67	2 (3%)	2/2	Fernandez-L et al. 2009
Cervical carcinoma	27	5 (18.5%)	Not available	Imoto et al. 2002
Cervical carcinoma	84	11 (13%)	Not available	Scotto et al. 2008
Cervical carcinoma	217	28 (13%)	Not available	Choschzick et al. 2012
Lung cancer	64	3 (5%)	Not available	Dai et al. 2003
Esophageal squamous cell carcinoma	42	4 (9.5%)	Not available	Imoto et al. 2001
Oral squamous cell carcinoma	24	17 (71%)	4/17	Snijders et al. 2005
Oral cancer	20	2 (10%)	Not available	Baldwin et al. 2005
Larynx and pharynx squamous cell carcinoma	56	5 (9%)	Not available	Hermsen et al. 2005
Hepatocellular carcinoma	25	2 (8%)	2/2	Zender et al. 2006
Ependimoma	24	1 (4%)	1/1	Modena et al. 2006
Mesothelioma	22	2 (9%)	2/2	Yokoyama et al. 2008
Soft tissue sarcoma	404	14 (3.5%)	6/14	Helias-Rodzewicz et al. 2010

Amplification event is defined as a more than two-fold copy number increase of a chromosomal region. It is common in cancers and it is associated with the overexpression of at least some of the amplified genes. Therefore genes mapping within amplicons are considered as candidate oncogenes. The cytogenetic analysis of amplified DNA highlights that it can be organized either as extrachromosomal copies, named double minutes, or as in-

tandem repeats within a chromosome, constituting the homogeneously staining region (HSR) (Albertson 2006).

Until now the only reported genetic alteration affecting YAP1 in tumors is 11q22 amplification. The size of the amplified DNA can vary from hundreds kilobases to megabases. Similar to all amplification events, this one also includes a large region of DNA that contains additional genes flanking YAP1 (Table 6). Among them some genes have been involved in cancer development. These are a cluster of matrix metalloproteinase (*MMP*) genes, two members of the BIRC family (*BIRC2* and *BIRC3* also known as the cIAP family) and the progesterone receptor (*PGR*).

Table 6. Genes contained in 11q22 amplicons of the cellular models under study (see results section).

GENE	GENE NAME	FUNCTION
ARHGAP42	Rho GTPase activating protein 42	GTPase activator
WDR82	WD repeat domain 82	Control of chromatin structure and cell cycle progression
PGR	Progesterone receptor	Receptor of steroid hormone progesterone
ANGPTL5	Angiopoietin-like 5	Angiogenesis promoter
KIAA1377		Neuronal functions
C11orf70	Chromosome 11 open reading frame 70	Not fully known
YAP1	Yes-associated protein 1	Organ size control
BIRC2	Baculoviral IAP repeat containing 2	Apoptosis Inhibitor
BIRC3	Baculoviral IAP repeat containing 3	Apoptosis Inhibitor
TMEM123	TMEM123 transmembrane protein 123	Cell surface receptor that mediates cell death
MMP7	Matrix metallopeptidase 7	Cell motility and cell invasion
MMP20	Matrix metallopeptidase 20	Cell motility and cell invasion
MMP27	Matrix metallopeptidase 27	Cell motility and cell invasion
MMP8	Matrix metallopeptidase 8	Cell motility and cell invasion
MMP10	Matrix metallopeptidase 10	Cell motility and cell invasion
MMP1	Matrix metallopeptidase 1	Cell motility and cell invasion
MMP3	Matrix metallopeptidase 3	Cell motility and cell invasion
MMP12	Matrix metallopeptidase 12	Cell motility and cell invasion
MMP13	Matrix metallopeptidase 13	Cell motility and cell invasion
DCUN1D5	Defective in cullin neddylation 1, domain containing 5	DNA damage regulator
DYNC2H1	Dynein, cytoplasmic 2, heavy chain 1	Intraflagellar transport

Matrix metalloproteinases (MMP) belong to a proteases family know as metzincin superfamily. Humans have 24 MMPs and in particular 10 of them are contained in the 11q22 amplicon (Table 6). These proteins act in the extracellular environment of cells and function degrading both matrix and non matrix proteins. These proteins are involved in the cleavage of cell surface receptors and play a role in cell proliferation, differentiation, wound healing, apoptosis, angiogenesis, morphogenesis, tissue repair and remodeling after injury and in progression of diseases such as cancer, arthritis and chronic ulcers (Page-McCaw et al. 2007).

Baculoviral IAP repeat containing 2 (BIRC2) and baculoviral IAP repeat containing 3 (BIRC3) genes encode for a member of IAP family of protein involved in apoptotic inhibition targeting directly caspase and pro-caspase (first of all caspase 3 and 7) (LaCasse et al. 1998).

IAP family proteins are multi-functional proteins which controls different cellular functions. These proteins indeed regulate not only caspases and apoptosis, but also mitogenic kinase signaling, inflammatory signaling, cell proliferation, as well as cell invasion and metastasis (LaCasse et al. 1998).

Progesterone receptor (PGR) is a nuclear hormone receptor and it is activated by the steroid hormone progesterone. Progesterone receptor is found in female reproductive tract, mammary glands, brain and pituitary gland and it is involved in ovulation, implantation, mammary gland development an in maintenance of pregnancy. The steroid hormones and their receptors are involved in the regulation of eukaryotic gene expression and affect cellular proliferation and differentiation in target tissues (Gadkar-Sable et al. 2005).

AIM OF THE THESIS

The Hippo pathway is a novel signaling pathway which, over the past years, has emerged as a complex signaling network with significant implications in cell contact inhibition, in organ size control, in cancer development and in regulation of stem cells and progenitor cells self-renewal and expansion.

YAP1 (Yes-associated protein 1) gene is a critical final effector of the Hippo pathway, located in 11q22 genomic region. Literature data report that 11q22 genomic region is amplified in individual cases from multiple human tumor types. Since amplicons usually span hundreds of kilobases, they typically contain several genes.

The aims of my thesis are to study whether YAP1 represents an oncogenic target of 11q22 amplicon and to corroborate the existence of YAP1 amplification in clinical series of different human tumor types.

The work is subdivided in three parts, each concerning different aspects of YAP1 oncogenic role and addressing the following questions:

- *Does YAP1 influence the tumorigenic properties of cancer cell lines?* I will identify established cancer cell lines that feature YAP1 amplification and overexpression and use them as a cellular model in my study. Endogenous YAP1 expression will be silenced by RNA interference strategies. I will then evaluate the effect of YAP1 silencing on multiple traits related to the malignant phenotype, under the hypothesis that YAP1 acts as an oncogene. If my hypothesis is correct then depletion of YAP1 should suppress the above mentioned phenotypes related to cell proliferation and tumorigenicity.

- *Which are the target genes regulated by YAP1?* YAP1 is a transcriptional coactivator, therefore, in order to identify the downstream genes and pathways that are critical YAP1 effectors in carcinogenesis, I will investigate YAP1 target genes, by gene expression profiling comparing YAP1-proficient with YAP1-silenced cells.

- *Is YAP1 amplification actually represented in our human tumour specimens' series?* I will investigate the frequency of YAP1 alterations in a panel of human tumor samples including non-small cell lung cancers, cervical carcinomas, central nervous system tumors and thyroid carcinomas.

RESULTS

1. YAP1 GENE IS AMPLIFIED IN A FRACTION OF CLINICAL SAMPLES FROM MULTIPLE HUMAN TUMORS

Literature data report that chromosome region 11q22, containing YAP1 gene, is amplified in a small percentage of samples from multiple human tumor types (Table 5, Introduction).

In order to expand these observations, I directly investigated the frequency of YAP1 copy number amplification in a panel of human tumor samples from different tumor types comprising cervical cancers, non small cell lung cancers (NSCLC), central nervous system tumors (CNS) and thyroid cancers (Figure 5).

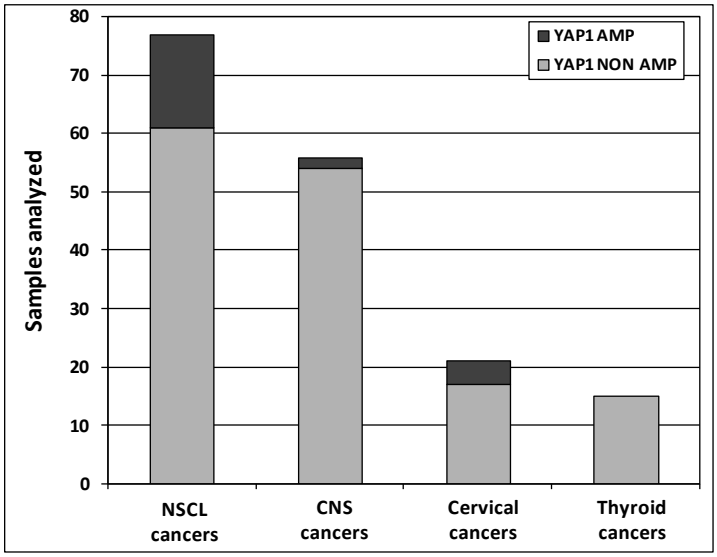

Figure 5. Frequency of YAP1 amplification in different types of human tumor samples. Number of cases displaying normal YAP1 copy number (in gray) or YAP1 copy number amplification (in black) in NSCL non small cell lung cancers samples (amplified cases 18/77; 23%), CNS central nervous system cancers samples (2/56; 3.6%), cervical cancers samples (4/21; 19%) and thyroid cancers samples (0/15; 0%).

In particular, 77 NSCLC samples arrayed on a tissue microarray were assayed using double-colour FISH, performed by my colleagues (Figure 6). Since cyclin D1 is present in the same chromosomal arm and this oncogene is frequently amplified in lung cancer (Betticher et al. 1996; Zhang et al. 1993), a double-colour FISH approach was applied using one probe specific for cyclin D1 gene (CCND1, 11q21, green signal) and another

probe specific for YAP1 gene (red signal). Among these NSCLC samples, 16 (21%) carried a large amplification which included both YAP1 and CCND1 genes, while 2 samples (2.6%) carried an amplification restricted to YAP1 only (Figure 6).

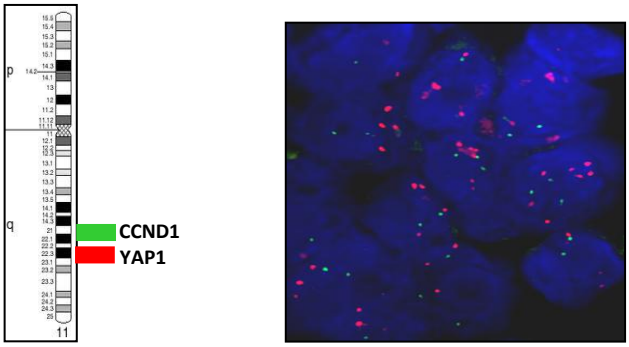

Figure 6. YAP1 amplification in non small cell lung cancer samples. FISH analysis was performed using YAP1 and CCND1 probes on 77 lung cancer samples analyzed in TMA. A large amplification which comprises both YAP1 and CCND1 was detected in 16 (21%) samples while in 2 (2.6%) samples a restricted YAP1 amplification was identified. The FISH picture shows a sample with an amplification restricted to YAP1 (Green = CCND1-containing BAC clone; Red = YAP1-containing BAC clone).

I investigated the YAP1 copy number status in the other clinical samples, which were available as individual paraffin blocks, by a quantitative PCR approach. The accuracy and reproducibility of the method was preliminarily investigated using normal DNA (2 copies of YAP1) and using cell lines that carried YAP1 amplification (as a positive control for YAP1 amplification) (Figure 7).

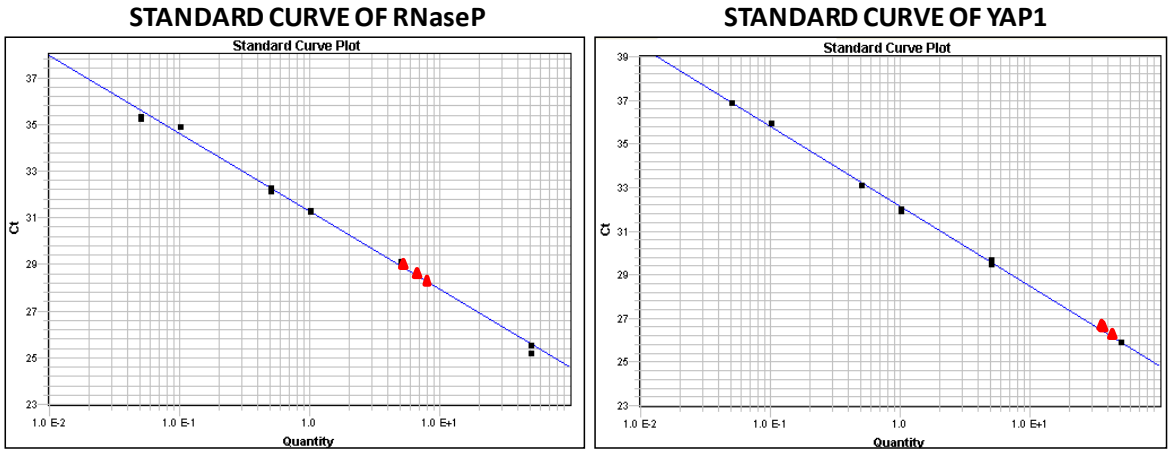

Figure 7. Standard curves of RNaseP and of YAP1. The standard curves were obtained from normal DNA. The triangles in red indicated a triplicate of one YAP1-amplified cell line.

In 56 CNS tumor samples I identified YAP1 copy amplification in 2 (3.6%) samples, including one low-copy amplification and one high-copy amplification.

None of the 15 thyroid cancer samples displayed YAP1 copy amplification.

Ultimately, I evaluated the YAP1 status in 21 advanced stage cervical cancer specimens. In 4/21 samples (19%) YAP1 amplification was detected, including high copy amplification in 3/4 and low copy amplification in 1/4 (Figure 8).

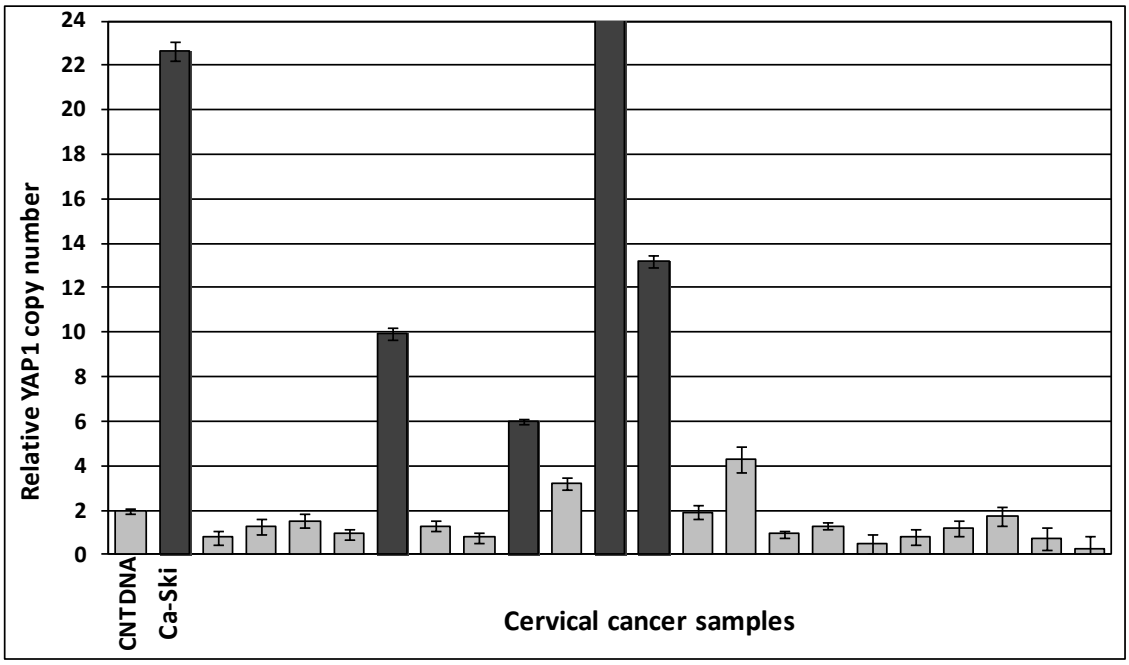

Figure 8. Relative YAP1 copy number in cervical cancer samples. Gene dosage analysis by qPCR in 21 cervical specimens revealing high/low YAP1 copy number amplification in 4 samples (black bars). Normal DNA (CNT DNA, grey bar, 2 copies of YAP1) was used as a control while Ca-Ski cell line was used as a positive control (black bar).

I then decided to check YAP1 protein expression by immunohistochemistry in the above mentioned cervical cancers. Immunohistochemistry was performed at Dept. of Pathology of Treviso Hospital, revealing that YAP1 protein level was higher in samples carrying YAP1 copy amplification compared to samples with normal YAP1 copy number (Figure 9).

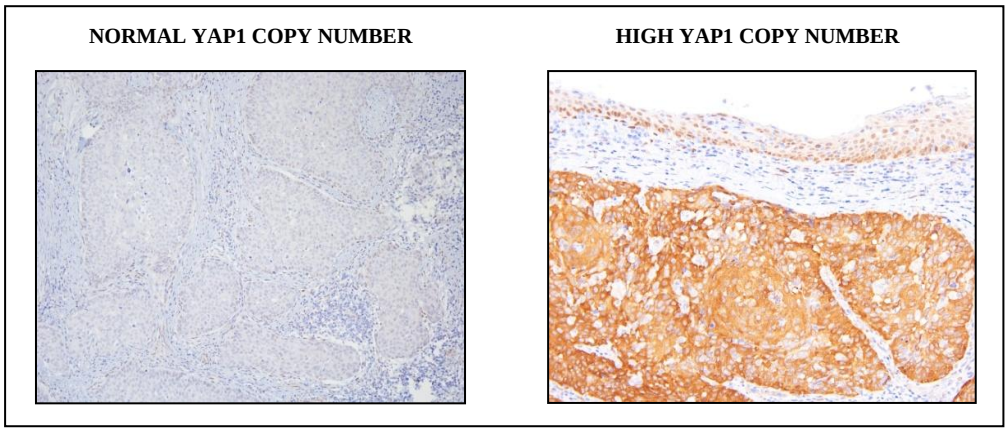

	AMP	NOT AMP
IHC 1+	0	12
IHC 2+/3+	4	5

Figure 9. Immunohistochemistry analysis performed on cervical cancer samples. Immunohistochemistry analysis related to a sample with a normal YAP1 copy number (left panel) and to a sample carrying YAP1 copy amplification (right panel). Fisher's exact test two-tailed p value = 0.0211.

To further analyze YAP1 copy number status in independent and larger collections of normal and neoplastic samples, I interrogated public (Sanger Centre) and private (Oncomine) microarray databases (Table 7) for the copy number status of genomic loci encompassing YAP1 gene. Analysis from Oncomine database *(www.oncomine.org)* revealed that deletion of YAP1 gene is a very rare event, in fact it is found only in 3/664 (0.5%) cancer cell lines and in 3/1629 (0.2%) cancer tissue samples. In contrast, YAP1 copy amplification event was found in a greater percentage of the same samples (Chi-square test $p<0.0001$). In fact, it was reported in 40/664 (6%) of cancer cell lines and in 31/1629 (1.9%) of cancer tissue samples. Moreover YAP1 amplification was present in 2/110 (1.8%) of primary cancer cell cultures and in 1/20 (5%) xenograft tumors (Table 7).

Based on SNP-based array-CGH data from the public Sanger Centre database (*http://www.sanger.ac.uk/genetics/CGP/CellLines/),* I identified 21/764 (3%) cell lines that carried 11q22-restricted high copy number amplification, encompassing YAP1 locus.

Table 7. Summary of YAP1 copy number data from Oncomine database.

NORMAL CELL LINES	YAP1 AMPLIFICATION (%)	YAP1 DELETION (%)	
10	0 (0%)	0 (0%)	
CANCER CELL LINES	YAP1 AMPLIFICATION (%)	YAP1 DELETION (%)	χ^2 p-value
664	40 (6%)	3 (0.5%)	< 0.0001
PRIMARY CANCER CELL CULTURES	YAP1 AMPLIFICATION (%)	YAP1 DELETION (%)	
110	2 (1.8%)	0 (0%)	
NORMAL TISSUE SAMPLES	YAP1 AMPLIFICATION (%)	YAP1 DELETION (%)	
45	0 (0%)	0 (0%)	
CANCER TISSUE SAMPLES	YAP1 AMPLIFICATION (%)	YAP1 DELETION (%)	χ^2 p-value
1629	31 (1.9%)	3 (0.2%)	< 0.0001
XENOGRAFT TUMORS	YAP1 AMPLIFICATION (%)	YAP1 DELETION (%)	
20	1 (5%)	0 (0%)	

Legend: The table collects the number and the percentage of YAP1 copy amplification and deletion events in normal cell lines, cancer cell lines, primary cancer cell cultures, normal tissue samples, cancer tissue samples and in xenograft tumors. YAP1 copy amplification is found in a significantly higher percentage of cancer cell lines and tissues, compared to YAP1 deletion. Chi-square based on the null hypothesis that the two anomalies are expected at the same frequency.

Interestingly, among the datasets available in Oncomine database there was a study (Scotto et al. 2008) that analyzed cervical squamous cell carcinomas and cervical cell lines (Figure 10). The study showed that amplification of genomic clones encompassing YAP1 is detected in 8/40 (20%) tissues in advanced stage, concordant with our data. Moreover, amplification was not present in earlier stages of disease suggesting that YAP1 copy amplification may be a specific event related to tumor progression in cervical cancer. Finally, Ca-Ski cell line was also included in the study and indeed revealed YAP1 amplification (Figure 10).

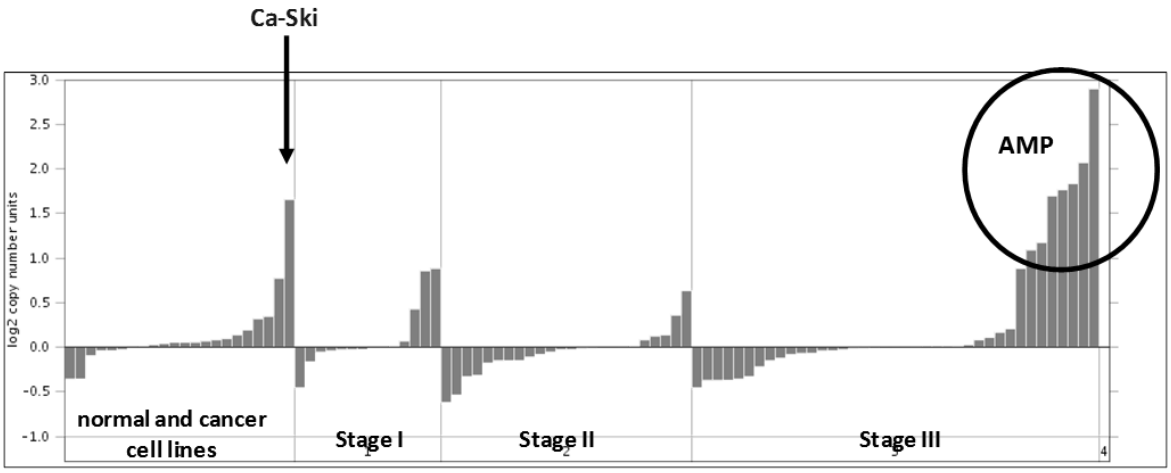

Figure 10. Schematization of Scotto and others research from Oncomine database. The study analyzed YAP1 copy number in cervical squamous cell carcinoma. Samples were grouped by stage. In addition, the analysis included both normal and cancer cell lines. YAP1 copy amplification was detected in advanced stage cancer samples.

2. IDENTIFICATION OF CANCER CELL LINES CARRYING 11q22 AMPLIFICATION AND OVEREXPRESSION

Preliminary experiments were performed in order to validate YAP1 amplification in our in-house stocks of established cancer cell lines and to confirm the presence of YAP1 overexpression.

I analyzed Ca-Ski cell line (Cervical squamous cell carcinoma), EKVX cell line (Non small cell lung-adenocarcinoma) and RO82 cell line (Follicular thyroid carcinoma) and indeed YAP1 high-copy number was confirmed in our batches of cells (Figure 11). Notably, both Ca-Ski and EKVX cell lines represent tumor histotypes in which I have also identified YAP1 copy number amplification in clinical samples. On the contrary, RO82 cell line represents a tumor histotype in which I did not identify YAP1 copy amplification in clinical samples, possibly because I have only analyzed a smaller number of thyroid cancer samples compared to the other tumor samples.

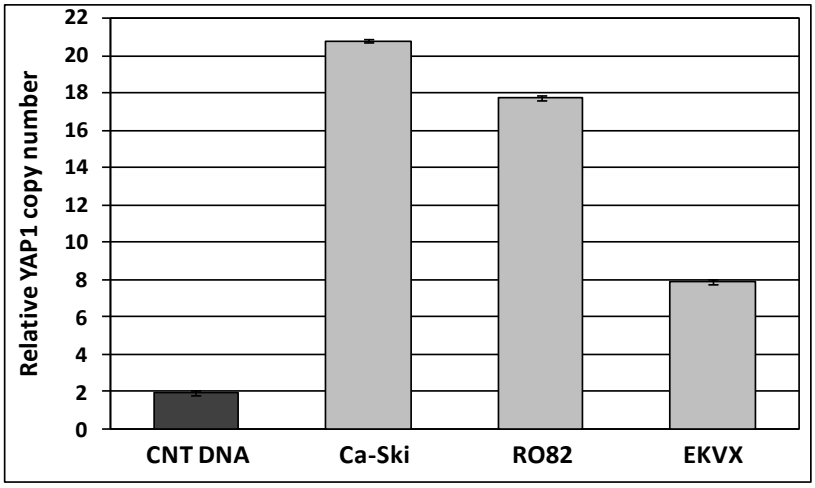

Figure 11. Evaluation of YAP1 copy amplification in Ca-Ski, RO82 and EKVX cell lines. Gene dosage analysis by qPCR shows YAP1 copy number amplification in Ca-Ski, RO82 and EKVX cell lines (grey bars). Normal DNA (2 copies of YAP1) was used as a control (black bar).

FISH analysis (performed at Cytogenetics unit, Istituto Nazionale Tumori, Milan) allowed us to define that YAP1 copy amplification is contained in a homogeneously staining region (HSP) in Ca-Ski cell line or as multiple interspersed copies (double minutes) in RO82 and in EKVX cell lines (Figure 12).

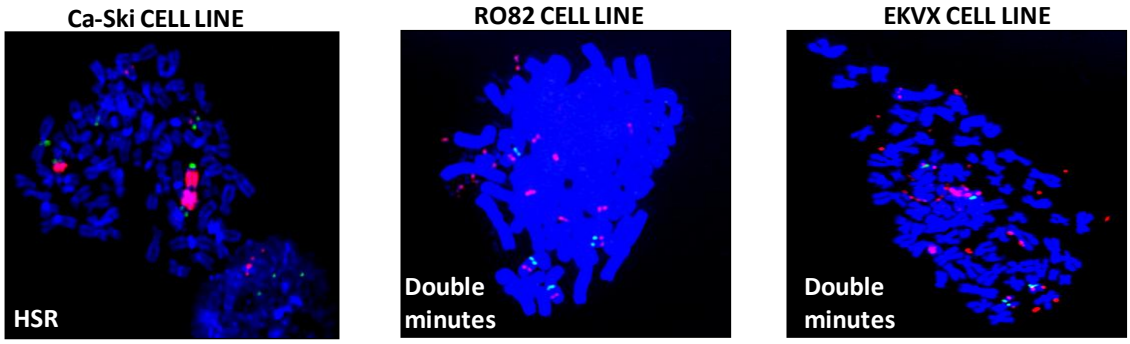

Figure 12. Evaluation of YAP1 copy amplification in Ca-Ski, RO82 and EKVX cell lines. FISH analysis confirmed the presence of the amplicon spanning YAP1 gene in Ca-Ski, RO82 and EKVX cell lines (Green = Control BAC clone; Red = YAP1-containing BAC clone).

I verified that YAP1 amplification was associated with protein overexpression by western blotting analysis. In fact, Ca-Ski, RO82 and EKVX cell lines show high YAP1 protein level compared to others tumor cell lines (Figure 13).

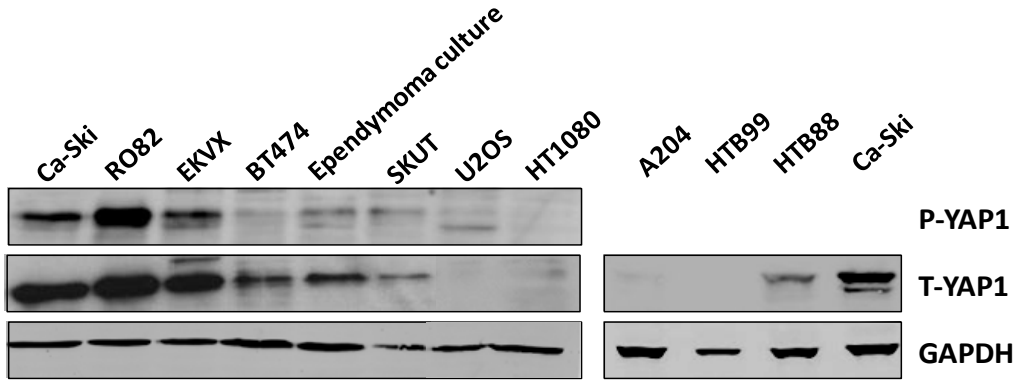

Figure 13. YAP1 protein level in cancer cell lines. Total and Phospho (Ser127) YAP1 protein level in Ca-Ski, RO82 and EKVX cell lines (high protein levels) and in other cancer cell lines (low protein levels). GAPDH (lower panel) was used as loading control.

In order to investigate the presence of mutations that could alter normal YAP1 protein functions, I performed mutational analysis by exon amplification and sequencing of the 9 exons of YAP1 in Ca-Ski, RO82 and EKVX cancer cell lines and I did not detect any mutation. In addition, Ca-Ski cell line carries mutated *PIK3CA*, while *CDKN2A*^{p16}*/RB* and *CDKN2A*^{p14}*/TP53* pathways inactivation occurs as a result of viral infection with HPV. In EKVX cell line *TP53* mutation is present and RO82 cell line carries both *TP53* and *CDKN2A* mutations (Table 8).

Table 8. Relevant characteristics of Ca-Ski, EKVX and RO82 cell lines.

CELL LINE	HISTOTYPE	HPV	STATUS *TP53*	STATUS *CDKN2A*	STATUS *PIK3CA*
Ca-Ski	Cervical squamous cell carcinoma	positive	wild type	wild type	Mutated 1633G>A
EKVX	Non small cell lung Adenocarcinoma	negative	Mutated 609_610GG>TT	wild type	wild type
RO82	Follicular thyroid carcinoma	negative	Mutated 668C>T	Homozygous deletion	wild type

Legend: HPV= Human Papilloma Virus

3. EFFECTIVE YAP1 SILENCING IN 11q22-AMPLIFIED CANCER CELL LINES

Endogenous YAP1 expression was modulated in Ca-Ski, EKVX and RO82 cell lines by RNA interference strategies. YAP1 silencing was performed using both short-hairpin RNA (shRNA) Lentiviral Particles and small interference RNA (siRNA).

Short-hairpin RNA (shRNA) expression vectors that I used carry GFP expression to track infected cells by immunofluorescence and puromycin resistance for stable selection. I used two different silencing sequences targeting YAP1 (shY1 and shY2) and, as a control, an artificial sequence that does not silence any human transcript (shOT, off target sequence). I measured YAP1 mRNA and protein expression in the bulk cell population upon puromycin selection. The YAP1 residual expression of mRNA was 20-50% and the YAP1 residual protein expression was 15-30% (Figure 14). I verified the YAP1 silencing in all experiments performed and the YAP1 residual expression was comparable to these values. In general, it was evident that shY2 construct silenced YAP1 with greater efficiency then shY1.

Small interference RNA (siRNA) is a short-term silencing system. A pool of three different sequences (siYAP1-A, siYAP1-B and siYAP1-C) targeting YAP1 (siYAP1) and, as a control, an artificial sequence that does not silence any human transcripts (siOT, off target sequence) were used and transfected directly into the cells. After 24 hours post-transfection, I evaluated that the mRNA was efficiently silenced with a residual expression of about 10-20%. The protein was efficiently downregulated with minimal expression between 48 and 96 hours. The level of mRNA and protein of siOT cells was comparable to parental cells (Figure 15). I verified the YAP1 silencing in all the experiments performed and the YAP1 residual expression was comparable to these values.

I checked that the three individual siRNAs effectively silenced YAP1 as much as an equal amount of the pool of the three combined siRNAs (Figure 16). I also verified that YAP1 protein level in parental and silenced cell lines was equally quantified by different antibodies, raised against recombinant total YAP1 (Santa Cruz monoclonal), Ser127 phosphorylated site (Cell Signaling polyclonal) and a recombinant peptide of YAP1 protein (Cell Signaling polyclonal) (Figure 16).

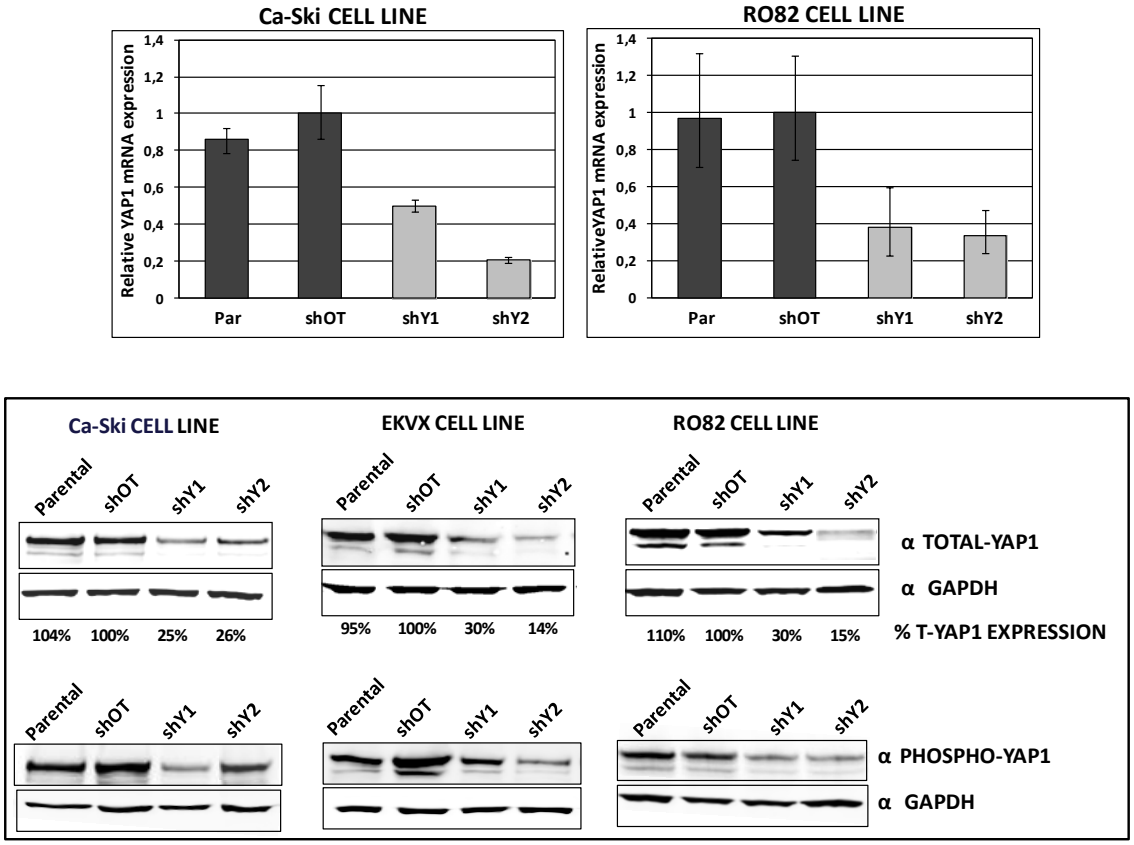

Figure 14. Evaluation of YAP1 mRNA and protein silencing in Ca-Ski, EKVX and RO82 cell lines using shRNA. Ca-Ski and RO82 mRNA (upper panel) and Ca-Ski, EKVX and RO82 protein bulk cell population after puromycin selection (lower panel) of parental cells, off target cells (shOT) and YAP1 silenced cells (shY1 and shY2). YAP1 mRNA expression level was determined by qPCR analysis. Protein level was defined by western blot analysis for the total YAP1 and for YAP1 phosphorylated form (Ser127) YAP1 residual protein expression level relative to the GAPDH.

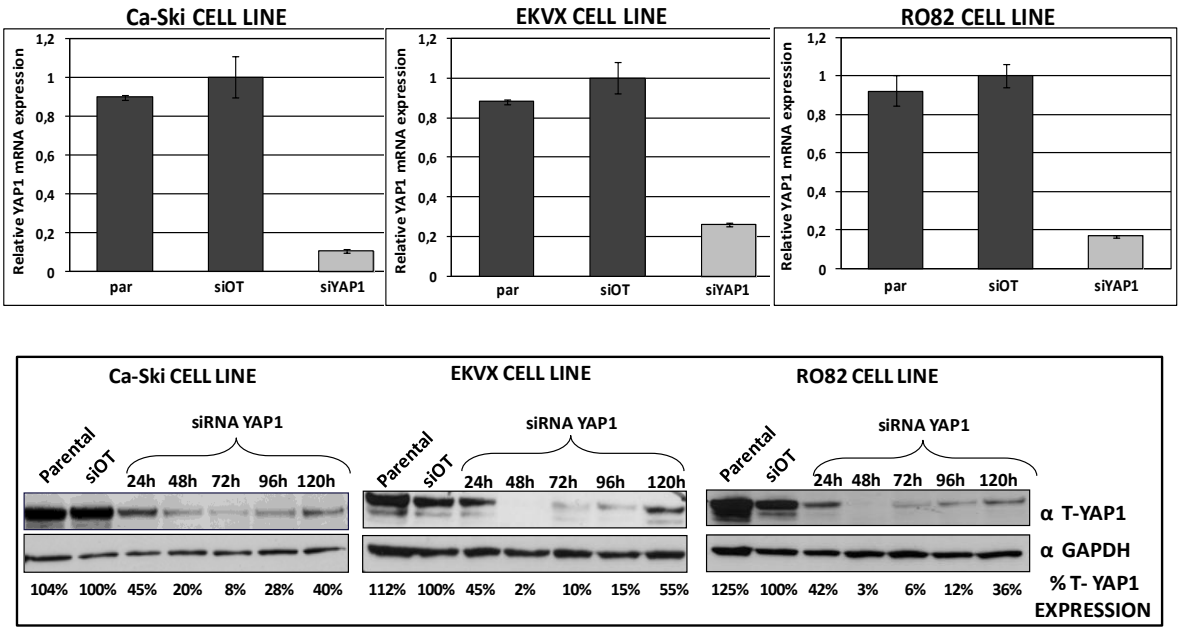

Figure 15. Evaluation of YAP1 mRNA and protein silencing in Ca-Ski, EKVX and RO82 cell lines using siRNA. Ca-Ski, EKVX and RO82 YAP1 relative expression level of parental cells, off target cells (siOT) and of YAP1 silenced cells (siYAP1), 24 hours post transfection, determined by qPCR analysis (upper panel). YAP1 protein level in Ca-Ski, EKVX and RO82 parental cells, off target cells (siOT) and YAP1 silenced cells (siYAP1) was determined by western blot analysis (lower panel). The panel shows a time-course analysis 24-120 hours after transfection with siYAP1. Note that YAP1 protein re-expression starts at 72-96 hours after transfection.

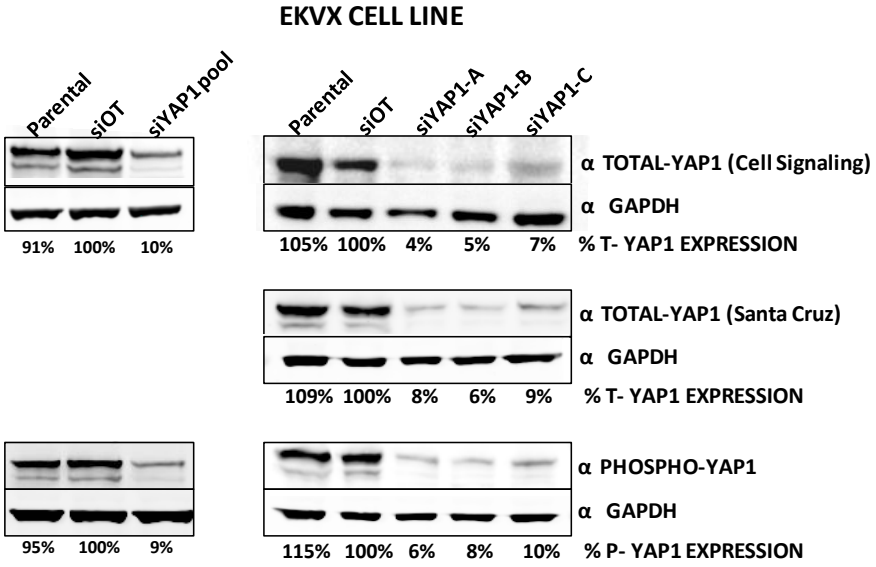

Figure 16. Evaluation of YAP1 protein silencing in EKVX cell line using siRNA. EKVX total and phospho YAP1 protein level of parental cells, off target cells (siOT) and of YAP1 silenced cells (siYAP1) determined by western blot analysis. On the left YAP1 silencing effect of the pool of the three different siRNAs targeting YAP1 and on right the YAP1 silencing effect of the single constructs (siYAP1-A, siYAP1-B, siYAP1-C). The panels show the residual YAP1 protein expression level detected using two different antibodies for total YAP1 (Santa Cruz and Cell Signaling) and one antibody for the YAP1 phosphorylated form at Ser127 relative to GAPDH.

4. EFFECT OF YAP1 SILENCING ON STABLE CLONES FORMATION

Short-hairpin RNA (shRNA) is a stable YAP1 silencing system characterized by GFP expression and puromycin resistance. Therefore puromycin selection allowed me to obtain a stable YAP1 silencing bulk cell population in Ca-Ski, EKVX and RO82 cell lines. From bulk cell population of these cell lines I tested the clonogenic capability, deriving monoclonal cell population from the bulk cell population by very low cell seeding.

YAP1 silencing constructs provided half of the clones compared to the control siOT construct in Ca-Ski and RO82. The GFP-positive clones were expanded and I confirmed the effective YAP1 silencing in these monoclonal cell populations (Figure 17).

On the contrary, in the EKVX cell line YAP1 silencing constructs formed very few clones compared to shOT construct, despite equal infection efficiency as detected by percentage of GFP positive cells in all the three constructs. YAP1 silencing was monitored after clones expansion revealing that none of the clones were robustly silenced (Figure 17). This result suggests that long-term silencing of YAP1 is counterselected particularly in EKVX cell line.

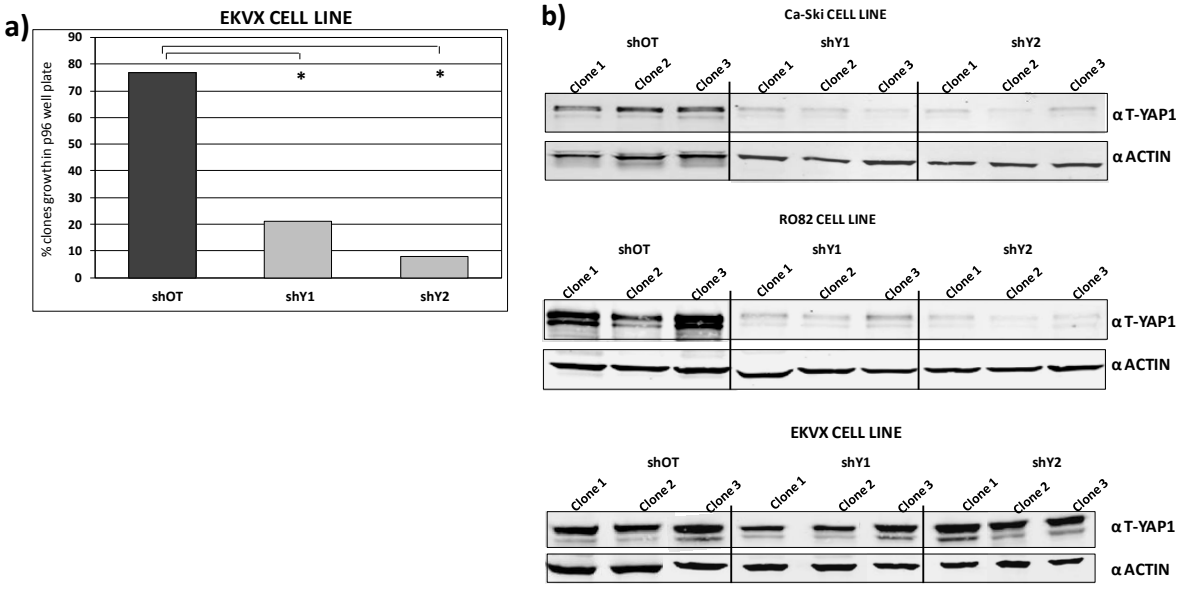

Figure 17. Evaluation of clones obtained from bulk cell population. a) Percentage of clones grown in 96-well plate and derivating from bulk cell population in EKVX shOT, shY1 and shY2 cells. $p<0.0001$ Fisher two-tailed exact test. **b)** Protein expression levels of YAP1 in shOT, shY1 and shY2 clones derived from Ca-Ski, EKVX and RO82 relative to Actin.

5. DOWNREGULATION OF YAP1 REDUCES *IN VITRO* CELL PROLIFERATION

Uncontrolled, aberrant cell proliferation is a common characteristic of cancer cells (Evan and Vousden 2001). Therefore, in order to evaluate whether YAP1 sustains the cell proliferation, I studied cell growth in Ca-Ski, EKVX and RO82 cell lines bulk population following sh-mediated stable silencing.

Using Sulforhodamine B assay, I detected that YAP1 silencing induced a moderate reduction in cell proliferation in all cell lines analyzed, which is statistically significant only in Ca-Ski cell line (Figure 18).

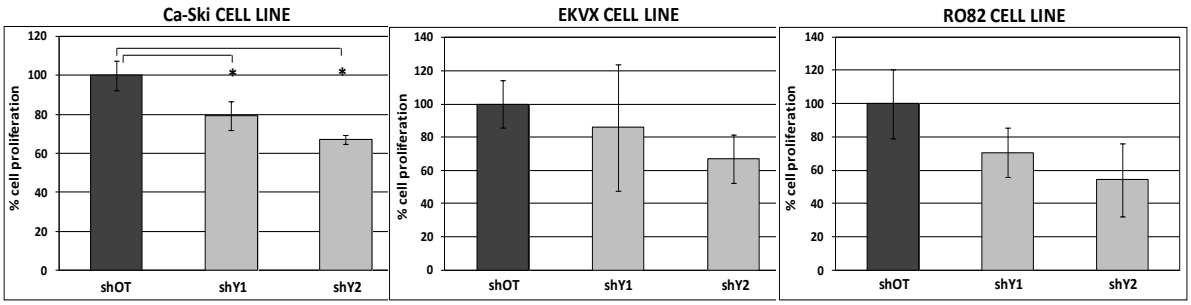

Figure 18. Evaluation of cell proliferation effect after YAP1 silencing. SRB assay was performed on Ca-Ski, EKVX and RO82 cell lines silenced for YAP1 using stable silencing system. The percentage of cell proliferation was evaluated 72 hours post seeding. The values correspond to the percentage calculate on the means from three independent experiments. The error bars denote the s.e.m. In Ca-Ski cell line paired t-test shOT versus shY1 p=0.0124, shOT versus shY2 p=0.0157, in EKVX cell line paired t-test shOT versus shY1 p=0.6741, shOT versus shY2 p=0.1337 and in RO82 cell line paired t-test shOT versus shY1 suggestive p=0.0537 shOT versus shY2 suggestive p=0.0833.

Cell growth has been also studied using cell counting and Trypan blue staining, which selectively stained dead cells. I performed the experiment on cell lines silenced for YAP1 through stable silencing system using control and shY2 constructs. Concordant with SRB assay, I observed that YAP1 silencing correlates with a reduction in viable cell count in all cell lines analyzed and at this time the effect was reached statistical significance only in Ca-Ski cell line (Figure 19, black bars, left y axis).

Furthermore, Trypan blue staining revealed very few dead cells in all three cell lines and I did not identify any difference in the percentage of dead cells between shOT cells and shY2 cells (Figure 19, grey bars, right y axis).

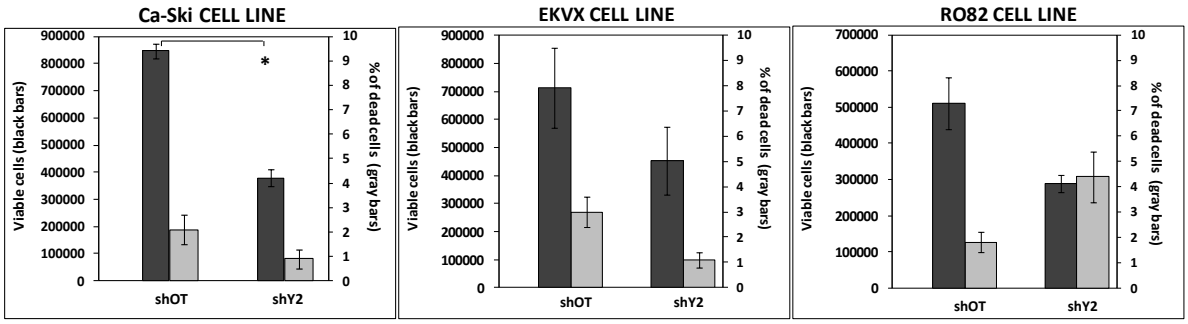

Figure 19. Evaluation of viable cells after YAP1 silencing. Cell counting and Trypan blue staining was performed on Ca-Ski, EKVX and RO82 cell lines silenced for YAP1 using stable YAP1 silencing system (shY2). The count of viable cells (left y axis) and the percentage of the dead cells (right y axis) were determined 72 hours after cells seeding. The values correspond to means of more than 3 samples from two independent experiments. The error bars denote the s.e.m. In Ca-Ski cell line unpaired t-test shOT versus shY2 p=0.0079, in EKVX cll line unpaired t-test shOT versus shY2 p=0.2977 and in RO82 cell line unpaired t-test shOT versus shY2 suggestive p= 0.0995.

6. YAP1 SILENCING INDUCES A MODERATE PERTURBATION OF THE CELL CYCLE

The DNA replication process and cell division can be described as a series of coordinated events that compose a cell cycle. Cell cycle machinery controls cell proliferation but cancer cells are characterized by an inappropriate cell proliferation. Therefore in these conditions, cells have alterations in the function or expression of the genes that control the cell cycle and display changes in normal cell progression (Malumbres and Carnero 2003).

In order to investigate whether YAP1 positively perturbs the cell cycle progression, I performed BrdU assay which quantified the percentage of cells in active S-phase as those incorporating BrdU in newly synthesized DNA during the BrdU pulse.

The assay was performed on Ca-Ski, EKVX and RO82 cell lines silenced using siRNA transient silencing system in order to avoid interferences between GFP and BrdU.

Upon BrdU pulse incorporation, I identified that YAP1 silencing induced a modest reduction of the proliferative cell compartment (cells in S phase of the cell cycle), which is statistically significant in RO82 cell line (Figure 20).

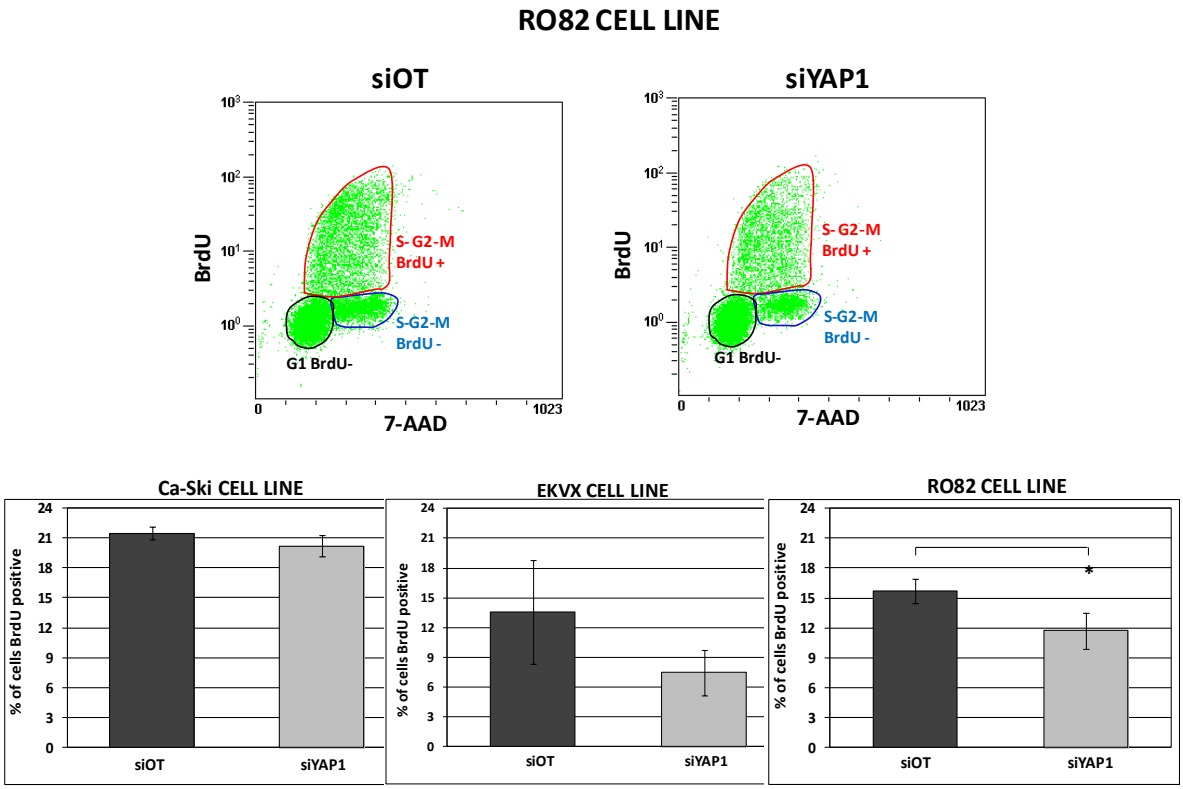

Figure 20. Evaluation of YAP1 silencing effect on cell cycle progression. BrdU assay was performed on Ca-Ski, EKVX and RO82 cell lines. Cells were pulsed with 1 or 2 hours of BrdU incorporation, depending of the cell line, washed and released for 1 additional hour in complete medium. The upper images show FACS analysis plots of siOT and siYAP1 RO82 cells where on the y axis are plotted the BrdU incorporation and on x axis the 7AAD (DNA content) staining. Based on the DNA contents and on the BrdU incorporation I divided the plot in 3 gates: G1 BrdU negative cells, S-G2-M BrdU negative cells and S-G2-M BrdU positive cells. The histograms summarized the results relative to BrdU positive cells in siOT and in siYAP1 cells. The values correspond to the percentage calculate on the means from three independent experiments. The error bars denote the s.e.m. In Ca-Ski cell line paired t-test siOT versus siYAP1 suggestive p= 0.0947, in EKVX cell line paired t-test siOT versus siYAP1 p=0.1875 and in RO82 cell line paired t-test siOT versus siYAP1 p=0.0215.

The p21 protein is implicated in the mechanisms of cell-cycle arrest, allowing DNA repair or apoptosis, upon DNA damage. In response to DNA damaging agents, the expression of p21 blocks the progression of the cell cycle at the G1/S transition by inhibiting the activity of Cdk2 and Cdk4/6 (Colozza et al. 2005).

Therefore I analyzed p21 protein expression level in Ca-Ski, EKVX and RO82 cell lines in YAP1 stably and transiently silenced cells and in control cells. I detected an increase of p21 protein level in YAP1 silenced cells compared to the off target cells in all YAP1-amplified cancer cell lines (Figure 21).

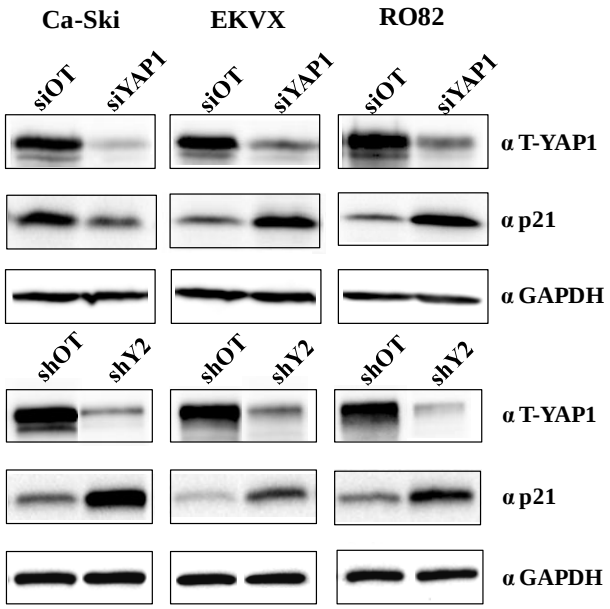

Figure 21. Evaluation of p21 protein expression level after YAP1 silencing. p21 protein expression level was analyzed by western blottig on Ca-Ski, EKVX and RO82 YAP1 silencing cells (siYAP1 and shY2) and off target cells (siOT and shOT). GAPDH was used as loading control.

These results regarding the BrdU incorporation and the p21 protein expression showed a moderate slowdown of the cell cycle progression in YAP1 silenced cells compared to control cells in all 11q22-amplified cancer cell lines.

7. YAP1 SILENCING STRONGLY REDUCES COLONY NUMBER IN ANCORAGE-INDEPENDENT GROWTH

Normal cells typically are not able to grow and form cell colonies in semisolid media because under these conditions undergo anoikis-mediated cell death. In contrast, cancer cells acquire the capability to grow without anchorage-dependence to the substrate, within a semi-solid medium such as agar (Guadamillas et al. 2011).

In order to evaluate whether YAP1 positively affected the anchorage independent growth I performed the soft agar assay in Ca-Ski, EKVX and RO82 cell lines, comparing the number of colonies grown in off target cells and in YAP1 stably silenced cells.

I detected that YAP1 silencing induced a strong and significant reduction in the number and size of colonies counted in all three cell lines analyzed, compared to the control cells (Figure 22).

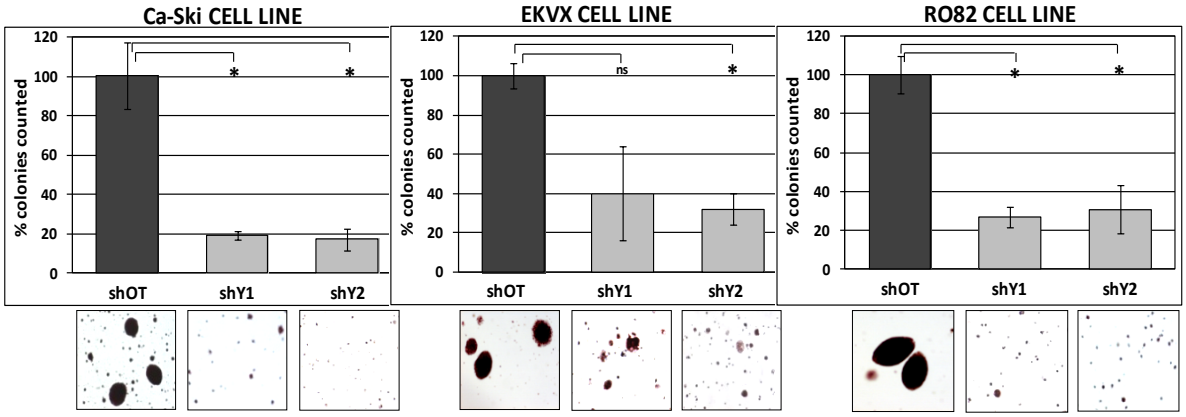

Figure 22. Evaluation of anchorage-independent growth after YAP1 silencing. Soft agar assay was performed on Ca-Ski, EKVX and RO82 cell lines silenced for YAP1 using stable silencing system. Colonies were counted from 60 mm dishes and one randomly chosen field was photographed (10x magnification). The values correspond to the percentage calculate on the means from three independent experiments. The error bars denote the s.e.m. In Ca-Ski cell line unpaired t-test shOT versus shY1 p=0.0091, shOT versus shY2 p=0.0095, in EKVX cell line unpaired t-test shOT versus shY1 p=0.1357, shOT versus shY2 p=0.0216 and in RO82 cell line unpaired t-test shOT versus shY1 p=0.0027, shOT versus shY2 p=0.0116.

8. YAP1 SILENCING REDUCES *IN VIVO* TUMORIGENIC POTENTIAL

In vivo cell expansion, following subcutaneous injection into nude mice, is a peculiar feature of cancer cell lines but not of normal differentiated cells (Cespedes et al. 2006). Although typically the anchorage-independent growth in soft agar assay correlates with *in vivo* tumorigenic capability, I felt it was important to directly verify in at least one cell line whether YAP1 supports the *in vivo* tumor growth, a crucial phenotype which is strongly associated with tumorigenic potential.

Therefore, I performed a subcutaneous injection of Ca-Ski sh-off target cells and of Ca-Ski sh-YAP1 stably silenced cells in both flanks of nude mice and I measured the tumors' growth at constant intervals (3 replicate experiments, 4 mice/condition, 36 mice in total).

A significant reduction in tumor volume was induced by YAP1 silencing. The effect detected was more evident in mice treated with shY2 cells (which silenced YAP1 protein more efficiently in biochemical assays) compared to shY1 cells (Figure 23).

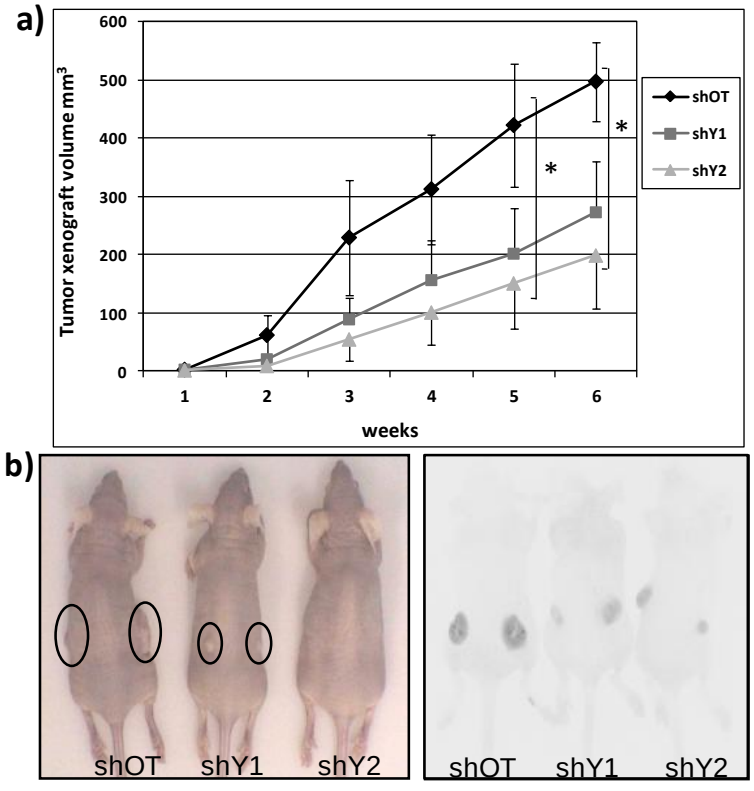

Figure 23. Evaluation of tumorigenicity in *in vivo* models after YAP1 silencing. a) Ca-Ski cell line control cells (shOT) and YAP1 silenced cells (shY1 and shY2) were injected in both flanks of nude mice. Tumors growth was monitored for 6 weeks after cells injection. The values correspond to means from three independent experiments. The error bars denote the s.e.m. In Ca-Ski cell line two-way ANOVA shOT versus shY2 $p \leq 0.05$. **b)** A representative picture (left) and GFP luminescence (right) of tumors grown in mice 6 weeks after cells injection.

9. YAP1 SILENCING PARTIALLY REDUCES SPHERE-FORMING CAPACITY

I performed sphere forming assay, which is based on the evaluation of the growth capacity of non-adherent multicellular aggregates (spheres) in the presence of growth factors and in the absence of serum. Usually, only normal cells that retain stemness/progenitor features, but not differentiated cells, are capable to grow in serum-free conditions and this assay is considered a surrogate *in vitro* marker of stemness/self-renewal capacity. Cancer cells often retain/acquire stemness features, at least in a subpopulation of cells that sustain tumor replenishment over time and, in particular, literature data suggest that the Hippo pathway may also be involved in the stem cell regulation (Lian et al. 2010). Therefore, I investigated this phenotype in Ca-Ski and EKVX cell lines. In fact, preliminary experiments performed on parental cell lines highlighted that RO82 was not able to form spheres in non-adherent cell conditions.

YAP1 silencing induces a reduction in the number of spheres counted both in Caski and in EKVX cell lines and the effect is more evident in Ca-Ski cell line (Figure 24).

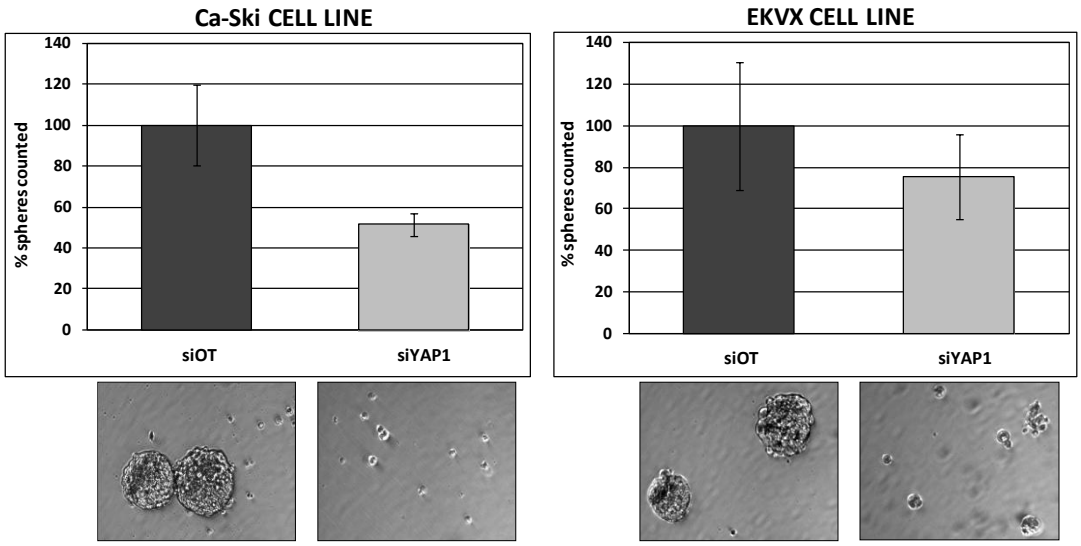

Figure 24. Sphere-forming ability after YAP1 silencing. Sphere-forming assay was performed on Ca-Ski and EKVX cell lines. Spheres growth was assessed using non adherent 6-well plates. Pictures were taken from a randomly chosen field (10x magnification). The values correspond to the percentage calculate on the means from three independent experiments. The error bars denote the s.e.m. In Ca-Ski cell line unpaired t-test siOT versus siYAP1 suggestive p= 0.0526 and in EKVX cell line unpaired t-test siOT versus siYAP1 p= 0.6435.

10. YAP1 SILENCING AFFECTS CELL MIGRATION IN Ca-Ski AND RO82 CELL LINES

Cell migration exerts an important role in the progression of various diseases including cancer. Active migration of tumor cells is a prerequisite for tumor cell invasion and for metastasis development (Yamaguchi et al. 2005). At this regard I performed wound healing assay, chemotaxis experiments and tracking experiments using video time-lapse microscopy on Ca-Ski, EKVX and RO82 cell lines, to establish whether YAP1 expression could sustain cell migration.

I initially performed these experiments on parental cell lines to assess and optimize the migration process in Ca-Ski and RO82 cellular model. EKVX cell line was not suitable for wound healing assay due to its migration inability.

I then performed wound healing assay in cell lines silenced for YAP1, using both shRNA and siRNA silencing systems. In Ca-Ski cell line the wound closed so rapidly (24 hours) that it was difficult to appreciate any significant difference after YAP1 silencing (Figure 21). In RO82 cell line it was evident that the wound healed more rapidly in control cells compared to YAP1 silenced cells, suggesting that the cell motility in YAP1 silenced cells is reduced with respect to the control cell condition (Figure 25).
Same results were obtained using either siRNA or shRNA cells for silencing YAP1.

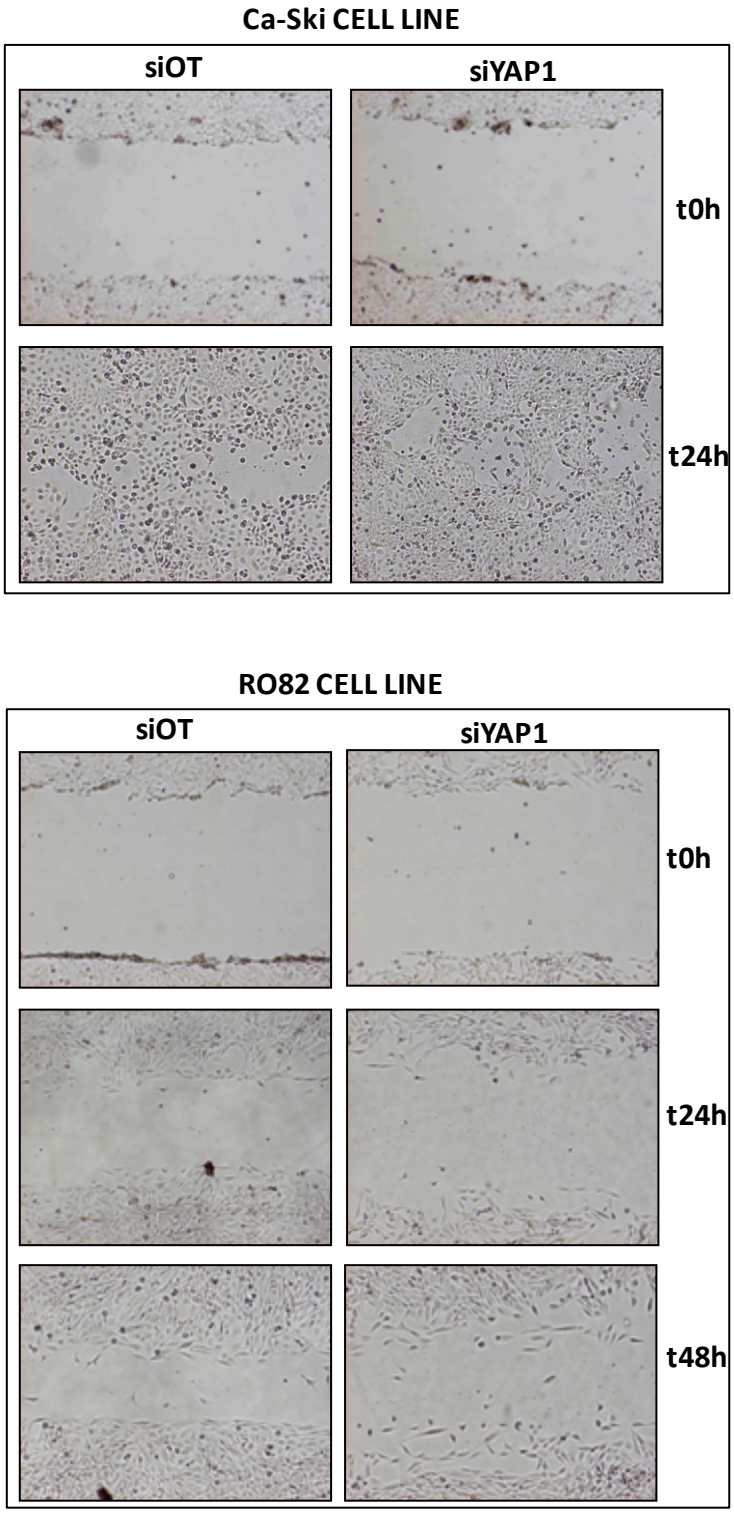

Figure 25. Evaluation of the effect of wound healing assay after YAP1 silencing. Wound healing assay was performed on Ca-Ski and RO82 cell lines depleted for YAP1 using either siRNA and shRNA silencing systems. The pictures show representative results obtained using siRNA cells (siOT and siYAP1). T0 represents the cells 24 hours post-transfection (10x magnification).

To further clarify the effect of YAP1 on cell migration I performed the chemotaxis experiments using the transwell chamber system. Chemotaxis studies the cell migration based on a particular chemical signal, such as the serum, as attractant. I detected both in Ca-Ski and in RO82 cell lines a significant reduction of cells migrated into the serum-containing lower chamber in siYAP1 cell condition compared to the control cells (Figure 26).

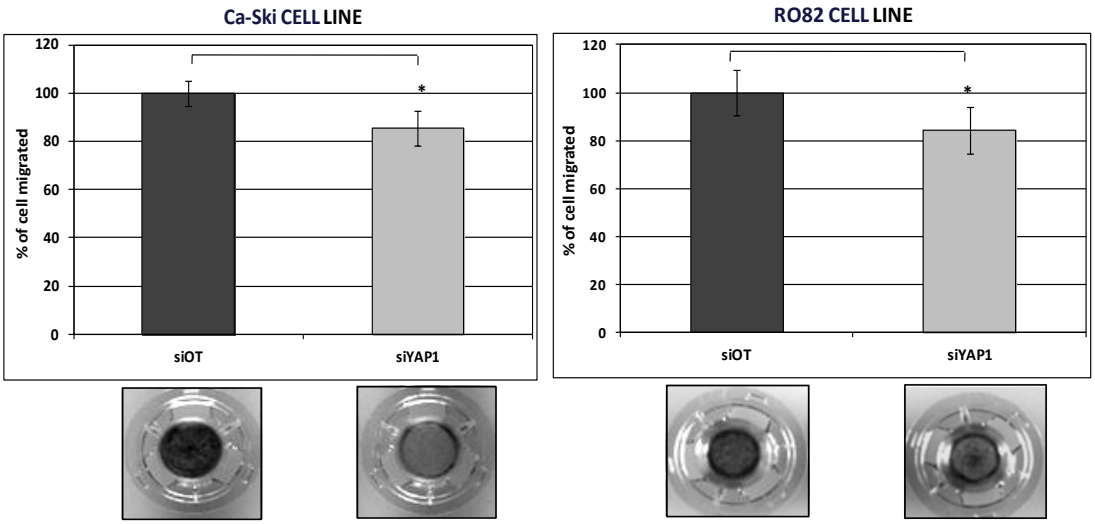

Figure 26. Evaluation of chemotaxis after YAP1 silencing. Chemotaxis experiment was performed on Ca-Ski and RO82 siOT and siYAP1 cells. The pictures show the cells migrated in low chamber of transwell stained with crystal violet. The values correspond to the means from three independent experiments. The error bars denote the s.e.m. In Ca-Ski cell line paired t-test siOT versus siYAP1 p=0.0487, in RO82 cell line paired t-test siOT versus siYAP1 p=0.0287.

In addition, to further investigate how migration activity could be affected by modulation of YAP1 expression and in order to obtain more quantitative measurements, video time-lapse microscopy (coupled with humidified, CO_2 controlled incubator) was performed on the above described cell lines. The cell movement lasts usually a few micrometers/minute and time-lapse at regular time intervals over several hours allows cell tracking to measure the distance covered by the cells within a time frame.

Tracking analysis experiments then allowed me to determine the distance covered by the cells recorded. In particular I evaluated the cell motility for 12 hours. In both cell lines YAP1 silenced cells showed a moderate reduction of the distance covered in 12 hours of observation, compared to the control cells (Figure 27).

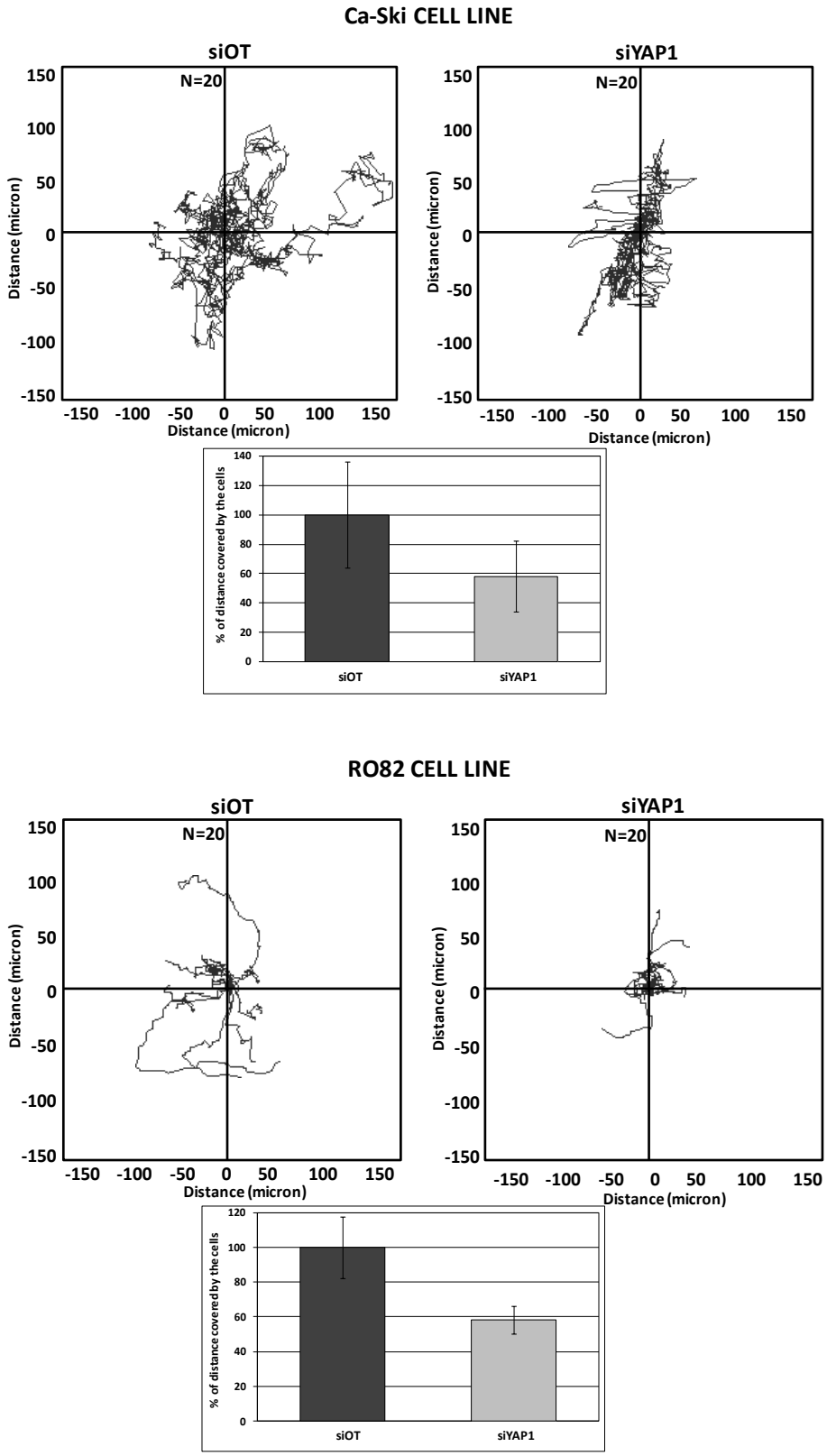

Figure 27. Evaluation of the distance covered by the cells after YAP1 silencing. Tracking experiment using time-lapse microscopy was performed on Ca-Ski and RO82 cells transfected with siRNA (siOT and siYAP1). The graphs show the distance covered by 20 cells (micron) for 12 hours. The values in the histograms correspond to the percentage calculate on the means from three independent experiments. The error bars denote the s.e.m. In Ca-Ski cell line paired t-test siOT versus siYAP1 suggestive p= 0.0648 and in RO82 cell line paired t-test siOT versus siYAP1 p= 0.1896.

11. YAP1 SILENCING INCREASES DNA DAMAGE RESPONSE IN Ca-Ski CELL LINE

The effect of the endogenous YAP1 silencing was also evaluated in response to pharmacological genotoxic treatment with cisplatin.

In Ca-Ski cell line I detected that YAP1 stable silencing induced a more prominent reduction of cell proliferation in response to cisplatin compared to the off target cells, suggesting that YAP1 silenced cells are more sensitive to the treatment compared to control cells (Figure 28).

On the contrary, in EKVX and RO82 cell lines I did not detect any difference in sensitivity to cisplatin between off target cells and YAP1 silenced cells.

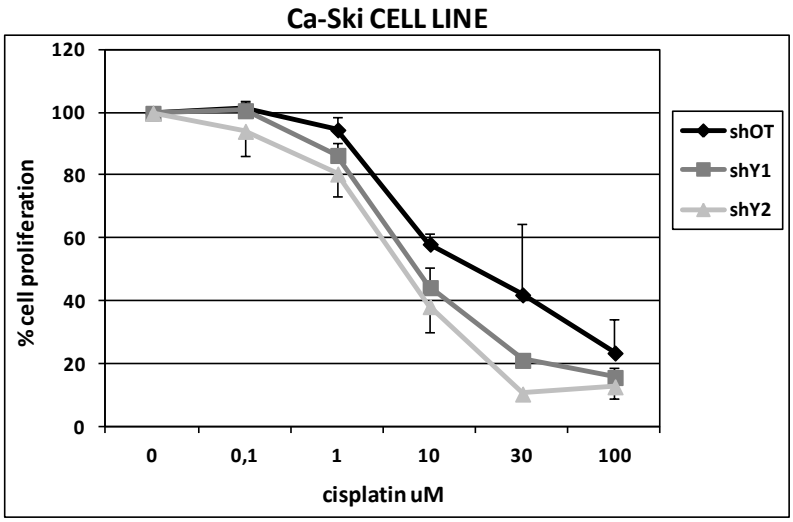

	shOT	shY1	shY2
IC50 (uM)	10.3	5.8	4.6
95% CI	6.1 to 17.4	4.4 to7.5	2.8 to 7.5

Figure 28. Evaluation of cisplatin response after YAP1 silencing. Percentage of cell proliferation in Ca-Ski off target cells and YAP1-silenced cells after cisplatin treatment. Cells were treated with 0.1, 1, 10, 30 and 100 uM of cisplatin and for each dose the reduction of cell proliferation was determined. The values correspond to means from two independent experiments. The error bars denote the s.e.m. The table below shows the values of IC50 and the 95% confidence interval of shOT, shY1 and shY2 cells.

Since cisplatin is known to induce apoptosis in addition to reduce cell proliferation, I investigated if the observed differences in response to cisplatin correlated with differences in apoptotic response after cisplatin treatment in YAP1 silenced and control Ca-Ski cells, using flow cytometry.

Following cisplatin treatment, I detected a statistically significant increase in annexin V and 7AAD positivity in YAP1 silenced cells compared to the off target cells and consequently the evidence that DNA damage induced a more prominent reduction of viability after YAP1 silencing in Ca-Ski cell line (Figure 29).

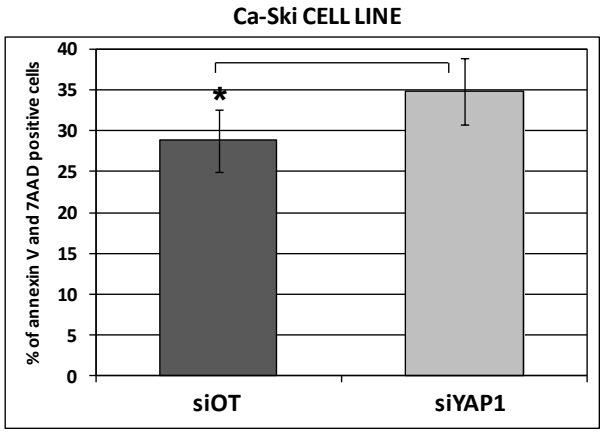

Figure 29. Evaluation of annexin V and 7AAD positivity in YAP1 silenced cells. Flow cytometer analysis was performed on Ca-Ski off target cells and YAP1 silenced cells with siRNA silencing cell system. Percentage of single or double annexin V and 7AAD positivity cells after cisplatin treatment with 100uM overnight. The values correspond to the percentage calculate on the means from three independent experiments. The error bars denote the s.e.m. Paired t-test siOT versus siYAP1 p=0.0107.

Moreover, I investigated in Ca-Ski cell line the activation of PARP and of caspases, which are essential mediators of the apoptosis process. I analyzed the initiator caspase 8, the effector caspase 3 and PARP protein levels and I detected the same activation level both in siOT and in siYAP1 cells after DNA damage (Figure 30). Therefore, under the experimental conditions tested, the greater sensitivity to cisplatin that I detected in YAP1 silenced cells compared to the control cells is not associated with increased in caspases activation (Figure 30).

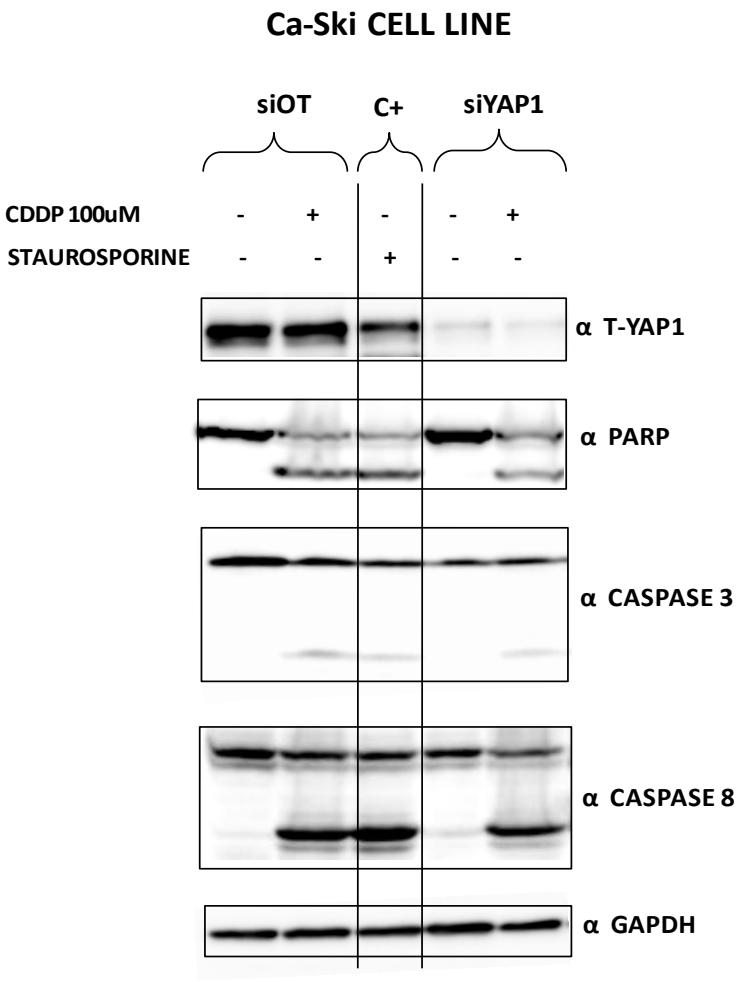

Figure 30. Evaluation of caspases and PARP protein levels after YAP1 silencing. Caspase 3, caspase 8 and PARP protein levels were analyzed by western blotting analysis in Ca-Ski siOT and siYAP1 cells after treatment with cisplatin 100 uM for 16 hours. The treatment with Staurosporine 1mM for 16 hours in siOT cells was used as positive control. GAPDH was used as loading control.

12. IDENTIFICATION OF TARGET GENES REGULATED BY YAP1 GENE IN 11q22-AMPLIFIED CANCER CELL LINES

Literature data report that YAP1 gene is a transcriptional cofactor (Yagi et al. 1999) but YAP1 target genes remain poorly characterized and therefore we performed gene expression profiling experiments with the aim to identify YAP1 target genes that may mediate an oncogenic stimulus in YAP1-amplified cell lines.

As described in the flowchart of Figure 31, YAP1 gene was silenced using short-term system, the RNA was extracted from siOT and siYAP1 cells at different times points and used in experiments of global gene expression analysis (Figure 31).

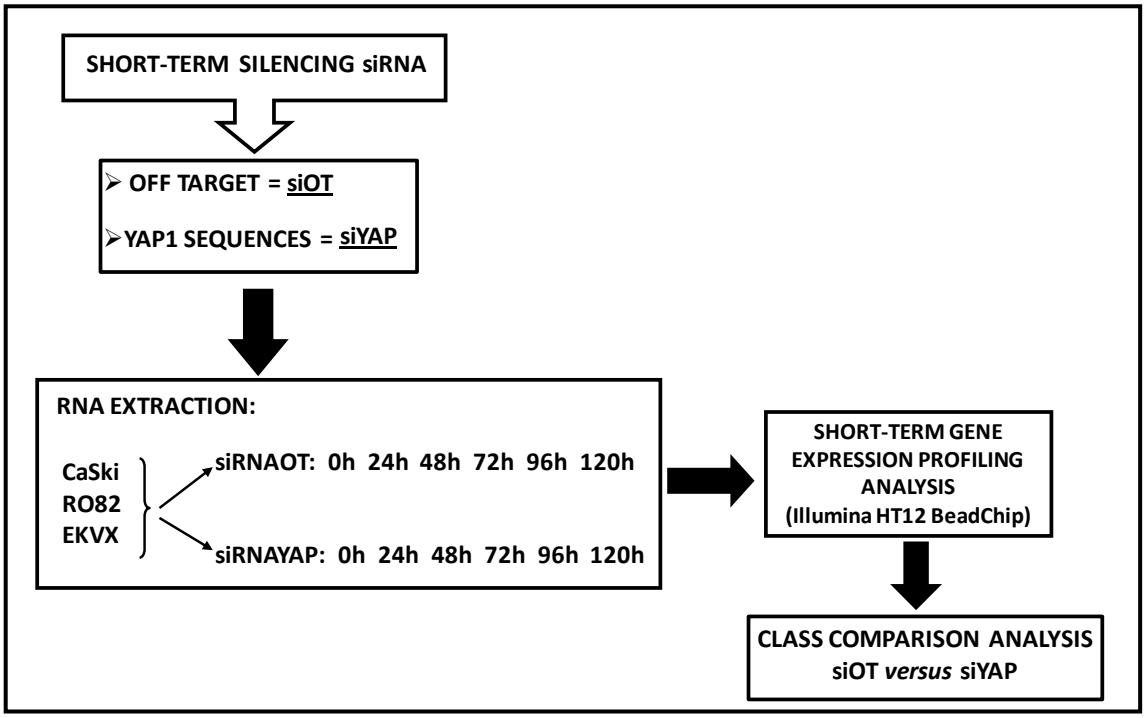

Figure 31. Flowchart of the gene expression profiling experiment.

Class comparison analyses comparing YAP1 proficient cells versus YAP1-silenced cells identified 707 statistically significantly modulated genes (p-value=0.002). Among these genes, 505 are down-regulated and 202 are up-regulated, thus suggesting that YAP1 is a transcriptional co-activator (Chi square p value < 0.0001), since such modulation of target genes occurs after YAP1 silencing.

Using different databases of functional annotation, I found that the 707 genes identified are significantly enriched for multiple gene ontologies related to cell proliferation and to cell movement molecular functions (Figure 33, left panel).

We next asked which genes, among the 707 differentially expressed, and ontologies were specifically regulated in the YAP1–amplified cancer cell lines analyzed. We therefore compared our YAP1-gene signature with 2 studies from the literature reporting gene expression profiling in normal cellular contexts in which YAP1 gene is overexpressed (Dong et al. 2007; Zhao et al. 2007). Among the 427 genes that could be compared across the three studies, I found that 86 genes out of 88 common genes are concordantly (up- or down-) co-regulated in our study and in at least one study from the literature (9/9 genes concordantly regulated in all analyses) (Figure 32). Indeed, these genes represent YAP1 targets modulated in multiple different normal and tumor cell contexts. Additional 339 genes are uniquely modulated in the 11q22-amplified cancer cell lines (Figure 32).

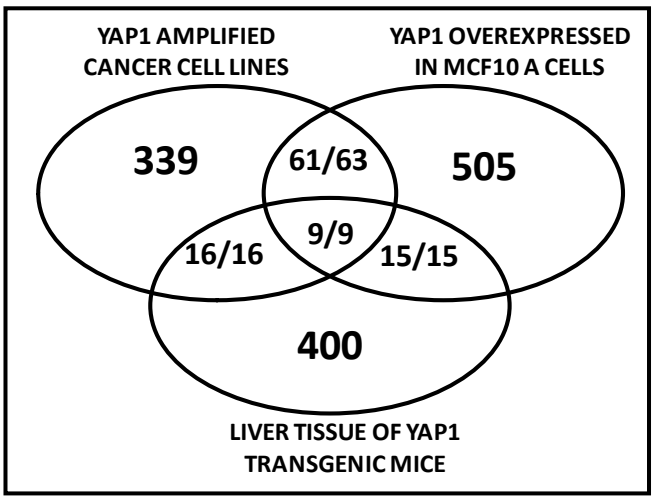

Figure 32. Comparison between target genes identified in YAP1 amplified cancer cell lines and in normal cells in which YAP1 gene is overexpressed. Number of unique and common target genes identified in YAP1 amplified cell lines and normal cellular contexts in which YAP1 gene is overexpressed. The fraction numerators indicate the number of genes which are concordantly co-regulated in the studies.

I functionally annotated the filtered 339 gene-list using Ingenuity functional annotation tool, revealing that they were mainly annotated for cell proliferation and for cell movement ontologies (Figure 33), similar to the global 707 gene-list. These results suggest that YAP1 amplification causes mainly a perturbation of "YAP1 wild-type" expression program, instead of the creation of an aberrant, ex-novo transcriptional program.

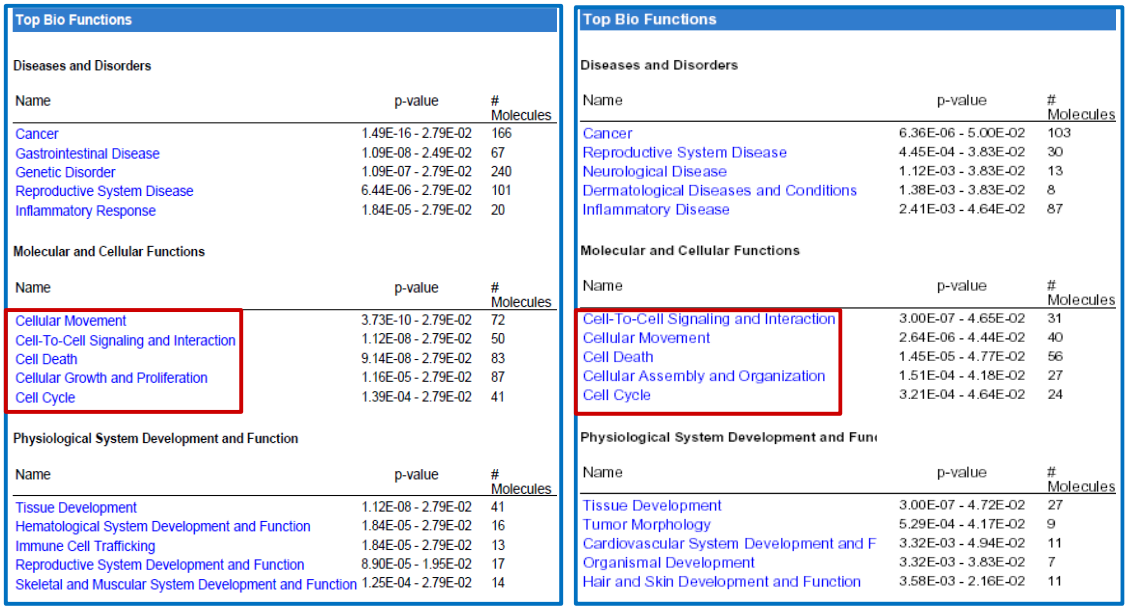

Top Bio Functions

Diseases and Disorders

Name	p-value	# Molecules
Cancer	1.49E-16 - 2.79E-02	166
Gastrointestinal Disease	1.09E-08 - 2.49E-02	67
Genetic Disorder	1.09E-07 - 2.79E-02	240
Reproductive System Disease	6.44E-06 - 2.79E-02	101
Inflammatory Response	1.84E-05 - 2.79E-02	20

Molecular and Cellular Functions

Name	p-value	# Molecules
Cellular Movement	3.73E-10 - 2.79E-02	72
Cell-To-Cell Signaling and Interaction	1.12E-08 - 2.79E-02	50
Cell Death	9.14E-08 - 2.79E-02	83
Cellular Growth and Proliferation	1.16E-05 - 2.79E-02	87
Cell Cycle	1.39E-04 - 2.79E-02	41

Physiological System Development and Function

Name	p-value	# Molecules
Tissue Development	1.12E-08 - 2.79E-02	41
Hematological System Development and Function	1.84E-05 - 2.79E-02	16
Immune Cell Trafficking	1.84E-05 - 2.79E-02	13
Reproductive System Development and Function	8.90E-05 - 1.95E-02	17
Skeletal and Muscular System Development and Function	1.25E-04 - 2.79E-02	14

Top Bio Functions

Diseases and Disorders

Name	p-value	# Molecules
Cancer	6.36E-06 - 5.00E-02	103
Reproductive System Disease	4.45E-04 - 3.83E-02	30
Neurological Disease	1.12E-03 - 3.83E-02	13
Dermatological Diseases and Conditions	1.38E-03 - 3.83E-02	8
Inflammatory Disease	2.41E-03 - 4.64E-02	87

Molecular and Cellular Functions

Name	p-value	# Molecules
Cell-To-Cell Signaling and Interaction	3.00E-07 - 4.65E-02	31
Cellular Movement	2.64E-06 - 4.44E-02	40
Cell Death	1.45E-05 - 4.77E-02	56
Cellular Assembly and Organization	1.51E-04 - 4.18E-02	27
Cell Cycle	3.21E-04 - 4.64E-02	24

Physiological System Development and Fun

Name	p-value	# Molecules
Tissue Development	3.00E-07 - 4.72E-02	27
Tumor Morphology	5.29E-04 - 4.17E-02	9
Cardiovascular System Development and F	3.32E-03 - 4.94E-02	11
Organismal Development	3.32E-03 - 3.83E-02	7
Hair and Skin Development and Function	3.58E-03 - 2.16E-02	11

Figure 33. Schematic of target genes annotation with Ingenuity tool. The molecular and cellular function related to the 707 statistically significantly modulated genes identified (left panel) and of the 339 genes which are specific for 11q22 amplified cancer cell lines (right panel).

Interestingly, I found that 5 of the genes identified as target of YAP1 are components of Hippo pathway (*STK3* (also known as *Mst2*), *STK4* (also known as *Mst1*), *LATS2*, *NF2* and *TEAD2*). *TEAD2* was upregulated following YAP1 silencing, while the other genes resulted down-regulated.

Considering that Hippo pathway is a cascade of phosphorylation events which inhibits YAP1, we can hypothesize that YAP1 downregulation mimics an over-activation of Hippo pathway (Figure 34).

Therefore, the observed down-regulation of the upstream -YAP1-inhibitory- components (*LATS2*, *NF2*, *STK3*, *STK4*) is consistent with the attempt to inactivate Hippo pathway and to release YAP1 inhibition. Concordantly, since TEAD2 is a Hippo downstream component which represents a transcription factor that promotes the expression of the YAP1 target genes, the observed up-regulation of TEAD2 after YAP1 silencing appears to counterbalance the siRNA-induced YAP1 deficiency.

Therefore, it seems that in YAP1-amplified cancer cell lines the transient YAP1 downregulation, by mimicking an over-activation of Hippo pathway, induces a feedback loop function on Hippo pathway components that tends to counterbalance the YAP1 silencing (Figure 34).

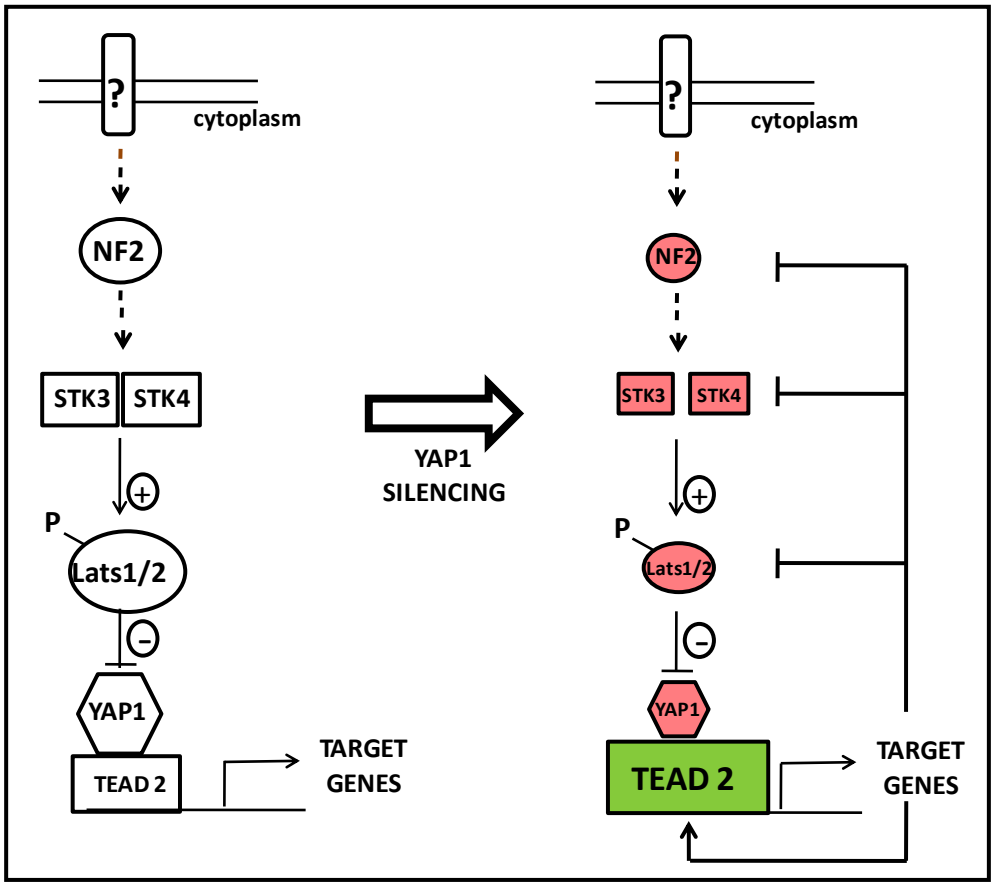

Figure 34. Schematic rapresentation of Hippo pathway components regulation following YAP1 silencing. The diagram highlights Hippo pathway components that resulted to be the target genes (down-regulated in red and up-regulated in green) following YAP1 silencing in cancer cell lines carrying YAP1 amplification.

I next performed the validation of individual YAP1 target genes identified by gene expression analysis using qPCR on independent silencing experiments. As an internal control, I also analyzed the modulation of *CTGF* gene (Bradham et al. 1991), one of the few known YAP1 target genes. I selected genes involved in the molecular ontologies whose expression was significantly perturbed by YAP1 silencing, including a group of genes involved in cell cycle regulation (*CCNA2*, *CCNG1*, *CDK2*, *SKP2*) (Aleem et al. 2004; Bates et al. 1996; Demetrick et al. 1996; Pagano et al. 1992; Tsai et al. 1991); the *ITGA5*

(Virtanen et al. 1990) and *NRG1* genes involved in cell-cell interaction; the genes *LATS2, NF2, STK3, STK4* and *TEAD2*, which are components of the Hippo pathway (Avruch et al. 2012); *GADD45A* gene which is involved in DNA repair (Hollander et al. 1993); *VEGFA* gene involved in angiogenesis (Mattei et al. 1996) and *ETS1* which is a transcription factor that acts as an oncogene via multiple pathways (Dittmer 2003) (Table 9).

Table 9. Genes significantly modulated by microarray experiment and then validated by qPCR.

GENE SYMBOL	ANNOTATION	EFFECT OF YAP1 SILENCING
CTGF	known YAP1 target gene	down
CCNA2	cell cycle regulation	down
CCNG1	cell cycle regulation	down
CDK2	cell cycle regulation	down
SKP2	cell cycle regulation	down
LATS2	hippo pathway component	down
NF2	hippo pathway component	down
STK3	hippo pathway component	down
STK4	hippo pathway component	down
TEAD2	hippo pathway component	up
GADD45A	DNA damage repair	down
ITGA5	cell-cell interaction	up
NRG1	cell-cell interaction	down
VEGFA	angiogenesis	up
ETS1	transcription factor	down

The analysis of the modulation of YAP1 target genes was performed after YAP1 short-term silencing in Ca-Ski, EKVX and RO82 cell lines, using siOT cells as the calibrator sample. In each cell line the mRNA was analyzed 72 hours after transfection when the expression level of the YAP1 protein is usually at its lowest.

In Ca-Ski cell line, 13 of 16 genes are modulated in agreement with the microarray data and in 13 genes the modulation results to be statistically significant (Figure 35).

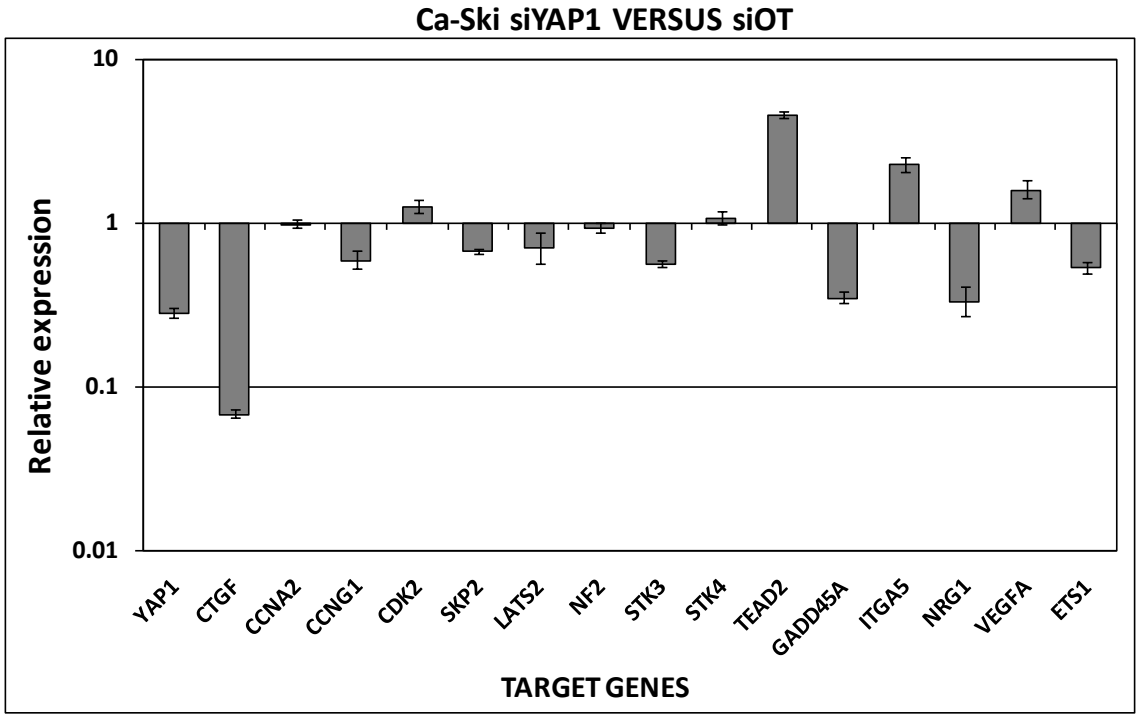

Figure 35. Relative expression of YAP1 target genes in Ca-Ski cell line after YAP1 silencing. qPCR analysis shown the modulation of YAP1 target genes after YAP1 silencing using siRNA. siRNA off target was used as a calibrator.

In EKVX cell line 13 of 16 genes are modulated in agreement with the microarray data and in 14 genes the modulation results to be statistically significant (Figure 36).

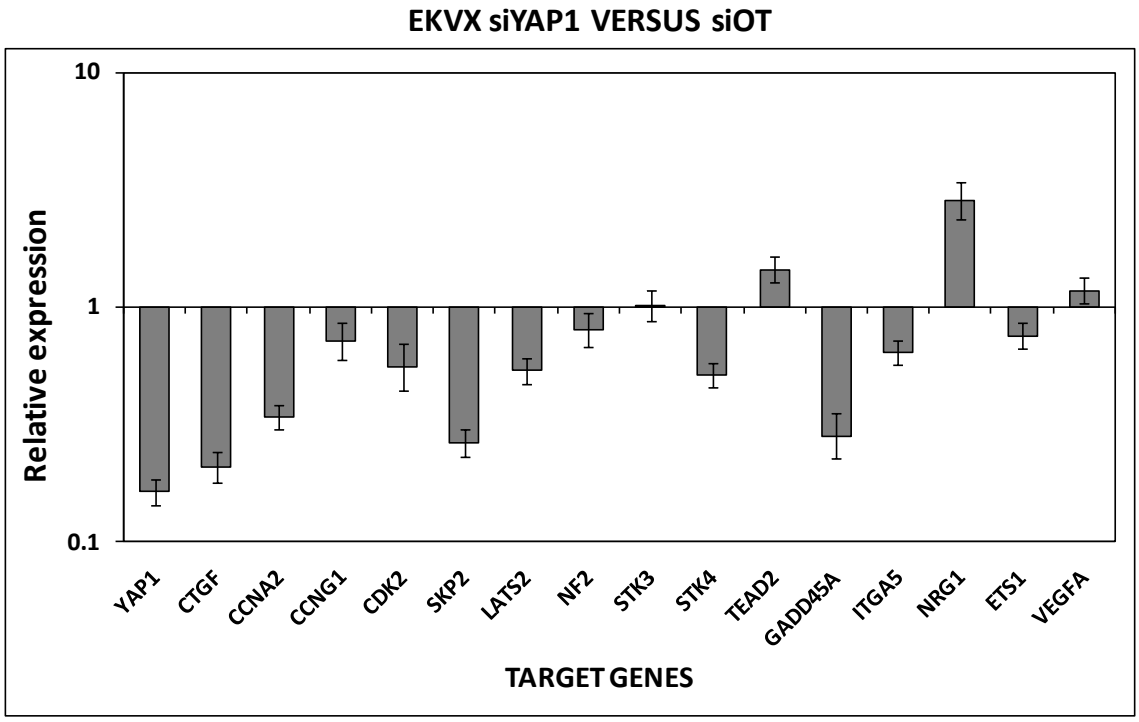

Figure 36. Relative expression of YAP1 target genes in EKVX cell line after YAP1 silencing. qPCR analysis shown the modulation of YAP1 target genes after YAP1 silencing using siRNA. siRNA off target was used as a calibrator.

In RO82 cell line 12 of 16 genes are modulated in agreement with the microarray data and in 10 genes the modulation results to be statistically significant (Figure 37).

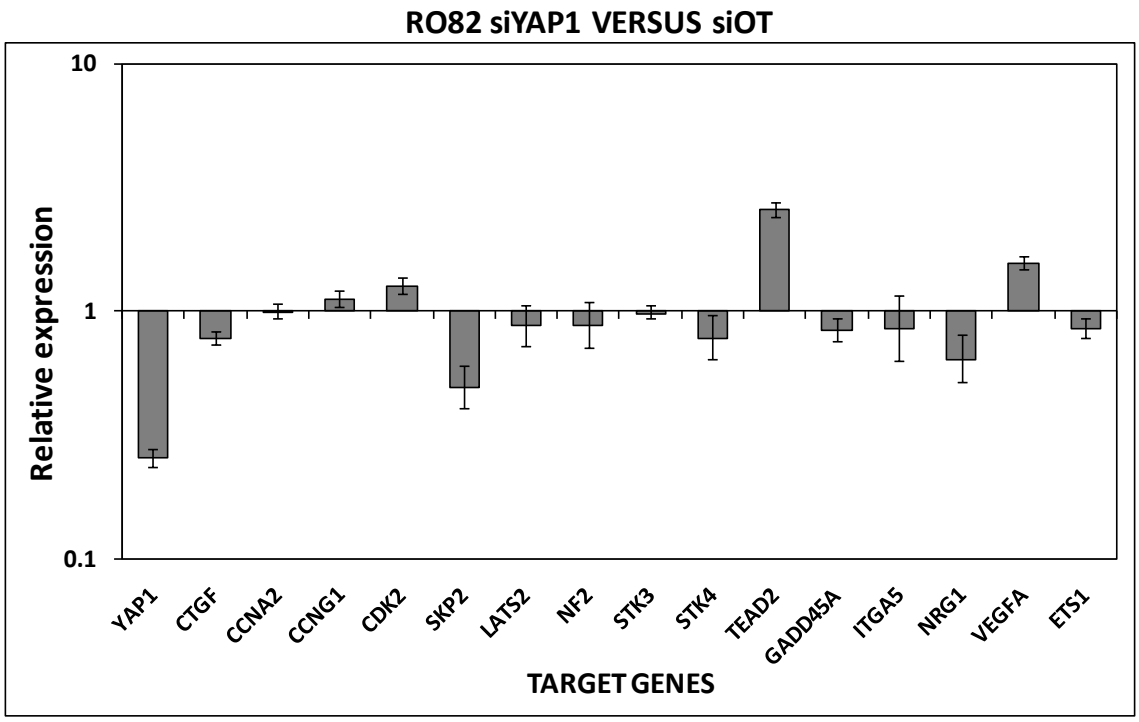

Figure 37. Relative expression of YAP1 target genes in RO82 cell line after YAP1 silencing. qPCR analysis shown the modulation of YAP1 target genes after YAP1 silencing using siRNA. siRNA off target was used as a calibrator.

Therefore, the validation experiments of YAP1 target genes using qPCR confirmed that the majority of genes are modulated in agreement with microarray data in all the cell lines analyzed.

DISCUSSION

1. IS YAP1 AN ONCOGENE OR A TUMOR SUPPRESSOR GENE?

Central to our understanding is the definition of the role of YAP1 in 11q22-amplified cancer cell lines. Here I demonstrate that YAP1 plays an important role in the tumorigenic phenotype, as it effectively supports multiple transformed properties in 11q22-amplified cancer cell lines.

In my experiments I exploited RNA interference strategies to silence YAP1 and compared YAP1 silenced cells and control cells from three cell lines (Ca-Ski, EKVX and RO82) that carried 11q22 copy number amplification and YAP1 overexpression. In fact, YAP1 silencing induced a moderate reduction of proliferation and a strong and significant reduction of anchorage independent growth in all three cell lines. Nevertheless, parental cell lines demonstrated a different expression of additional cellular phenotypes investigated, such as migration capacity, and were therefore affected differently by YAP1 silencing. The reason can be attributed to the different lineage and (epi)-genetic background of the individual cell lines. In addition, I cannot exclude a differential contribution of the multiple YAP1 isoforms expressed in individual cell lines, which may regulate at least partially different phenotypes.

Recent evidences have already described YAP1 as driving oncogenesis. In fact, YAP1 is amplified in human hepatocellular cancer and cooperates with *myc* oncogene to induce tumor growth in nude mice (Zender et al. 2006). In non transformed MCF10A mammary cells YAP1 ectopic overexpression induces alterations characteristic of transforming phenotypes (Overholtzer et al. 2006). In addition, it has been reported in transgenic mice model systems that the liver-specific YAP1 overexpession induced a dramatic increase of liver organ size eventually leading to cancer development (Camargo et al. 2007; Dong et al. 2007). Moreover, recent data indicated that YAP1 activity correlates with high histological grade and metastasis in breast cancer (Cordenonsi et al. 2011).

Noteworthy, on the contrary several studies described a proapoptotic function of YAP1. In fact, after DNA damage, YAP1 functions as a crucial co-activator of TP73-mediated apoptosis in TP53 null cells (Strano et al. 2001; Strano et al. 2005), after phosphorylation of YAP1 at tyrosine 357 (Levy et al. 2008), following YAP1 dissociates to Akt that induced its translocation from cytoplasm to the nucleus (Basu et al. 2003), as well

as a result of RASSF1A activation (Matallanas et al. 2007). Then, it was described the existence of the pro-apoptotic autoregulatory feedback loop between TP73, YAP1 and the promyelocytic leukemia (PML) tumor suppressor gene (Lapi et al. 2008). YAP1 was also proposed to be a tumor suppressor in breast cancer (Yuan et al. 2008), which is in seeming discrepancy with data from Cordenonsi and co-workers (Cordenonsi et al, 2011).

Based on these evidences I can speculate that YAP1 gene may act as oncogene or oncosuppressor according to the target cells in which it is deregulated and/or the cellular context (mutational load, stage of pathology). Literature data have already reported evidences on genes which exert both oncogene-like and tumor suppressor-like functions in different systems. It is well established that multiple cellular proto-oncogenes (such as c-*Myc, Ras, E2F*, *c-Jun* or *c-Fos*) may either promote cell proliferation or trigger oncogene-induced apoptosis or senescence if overexpressed in a normal cell context. This latter effect represents a safe-guard mechanism to prevent the consequences of aberrantly sustained oncogenic signaling. Therefore, in order to proliferate aberrantly and avoid oncogene-induced apoptosis, cancer cells need to accumulate multiple genetic defects that override these safe-guard mechanisms (Hermeking and Eick 1994; Lowe and Ruley 1993; Lowe et al. 1994; Serrano et al. 1997). The *E-cadherin* is a tumor suppressor gene in epithelial cells and its loss is detected in many carcinomas. Nonetheless, recent evidences reported that the re-expression of E-cadherin in such tumor cells is associated with an increased tumorigenesis and correlates with increased proliferation and invasiveness in a subset of high-grade gliomas (Lewis-Tuffin et al. 2010). Also *p21*, which acts as an established tumor suppressor gene, has been recently reported to act as an oncogene. In mouse models the elimination of p21 in TP53-deficient mice resulted in a substantially longer survival of TP53-null and TP53-haploinsufficient mice due to decrease of thymic lymphomas incidence (De la Cueva et al. 2006). On the other hand, the human gene *Ptpn11*, which encodes the tyrosine phospatase Shp2, may act as a proto-oncogene and inherited and somatic activating mutations have been detected in several types of leukemia but recent evidences suggest a tumor suppressor effect of Ptpn11/Shp2 in hepatocellular carcinogenesis (Bard-Chapeau et al. 2011). Also Notch signaling exerts a dual role in cancer, as it acts as a proto-oncogene in lymphocytes and mammary tissue while it exerts a potent tumor suppressive function in some solid and hematological tumors including hepatocellular carcinoma, chronic myelomonocytic leukemia, head and neck squamous cell carcinomas and skin (Lobry et al. 2011).

2. IS YAP1 AMPLIFICATION A SUBSTANTIAL EVENT IN HUMAN TUMOR SAMPLES?

Several studies reported that the 11q22 locus is amplified in human tumor samples (see Table 5, Introduction). The majority of the data published until now detected 11q22 amplification in different tumor types without directly investigating the YAP1 copy alteration. To fill this gap, in my PhD thesis I provided direct evidence of YAP1 copy amplification in 3-23% of samples from multiple tumor types, providing compelling evidence that it represents a cancer associated alteration in a fraction of multiple tumor types.

In particular, I detected YAP1 copy amplification in 4/21 (19%) advanced cervical cancer samples. Several literature data studied 11q22 copy number amplification in cervical cancer samples (Choschzick et al. 2012; Imoto et al. 2002; Scotto et al. 2008). In Scotto study the authors found 11q22 copy amplification predominantly in samples in advanced stage of the pathology. These evidences, together with my data on the direct YAP1 copy amplification, support that YAP1 is the target of the amplification at 11q22 locus in cervical carcinoma. Whether YAP1 copy amplification event represents a marker of cervical cancer progression and prognosis remains an intriguing but unexplored issue.

3. IS YAP1 THE UNIQUE ONCOGENIC TARGET GENE IN 11q22 AMPLIFICATION EVENTS?

Genes mapping within amplicons are considered as candidate oncogenes. Amplification is an important mechanism for gene copy number gain, for protein overexpression and sustained oncogene activation in tumor cells. Most amplification events include a relatively large region of DNA that contains several genes that can be considered possible targets of the amplification event. In my PhD thesis, I strongly demonstrated that YAP1 represents an oncogenic target of 11q22-restricted amplification events.

The 11q22 amplicons from the cancer cell lines under study include, in addition to YAP1, several genes which could be considered as possible candidate oncogenes (Table 6, Introduction, for a list of genes included in 11q22 amplicon). Literature data described *BIRC2* (*cIAP1*) and *BIRC3* (*cIAP2*) apoptosis inhibitor proteins as oncogenic targets of 11q22 amplification event in different tumor samples (Baldwin et al. 2005; Choschzick et

al. 2012; Dai et al. 2003; Imoto et al. 2001; Imoto et al. 2002; Lambros et al. 2005; Reardon et al. 1997; Snijders et al. 2005; Zender et al. 2006). Evidences reported that BIRC2 cooperates with YAP1 to accelerate tumorigenesis and promote mouse liver carcinogenesis (Zender et al. 2006). In addition, several members of *MMP* gene family, known to be involved in extracellular matrix remodeling, in cell invasion and metastasis development (Chakraborti et al. 2003), have been proposed as oncogene targets of the 11q22 amplicon (Lockwood et al. 2007; Roman et al. 2008). Finally, Progesterone receptor (*PGR*) is only 1 Mb proximal to YAP1 and its co-amplification may play a role in breast cancer. Therefore, the combined oncogenic role of co-amplified genes within 11q22 cannot be ruled out and remains a complex and fascinating issue to be explored.

4. DOES YAP1 AMPLIFICATION REPRESENT ONLY ONE OF MULTIPLE STRATEGIES OFFERED TO CANCER CELLS IN ORDER TO INACTIVATE HIPPO PATHWAY?

Based on the crucial role of YAP1 as effector protein of the Hippo pathway, one might ask whether YAP1 deregulation has the prominent role to perturb such pathway in cancer cells. Nevertheless, I and others observed that YAP1 amplification represents the only known mechanism of YAP1 gene alteration and it is a relatively rare event. Indeed, review of the literature evidences that multiple components of the Hippo network do suffer genetic alteration/deregulated expression in human cancer development (Table 10), suggesting that Hippo pathway deregulation may be a frequent occurrence in cancer cells and that YAP1 amplification may represent one of multiple events possibly deregulating the Hippo pathway in cancer. Notably, the evidence that reported genetic alterations have the consequence to inactivate YAP1/TAZ upstream components (Table 10) is in accordance with the essential role of Hippo pathway (paragraph 2, Introduction), and is functionally equivalent to YAP1 amplification/overexpression.

Table 10. Genetic alterations of different Hippo pathway components associated with human tumor development, based on literature data.

HIPPO COMPONENT	GENETIC ALTERATION	TUMOR TYPE	REPRESENTATIVE REFERENCES
LATS2	Deletion	Mesothelioma	Murakami et al. 2011
	Hypermethylation	Astrocytoma; Breast c.	Jiang et al. 2006; Takahashi et al. 2005
MOB1	Decreased expression	Colorectal c., Lung c.	Sasaki et al. 2007
WW45	Homozygous deletion	Renal c.	Tapon et al. 2002
NF2	Mutation	Sporadic Schwannoma, Mesotelioma	Evans et al. 2000
MST1/2	Hypermethylation	Soft tissue sarcoma	Seidel et al. 2007
	Decreased expression	Colorectal c., Prostate c.	Cinar et al. 2007; Minoo et al. 2007
FAT	Deletion	Breast c., Oral c., astrocytoma	Chosdol et al. 2009; Nakaya et al. 2007; Qi et al. 2009
RASSF1A	Promoter methilation	Lung c., Breast c., Prostate c., Nasopharyngeal c.	Burbee et al. 2001; Kuzmin et al. 2002

5. WHICH ARE THE CRITICAL TARGET GENES MEDIATING YAP1 ONCOGENIC FUNCTION?

YAP1 is a transcription co-factor which represents the final effector of the tumor suppressor Hippo pathway and, in response to growth signals or stimuli, YAP1 translocates into the nucleus to mediate the transcription of target genes (Liu et al. 2012). Literature data, regarding gene expression profiling in normal cellular contexts in which YAP1 gene is overexpressed, previously reported YAP1 target genes: *CTGF* gene, involved in cell growth (Zhao et al. 2008), *Ki67*, *c-myc*, *SOX4* and *APF* genes associated with epatocyte proliferation and several negative regulators of apoptosis such as *BIRC5*, *BIRC2* and of *MCL1* (Dong et al. 2007). As already described, *BIRC2* is coamplified with YAP1. The induction of *BIRC2* expression by YAP1 suggesting a feed-forward mechanism by which the YAP1/BIRC2 amplicon mediates the anti-apoptotic function (Dong et al. 2007). On the contrary, in pro-apoptotic condition literature data report *BBC3/puma* as a critical pro-apoptotic target genes (Matallanas et al. 2007) mediated by the interaction between YAP1 and TP73, whereas *Bax* and *p53AIP1* are selectively activated in response to cisplatin treatment (Strano et al. 2005).

I identified the downstream genes and pathways which are candidate critical YAP1 effectors in tumorigenesis, by gene expression profiling experiments comparing YAP1-

proficient with YAP1-silenced/deficient cells. Concordant with literature data, my data include already known YAP1 target genes, as *CTGF* and *BIRC2*. My results indicate that YAP1 target genes are mainly annotated for cell proliferation, cell to cell signaling and cellular movement ontologies. In addition, several YAP1 target genes such as *LATS2*, *NF2*, *STK3, STK4* and *TEAD2*, all components of the Hippo pathway (Pan 2010), are transcriptionally modulated upon YAP1 silencing. In particular, I found that the Hippo downstream component *TEAD2*, which is a transcription factor that interacts with YAP1 to promote the expression of the Hippo responsive genes, results to be upregulated after YAP1 silencing. All the other modulated genes represent negative growth regulators acting in a kinase cascade that ultimately inactivates YAP1 and I revealed that they are downregulated upon YAP1 silencing. Therefore, my results provide evidence that in the cancer cell lines under study YAP1 perturbation exerts a feedback loop function into the Hippo signaling pathway, contributing to its homeostasis and therefore supporting its oncogenic role in these cell models.

6. THE DIFFERENTIAL CONTRIBUTION OF YAP1 AND TAZ TO THE TUMORIGENIC PHENOTYPE REMAINS UNRESOLVED

TAZ gene is a YAP1 paralog in mammals similarly regulated by the Hippo pathway (Kanai et al. 2000) (paragraph 2, Introduction for details). Therefore, the final effectors of Hippo pathway are YAP1 and TAZ. Salvador-Warts-Hippo pathway in fact induces phosphorylation and inhibition of both genes at specific serine residues. Similar to YAP1, TAZ also is involved in cell proliferation, in cell migration and in cell invasion (Chan et al. 2008; Lei et al. 2008). Moreover it plays a critical role in cell fate decisions and in stem cell proliferation and it sustains self-renewal and tumor-initiation capacities in breast CSCs (Cordenonsi et al. 2011) and is involved in the regulation of cell cytoskeleton together with YAP1 (Dupont et al. 2011). Differently from YAP1, literature data does not report copy number amplification of TAZ in tumor samples. In one study, focusing on mammary tumors, TAZ overexpression is reported in 21% of primary breast cancer (Chan et al. 2008).

The majority of the literature data describes YAP1/TAZ as the final effectors of the Hippo pathway but most reports do not discriminate whether they exert their functions in combination and do not elucidate the individual role and involvement of each of these two proteins. My experiments specifically analyzed the contribution of the Hippo pathway final

effector YAP1 in carcinogenesis in the context of 11q22-amplified cancer cell lines and the results allowed us to define that YAP1 has an oncogenic role, without evaluating TAZ contribution. Indeed, it will be of interest to further delineate the individual contribution of either YAP1 or TAZ to cancer development.

MATERIAL AND METHODS

1. CANCER CELL LINES

The 11q22-amplified cancer cell lines Ca-Ski and EKVX were purchased from American Type Culture Collection (ATCC), RO82 cell line from Interlab Cell Line Collection, Genova, Italy (ICLC).

Ca-Ski (cervical squamous cell carcinoma) and EKVX (non small cell lung Adeno-carcinoma) cell lines were grown in RPMI 1640 (Sigma) supplemented with 10% heat-inactivated FBS (Lonza), RO82 cell line (Follicular thyroid carcinoma) was grown in DMEM (Sigma), Ham's F12 (Lonza), MCDB 105 (Sigma) (2:1:1) supplemented with 10% heat-inactivated FBS (Lonza). Cells were grown in a humidified incubator at 37°C and 5% CO_2 (Thermo Electron Corporation). Cell identity was monitored by microsatellite typing and absence of mycoplasma contamination was checked regularly.

2. TUMOR SAMPLES

Paraffin sections of 21 human cervical cancer samples, 15 human thyroid cancer samples, 56 human SNC tumor samples and of 77 human non small cell lung cancer samples were obtained from the Departments of Pathology of collaborating centers (Treviso General Hospital, Italy; "Fondazione Pascale" of Naples, Italy and "Fondazione Istituto Nazionale Tumori" of Milan, Italy).

3. GENERATION OF YAP1 STABLE KNOCKDOWN BY shRNA LENTIVIRAL TRANSDUCTION AND BY siRNA TRANSIENT KNOCKDOWN

Synthetic small-interfering RNAs (siRNA) are double-stranded, short (usually 21-bp) RNA molecules. The siRNA are incorporated into a multi-subunit complex RNA-induced silencing complex (RISC). The sense strand is degraded while the antisense strand directs RISC to mRNA target that has a complementary sequence. RISC cleaves the mRNA leading to target gene silencing.

Transient YAP1-silenced cells (siYAP1) were obtained by transfection using the Dharmafect Transfection Reagent (Thermo Scientific) using a pool of 3 different pre-designed sequences of small-interfering RNAs (siRNA). The sequences are referred as AM16708A-107951, AM16708A-107952, AM16708A-114602 (Ambion) (Figure 38). An independent sequence of siRNA (siRNAOT, off target), which does not target any human mRNA, was used as negative control and the sequence is referred as AM4611 (Ambion).

Cells at density of $3x10^5$/6-well plate were seeded and, 24 hours after seeding, cells were transfected with siRNA:

- TUBE 1

  1 uL siRNA
  199 uL serum free medium (Sigma)

- TUBE 2

  5 uL Dharmafect 3 (EKVX) Dharmafect 4 (Ca-Ski and RO82) (Thermo Scientific)
  195 uL serum free medium (Sigma)

		Tube 1 diluted siRNA		**Tube 2 diluted Dharmafect**			
Plating format	Surface area	Volume of 50 uM siRNA	Serum free medium	Volume of Dharmafect reagent	Serum free medium	Complete medium	Total transfection volume
6 well	9.6 cm^2	1 uL	199 uL	5 uL	195 uL	1600 uL	2000 uL

Cells were collected at appropriate time points depending on the experiments to perform and YAP1 silencing was checked at the protein level by western blot and at the mRNA level by qPCR analysis.

Short hairpin RNA (shRNA) is a molecule of RNA that makes a hairpin turn that, in our constructs, is transcribed from Lentiviral vectors. Once the shRNA is transcribed in the nucleus, it enters the cellular RNA interference machinery.

Stable YAP1-silenced cells (shYAP1) were obtained by infection using shRNA Lentiviral Particles (Thermo Scientific). Short-hairpin RNA (shRNA) expression vectors carry GFP expression to track infected cells by immunofluorescence and puromycin resistance for selection of stably infected cells. Two silencing sequences targeting YAP1 (shY1 and shY2) were used to silence YAP1 transcript. The sequences are referred as SH-

012200-02-10 (shY1) and as SH-012200-03-10 (shY2) (Thermo Scientific) (Figure 38). An independent sequence of shRNA (shOT, off target) was used as negative control and the sequence is referred as s-004000-02 (Thermo Scientific).

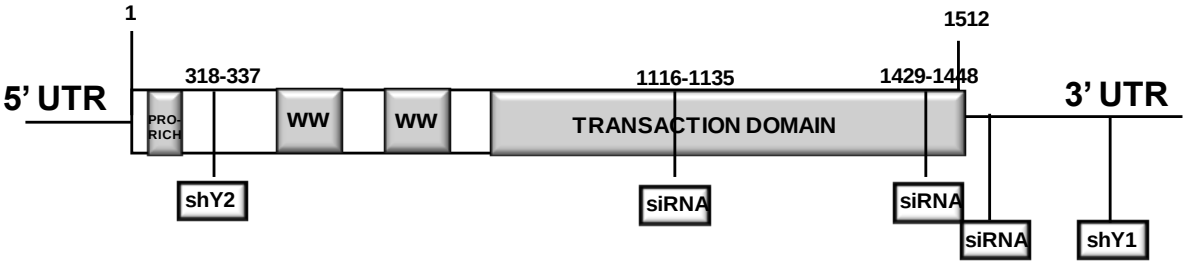

Figure 38. Mapping of siRNAYAP1 and shRNAYAP1 sequences on YAP1 mRNA.

Cells at density of $3x10^5$/6-well plate were seeded and, 24 hours after seeding, cells were infected with viral particles. Polybrene (Sigma) 6 ug/mL (EKVX cell line) or 4 ug/mL (Ca-Ski and RO82 cell lines) was added to the cells. Viral particles were diluted to medium and then were added to the cells. Cells were infected with MOI (multiplicity of infection) 5-10 (ie n=5-10 viral particles per cell seeded) and, 72 hours post infection, cells were selected using puromycin (Sigma).
Bulk cell population was collected and screened for YAP1 expression by Western Blot and qPCR analysis after puromycin selection.

4. RNA EXTRACTION

Total RNA was extracted using EZ1 RNA cell mini kit (Qiagen) and Bio-Robot EZ1 (Qiagen) according to the manufacturer's instructions. Cells were efficiently lysed using a solution of phenol and guanidine thiocyanate, designed to inhibit RNase and to facilitate lysis of cells. RNA was purified from lysates thought the binding to the silica surface of the magnetic particles in the presence of a chaotropic salt. The particles are separated from the lysates using a magnet, and the DNA is removed by treatment with RNse-free DNase. The RNA is then efficiently washed and eluted in elution buffer.

5. RETROTRASCRIPTION

RNA (500 ng) was retro-transcribed in cDNA as described:

1 μL Random Primers 250 ng (Invitrogen)

1 μL dNTPs MIX 10 Mm (Invitrogen)

10 μL RNA (1 ug/10 uL)

1 μL H_2O milliQ

The samples were incubated for 5 minutes at 65°C and then for 1 minute on ice.

A mix to add to the RNA was thus prepared:

4μL First Strand Buffer 5X (Invitrogen)

1μL DTT 0.1 M (Invitrogen)

1μL RNase OUT Recombinant RNase Inhibitor (Invitrogen)

1μL Super Script III RT (Invitrogen)

7 μL of the mix was added to each sample. The samples were loaded in Thermal Cycler Mastercycler (Eppendorf) with this thermal profile:

STAGE	TEMPERATURE	TIME
Hold	50°C	60 minutes
Hold	70°C	15 minutes

The cDNA was diluited 1:5 in a H_2O milliQ

6. DNA EXTRACTION

DNA was extracted from paraffin sections of human tumor samples (cervical cancers, thyroid cancers and SNC tumors) using EZ1 DNA paraffin-embedded tissue (Qiagen) and Bio-Robot EZ1 (Qiagen) according to the manufacturer's instructions. In order to remove the paraffin to the samples block, the sections were incubated with xilene, centrifuged and washed with ethanol. Samples were efficiently lysed at 65°C overnight in a solution of guanidine hydrochloride in combination with proteinase K, which is the lysis enzyme. DNA was purified from lysates through the binding to the silica surface of the

magnetic particles in the presence of a chaotropic salt. The particles are separated from the lysates using a magnet. The DNA is then washed and eluted in elution buffer.

DNA was extracted from the blood donor using DNA blood kit (Qiagen) and Bio-Robot EZ1 (Qiagen) according to the manufacturer's instructions and DNA was purified from 200 μL of whole blood.

Using the same methodology, DNA was extracted from cells using DNA tissue culture cells (Qiagen) and Bio-Robot EZ1 (Qiagen).

7. qRT-PCR

The cDNA (25 ng) was used as template in 20 μL of the PCR reaction. Relative quantification of gene expression was performed in triplicate using TaqMan Assays ^{on} Demand on a ABI Prism 7900HT Sequence Detection System (Applera) by comparative Ct method, using the HPRT gene (HPRT PDAR, 4326321E) (Applied Biosystem) as endogenous reference control and off target cells (sOT and shOT) (Applied Biosystem) as calibrators. Different assay were used as reported.

GENE SYMBOL	ASSAY
CCNA2	Hs00996788-m1
CCNG1	Hs00171112_m1
CDK2	Hs011548894_m1
CTGF	Hs000170014_m1
ETS1	Hs00428287_m1
GADD45A	Hs00169255_m1
ITGA5	Hs01547673_m1
LATS2	Hs00324396_m1
NF2	Hs00966302_m1
NRG1	Hs00247620_m1
SKP2	Hs01021864_m1
STK3	Hs00169491_m1
STK4	Hs001789779_m1
TEAD2	Hs0036621_m1
VEGFA	Hs00900055_m1
YAP1	Hs00371735_m1

A mix to add to the cDNA was thus prepared:

10 μL Taqman Gene expression Master Mix (Applied Biosystem)

4 μL Nuclease Free Water

1 μL Specific assay (Applied Biosystem)

15 uL of the mix were added to the 5 uL of the cDNA of each samples.

The samples were run with this thermal profile:

STAGE	TEMPERATURE	TIME
Hold	50°C	2 minutes
Hold	95°C	10 minutes
40 Cycles	95°C	15 seconds
	60°C	1 minute

The expression data of Real Time PCR were analyzed by the SDS software-RQ Manager 1.2, applying "Automatic Baseline Settings" and a threshold of 0.05, in order to obtain the Ct and the standard deviation. RQ (Relative Quantity) was calculated for each different genes normalize to an endogenous reference and relative to a calibrator, as described by this formula:

$2^{-\Delta\Delta CT}$ in which:

$$\Delta CT = CT_{target} - CT_{reference}$$

$$\Delta\Delta CT = \Delta CT_{sample} - \Delta CT_{calibrator}$$

8. qRT-PCR FOR GENE COPY NUMBER

Quantitative PCR was used to determine YAP1 copy number status of cell lines and of tumor samples (cervical cancer samples, thyroid cancer samples and SNC tumor samples).

In order to determine gene copy number, quantitative PCR used relative quantification method with standard curves. YAP1 assay used was Hs02837638_cn (Applied Biosystem) and RNaseP assay used was 4401631 (reference gene) (Applied Biosystem). Normal donor DNA was used as a normal copy number control while Ca-Ski cell line was used as a control of amplification for tumor cancer samples.

A mix to add to DNA was thus prepared:

10 μL	Taqman Gene expression 2X Master Mix (Applied Biosystem)
4 μL	Nuclease Free Water
1 μL	Copy number assay (Applied Biosystem)

15 uL of the mix were added to the 5 uL (between 1 to 20 ng) of the DNA of each sample. The samples were run with this thermal profile:

STAGE	TEMPERATURE	TIME
Hold	50°C	2 minutes
Hold	95°C	10 minutes
40 Cycles	95°C	15 seconds
	60°C	1 minute

The expression data of Real Time PCR were analyzed by the SDS software 2.3, in order to obtain the Ct and the standard deviation. In each experiment, standard curves were analyzed for both reference gene (RNaseP) and target gene (YAP1) using serial diluitions of a normal control DNA, in the template DNA range from 0.05 ng to 50 ng. Using the standard curves of reference gene and target gene, the mean Ct of individual samples were converted to nanogram equivalent of template DNA. The obtained values were converted to target gene copy number by normalizing over a normal donor DNA as calibrator.

9. FLUORESCENT IN SITU HYBRIDIZATION (FISH)

FISH analysis was performed on cells smeared over a positively charged slide and on human non small cell lung cancer samples that were arrayed on a tissue microarray. FISH analysis was performed at "Fondazione Istituto Nazionale Tumori" of Milan, Italy.

BAC probes DNA used for FISH was extracted using QIAprep Midiprep (Qiagen), verified by sequence tagged site content mapping and labeled with Spectrum Orange deoxyuridine triphosphate or Spectrum Green deoxyuridine triphosphate (Vysis, Downers Grove, IL) by use of a Nick Translation Kit (Vysis) according to the manufacturer's instructions. In double-color interphase FISH, one specific probe for cyclin D1 gene (CCND1, 11q21, green signal) and anther specific probe for YAP1 gene (YAP1, 11q22, red

signal) were used. The FISH hybridization signals were analyzed in an Olympus BX51 microscope coupled to a charge-coupled device camera COHU 4912 (Olympus). The images captured were analyzed using the Mac Probe software (PowerGene Olympus). A minimum of 100 nuclei were counted.

10. PROTEIN ANALYSES

For western blotting, protein lysates were prepared in RIPA buffer (TBS 1X, 1% Nonidet P-40, 0.5% Sodio Deoxicolato, 0.1% SDS, 0.04% Sodio Azide, PMSF 1X in DMSO, protease inibithor cocktail 1X in DMSO) (Santa Cruz Biotecnology).
Forty ug of cell lysates were loaded on 4-15% gradient gels (Biorad) and electro-blotted onto polyvinylidene difluoride membranes (Amersham Biosciences). Subsequently, membranes were incubated for 1 hour at room temperature in a solution of TBST [10 mmol/L Tris-HCl (pH 8.0), 0.15 mol/L NaCl, and 0.05% Tween 20] supplemented with 5% nonfat dry milk. For immunodetection, the anti-YAP1 antibody (Cell Signaling, 4912) was used diluted 1:1000, the anti-YAP1 antibody (Santa Cruz mouse monoclonal, sc-101199) was used diluted 1:500, the anti-phospho YAP1 (Ser127) antibody (Cell Signaling, 4911) was used diluted 1:1000, the anti-p21 antibody was used diluted 1:250 (BD Transduction Laboratories), the anti-caspase 3 antibody diluted 1:1000 (Cell Signaling, 9662), the anti-caspase 8 antibody was used diluted 1:1000 (Cell Signaling, 9746) and anti-PARP antibody was used diluted 1:500 (Santa Cruz, sc-8007). Protein loading equivalence was assessed using the anti-GAPDH antibody diluted 1:8000 (Santa Cruz sc-32233) or using the anti-TUBULIN ß antibody diluted 1:10.000 (Clone 2-28-33, Sigma). After overnight incubation at 4°C with the primary antibody, membranes were washed in TBST 0.1% Tween. Immunoreactivity was detected by AlexaFluor680 or IRDye800CW-conjugated goat-antimouse or goat-antirabbit antibodies diluted 1:2000 (Invitrogen and Li-Cor, respectively). Protein expression was analyzed using Odyssey infrared imaging system (Li-Cor) and the data were normalized on siOT and on shOT.

Immunohistochemistry was performed on 21 human cervical cancer samples retrieved from the Pathological Department of the Treviso General Hospital. Protein expression of YAP1 was investigated by immunohistochemistry using anti-YAP1 antibody diluted 1:25 (Cell Signaling, 4912). Endogenous peroxidase was blocked with 0.3%

hydrogen peroxide in methanol for 30 minutes. Immunohistochemistry analysis was performed using Ultra vision detection system (LabVision), upon heat-induced epitope retrieval. Intensity scoring of tumor cells was performed by pathologist based on a 4-tiered scale. The comparisons between two classes were performed by Fisher two tailed extract test using Prism 5 software (GraphPad Inc.), by grouping negative/1+ cases and 2+/3+ cases. The p-values < 0.05 were considered statistically significant.

11. SULFORHODAMINE B STAINING ASSAY (SRB ASSAY)

SRB assay is used for cell proliferation rate determination, based on the measurement of cellular protein content. The assay relies on the ability of the Sulforhodamine B to bind to protein components of the cells (Vichai and Kirtikara 2006).

Preliminary experiments were performed in order to determine the optimal cell density to plate. Cells were grown for 72 hours at density of $5x10^3$/96-well plate (Ca-Ski cell line) and at density of $1x10^4$ cells/96-well plate (EKVX and RO82 cell lines). After culture, cells were fixed using cold 50% trichloroacetic acid for 1 hour, washed in deionized water, dried and stained with 0.4% (w/v) Sulforhodamine B (Sigma) diluted in 1% (vol/vol) acetic acid for 20 min, after which the excess dye was removed by washing repeatedly with 1% acetic acid and plates were air-dried. The protein-bound dye dried was dissolved in 10 mM Tris base solution. The absorbance of protein biomass, that is proportional to the cell number, was read at 550 nm, using the microplate reader Infinite 200 (TECAN). In another plate the cells were grown in the same condition (time zero plate), fixed and stained after overnight cell adhesion and served for background subtraction and calculation of relative absorbance values.

The percentage of cell growth was determined applying the following formula:

$$\% \text{ cell growth} = \frac{\text{mean } OD_{day3} - \text{mean } OD_{day0}}{\text{mean } OD_{day0}} \times 100$$

The data showed the means and the s.e.m of three independent experiments. The comparisons between two classes were performed by two-sample paired t-test using Prism 5 software (GraphPad Inc.). The p-values < 0.05 were considered statistically significant.

The SRB assay is also the most widely used methods for *in vitro* cytotoxicity screening. Cells at density of $5x10^3$/96-well plate were treated with Cisplatin (Teva) at different doses (0.1, 1, 10, 30 and 100 uM). Cisplatin was added 24 hours post-plating at the indicated concentrations.

The percentage of inhibition of cell proliferation after drug treatment was determined applying the following formulas:

$$\% \text{ cell growth} = \frac{\text{mean OD}_{\text{sample}} - \text{mean OD}_{\text{day0}}}{\text{mean OD}_{\text{control}} - \text{mean OD}_{\text{day0}}} \times 100$$

$$\% \text{ growth inhibition} = 100 - \% \text{ cell growth}$$

The data showed the means and the s.e.m of two independent experiments.

The IC50 (concentration of drug inhibiting 50% of cell growth) was calculate using Prism 5 software (GraphPad Inc.) applying "non-linear fitting dose response". On the basis of the data entered, the software derives a function on the basis of which calculates the IC50.

12. CELL COUNTING USING TRYPAN BLUE STAINING

Trypan Blue dye selective staining dead cells. Dye enters into the dead cells which lack of integrity of the cell membrane.

Cells were plated at density of $2x10^5$/6-well plate. After 72 hours from seeding, cells suspension (about 1000 cells/1 uL) was stained with 1/10 of Trypan Blu stain solution (Lonza). After 2 minutes of incubation with Trypan Blu, 10 uL of stained cells were put into the microscope slides (Kova). Vital cells (not blu) and dead cells (blu) were counted in 3 of 9 quadrants of the counting slide chamber.

The data showed the means and the s.e.m of two independent experiments. The comparisons between two classes were performed by two-sample unpaired t-test using Prism 5 software (GraphPad Inc.). The p-values < 0.05 were considered statistically significant.

13. BROMODEOXYURIDINE (BrdU) ASSAY

Bromodeoxyuridine (BrdU), which is an analog of the DNA precursor thymidine, is incorporated into newly synthesized DNA and processing thought the S phase of the cell cycle.

BrdU Flow Kit Staining (BD Pharmingen) was used to quantify cells that were actively synthesizing DNA. Cells at density of $1x10^6$/100 mm dish were pulsed with 1 hour of BrdU incorporation (Ca-Ski and RO82 cell lines) and with 2 hours of BrdU incorporation (EKVX cell line). After BrdU pulse, the cells were washed and released for additional 1 hour in complete medium. According to the manufacturer's instructions, cells were permealized, fixed and then treated with DNase for 1 hour at 37°C. The BrdU incorporation is stained with specific fluorescent anti BrdU antibody for 20 minutes shielded from light. The staining of total DNA was performed using 7 amino actinomycin D (7AAD), which is a fluorescent dye for labeling DNA. Stained cells (cells-associated BrdU) were measured with flow cytometer (Beckman Coulter) and the data were then analyzed with flow cytometer analysis software (Beckman Coulter).

The data showed the means and the s.e.m of three independent experiments. The comparisons between two classes were performed by two-sample paired t-test using Prism 5 software (GraphPad Inc.). The p-values < 0.05 were considered statistically significant.

14. ANCHORAGE-INDEPENDENT GROWTH

Anchorage-independent growth evaluates the colonies growth in a semisolid culture medium. Cells at density of $5x10^4$/60 mm dish (Ca-Ski and RO82 cell lines) and at density of $1x10^5$/60 mm dish (EKVX cell line) were resuspended in 0.35% agar (Sigma) complete medium (top agar) and seeded on 0.5% bottom agar medium. Fresh top agar was added weekly. After two weeks, plates were stained with iodonitrotetrazolium violet (Sigma) and colonies formation were photographed and counted at the microscope (Olympus).

The data showed the means and the s.e.m of three independent experiments. The comparisons between two classes were performed by two-sample unpaired t-test using Prism 5 software (GraphPad Inc.). The p-values < 0.05 were considered statistically significant.

15. *IN VIVO* TUMORIGENICITY ASSAY

Experiments on animals were performed in accordance with national regulations and were approved by the CRO ethical committe for animal experimentations. All experiments conform to the relevant regulatory standards.

Cells in concentration of $1x10^6$ were resuspended in 80 uL of PBS, were injected into each flank of six-week-old immunocompromised athymic nude mice (Hsd:Athymic nude-nu, Harlan). Tumor size was monitored weekly. Mice were sacrificed when the tumors reached a diameter of 1.2-1.5 cm or after 6 weeks of monitoring. Tumor volume was calculated as $1/2r^3$.

The data showed the means and the s.e.m of three independent experiments. Two classes' comparisons with multiple measurement points have been performed by two-way analysis of variance (ANOVA) using Prism 5 software (GraphPad Inc.). The p-values < 0.05 were considered statistically significant.

16. SPHERE FORMING ASSAY

Single cell suspensions derived from monolayer cultures were seeded at density of $6x10^3$/60 mm dish in ultra low attachment plates (Corning) and maintained in a serum free RPMI medium (Sigma) supplemented with 4 ug/ml heparin (Sigma). Every other day culture medium was enriched with fresh 20 ng/ml EGF (Peprotech), 10 ng/ml bFGF (Peprotech) and B27 (Sigma).

Cells were incubated for 10 days in a humidified incubator at 37°C and 5% CO_2 (Thermo Electron Corporation). The number of spheres (>50 cells/sphere) per well was then counted after 10 days from seeding.

The data showed the means and the s.e.m of three independent experiments. The comparisons between two classes were performed by two-sample unpaired t-test using Prism 5 software (GraphPad Inc.). The p-values < 0.05 were considered statistically significant.

17. GENERATION OF STABLE CLONES

Stable clones were derived from the bulk cell population after puromycin selection. Cells were seeded at density of 5/96-well plate and were grown in selective medium for 15 days. 12 GFP-positive clones were expanded up to 100 mm dish and were performed a protein lysate for tested YAP1 expression by western blotting.

The comparisons between two classes were performed by Fisher two tailed extract test using Prism 5 software (GraphPad Inc.). The p-values < 0.05 were considered statistically significant.

18. WOUND HEALING ASSAY

For the evaluation of cell motility, exponentially growing cells at density of $8x10^5$/60 mm dish were plated in order to create a dense monolayer. Cell monolayer was scratched using a pipette tip. Complete medium was added after washing in PBS, and wound closure was monitored every 24 hours and pictures were taken by microscope (Olimpus). The pictures were related to one representative experiment out of three.

19. CHEMOTAXIS ASSAY

Transwell permeable supports, 6.5 mm diameter inserts, 8.0 um pore size, polycarbonate membranes (Corning Inc.) were used to perform migration assay.

Cells at density of $1x10^5$/96-well plate were seeded in the upper chamber of the transwell insert in serum free medium (Sigma). The lower chamber of the transwell was filled with 600 uL of culture medium containing 10% fetal bovine serum. Cells were incubated at 37°C and 5% CO_2 (Thermo Electron Corporation) for 16 h. The transwells were then removed from the 24-well plates and stained with 0.1% Crystal Violet (Sigma) in 25% methanol. Non-migrated cells were scraped off the top of the transwell with a cotton swab. Migrated cells were quantified by eluting crystal violet with 1% SDS and reading the absorbance at 550 nm using the microplate reader Infinite 200 (TECAN). In parallel, equal

amounts of cells were plated in 96-well plate fixed and stained after overnight cell adhesion which served for background subtraction and for calculation of relative absorbance values.

The data showed the means and the s.e.m of three independent experiments. The comparisons between two classes were performed by two-sample paired t-test using Prism 5 software (GraphPad Inc.). The p-values < 0.05 were considered statistically significant.

20. TIME-LAPSE VIDEO MICROSCOPY

For the evaluation of cell motility cells were seeded at density of $3x10^3$/24-well plate. After overnight cell adhesion, cells were incubated at 37°C in 5% CO_2 atmosphere in the Leica Time LapseAF6000LX workstation equipped with the Leica DMI 6000 motorized microscope and an environmental chamber for the proper setting of temperature humidity and CO_2 concentration. The AF6000 Software (Leica) allows the acquisition of the images on the desiderate frames and periods of time. Images were collected every 5 minutes for 12 hours and were used to create a video that was analyzed with a cell tracking software (Leica) to collect different locomotion parameters. Cells were randomly selected and their x/y coordinates tracked using the IM2000 software (Leica), which allows manual cell tracking in order to obtain the total distance covered (micron) by the cells.

The data showed the means and the s.e.m of three independent experiments. The comparisons between two classes were performed by two-sample paired t-test using Prism 5 software (GraphPad Inc.). The p-values < 0.05 were considered statistically significant.

21. APOPTOSIS ANALYSIS

Guava flow cytometer instrument (Millipore) was used to perform apoptosis analysis using Guava Nexin protocol (Millipore). This assay could distinguish the cells in four populations:

- Non-apoptotic cells: Annexin v (-) and 7-AAD (-)
- Early apoptotic cells: Annexin v (+) and 7-AAD (-)
- Dead cells: Annexin v (+) and 7-AAD (+)
- Late stage apoptotic cells: Annexin v (-) and 7-AAD (+)

Cells were seeded at density of $1x10^5$/6-well plate and were treated with cisplatin (Teva) 100 uM for 16 hours. Cells (cells concentration should be between $2x10^5$ and $1x10^6$cells/mL) were harvested and incubated with 100 uL of Guava Nexin Reagent for 20 minutes at room temperature shielded from light. The data were acquired on the Guava instrument (Millipore) and then analyzed using Nexin Guava Analysis Software (Millipore).

The data showed the means and the s.e.m of three independent experiments. The comparisons between two classes were performed by two-sample paired t-test using Prism 5 software (GraphPad Inc.). The p-values < 0.05 were considered statistically significant.

22. BIOINFORMATIC ANALYSIS

We identified YAP1 target genes in 11q22-amplified cancer cell lines by gene expression profiling experiments. Class comparison analysis performed using the BRB Array Tool software from the US National Cancer Institute (linus.nci.nih.gov/BRB-ArrayTools.html) and comparing YAP1 proficient cells versus YAP1-silenced cells. Differential expression levels of probe sets were considered statistically significant if $p < 0.001$ by random variance t tests. A multivariate permutation test was applied to provide 90% confidence that the false discovery rate was less than 10%. Such stringent significance threshold was used to limit the number of false-positive findings. The statistically significantly modulated genes identified were functionally annotated using Ingenuity bioinformatic tool.

The analysis of YAP1 copy number (deletion or amplification) status in independent datasets was performed using Oncomine *(www.oncomine.org)* and Sanger Centre *(www.sanger.ac.uk/genetics/CGP/CellLines)* database repositories, two cancer microarray databases which contain gene copy number data collected from the literature and proprietary datasets. Data are related to normal cell lines, cancer cell lines, primary cancer cell cultures, normal tissue samples, cancer tissue samples and xenograft tumors.

The comparison between YAP1 deletion and amplification was performed in order to test the null hypothesis that the two anomalies are expected at the same frequency by Chi-square using Prism 5 software (GraphPad Inc.). The p-values < 0.05 were considered statistically significant.

REFERENCES

Alarcon, C., Zaromytidou, A. I., Xi, Q., Gao, S., Yu, J., Fujisawa, S., et al. (2009). Nuclear CDKs drive Smad transcriptional activation and turnover in BMP and TGF-beta pathways. *Cell*, 139(4), 757-769.

Albertson, D. G. (2006). Gene amplification in cancer. *Trends in genetics : TIG*, 22(8), 447-455.

Aleem, E., Berthet, C., Kaldis, P. (2004). Cdk2 as a master of S phase entry: fact or fake?. *Cell cycle (Georgetown, Tex.)*, 3(1), 35-37.

Avruch, J., Zhou, D., Fitamant, J., Bardeesy, N., Mou, F., Barrufet, L. R. (2012). Protein kinases of the Hippo pathway: regulation and substrates. *Seminars in cell & developmental biology*, 23(7), 770-784.

Azzolin, L., Zanconato, F., Bresolin, S., Forcato, M., Basso, G., Bicciato, S., et al. (2012). Role of TAZ as Mediator of Wnt Signaling. *Cell*, 151(7), 1443-1456.

Baldwin, C., Garnis, C., Zhang, L., Rosin, M. P., Lam, W. L. (2005). Multiple microalterations detected at high frequency in oral cancer. *Cancer research*, 65(17), 7561-7567.

Bard-Chapeau, E. A., Li, S., Ding, J., Zhang, S. S., Zhu, H. H., Princen, F., et al. (2011). Ptpn11/Shp2 acts as a tumor suppressor in hepatocellular carcinogenesis. *Cancer cell*, 19(5), 629-639.

Basu, S., Totty, N. F., Irwin, M. S., Sudol, M., Downward, J. (2003). Akt phosphorylates the Yes-associated protein, YAP, to induce interaction with 14-3-3 and attenuation of p73-mediated apoptosis. *Molecular cell*, 11(1), 11-23.

Bates, S., Rowan, S., Vousden, K. H. (1996). Characterisation of human cyclin G1 and G2: DNA damage inducible genes. *Oncogene*, 13(5), 1103-1109.

Bennett, F. C. & Harvey, K. F. (2006). Fat cadherin modulates organ size in Drosophila via the Salvador/Warts/Hippo signaling pathway. *Current biology : CB*, 16(21), 2101-2110.

Betticher, D. C., Heighway, J., Hasleton, P. S., Altermatt, H. J., Ryder, W. D., Cerny, T., et al. (1996). Prognostic significance of CCND1 (cyclin D1) overexpression in primary resected non-small-cell lung cancer. *British journal of cancer*, 73(3), 294-300.

Bradham, D. M., Igarashi, A., Potter, R. L., Grotendorst, G. R. (1991). Connective tissue growth factor: a cysteine-rich mitogen secreted by human vascular endothelial cells is related to the SRC-induced immediate early gene product CEF-10. *The Journal of cell biology*, 114(6), 1285-1294.

Burbee, D. G., Forgacs, E., Zochbauer-Muller, S., Shivakumar, L., Fong, K., Gao, B., et al. (2001). Epigenetic inactivation of RASSF1A in lung and breast cancers and malignant phenotype suppression. *Journal of the National Cancer Institute*, 93(9), 691-699.

Cai, J., Zhang, N., Zheng, Y., de Wilde, R. F., Maitra, A., Pan, D. (2010). The Hippo signaling pathway restricts the oncogenic potential of an intestinal regeneration program. *Genes & development*, 24(21), 2383-2388.

Camargo, F. D., Gokhale, S., Johnnidis, J. B., Fu, D., Bell, G. W., Jaenisch, R., et al. (2007). YAP1 increases organ size and expands undifferentiated progenitor cells. *Current biology : CB*, 17(23), 2054-2060.

Cespedes, M. V., Casanova, I., Parreno, M., Mangues, R. (2006). Mouse models in oncogenesis and cancer therapy. *Clinical & translational oncology : official publication of the Federation of Spanish Oncology Societies and of the National Cancer Institute of Mexico*, 8(5), 318-329.

Chakraborti, S., Mandal, M., Das, S., Mandal, A., Chakraborti, T. (2003). Regulation of matrix metalloproteinases: an overview. *Molecular and cellular biochemistry*, 253(1-2), 269-285.

Chan, S. W., Lim, C. J., Chong, Y. F., Pobbati, A. V., Huang, C., Hong, W. (2011). Hippo pathway-independent restriction of TAZ and YAP by angiomotin. *The Journal of biological chemistry*, 286(9), 7018-7026.

Chan, S. W., Lim, C. J., Guo, K., Ng, C. P., Lee, I., Hunziker, W., et al. (2008). A role for TAZ in migration, invasion, and tumorigenesis of breast cancer cells. *Cancer research*, 68(8), 2592-2598.

Chen, H. I. & Sudol, M. (1995). The WW domain of Yes-associated protein binds a proline-rich ligand that differs from the consensus established for Src homology 3-binding modules. *Proceedings of the National Academy of Sciences of the United States of America*, 92(17), 7819-7823.

Cho, E., Feng, Y., Rauskolb, C., Maitra, S., Fehon, R., Irvine, K. D. (2006). Delineation of a Fat tumor suppressor pathway. *Nature genetics*, 38(10), 1142-1150.

Choschzick, M., Tabibzada, A. M., Gieseking, F., Woelber, L., Jaenicke, F., Sauter, G., et al. (2012). BIRC2 amplification in squamous cell carcinomas of the uterine cervix. *Virchows Archiv : an international journal of pathology*, 461(2), 123-128.

Chosdol, K., Misra, A., Puri, S., Srivastava, T., Chattopadhyay, P., Sarkar, C., et al. (2009). Frequent loss of heterozygosity and altered expression of the candidate tumor suppressor gene 'FAT' in human astrocytic tumors. *BMC cancer*, 9, 5-2407-9-5.

Cinar, B., Fang, P. K., Lutchman, M., Di Vizio, D., Adam, R. M., Pavlova, N., et al. (2007). The pro-apoptotic kinase Mst1 and its caspase cleavage products are direct inhibitors of Akt1. *The EMBO journal*, 26(21), 4523-4534.

Colozza, M., Azambuja, E., Cardoso, F., Sotiriou, C., Larsimont, D., Piccart, M. J. (2005). Proliferative markers as prognostic and predictive tools in early breast cancer: where are we now?. *Annals of Oncology : Official Journal of the European Society for Medical Oncology / ESMO*, 16(11), 1723-1739.

Cordenonsi, M., Zanconato, F., Azzolin, L., Forcato, M., Rosato, A., Frasson, C., et al. (2011). The Hippo transducer TAZ confers cancer stem cell-related traits on breast cancer cells. *Cell*, 147(4), 759-772.

Creasy, C. L. & Chernoff, J. (1995)a. Cloning and characterization of a human protein kinase with homology to Ste20. *The Journal of biological chemistry*, 270(37), 21695-21700.

Creasy, C. L. & Chernoff, J. (1995)b. Cloning and characterization of a member of the MST subfamily of Ste20-like kinases. *Gene*, 167(1-2), 303-306.

Dai, Z., Zhu, W. G., Morrison, C. D., Brena, R. M., Smiraglia, D. J., Raval, A., et al. (2003). A comprehensive search for DNA amplification in lung cancer identifies inhibitors of apoptosis cIAP1 and cIAP2 as candidate oncogenes. *Human molecular genetics*, 12(7), 791-801.

De la Cueva, E., Garcia-Cao, I., Herranz, M., Lopez, P., Garcia-Palencia, P., Flores, J. M., et al. (2006). Tumorigenic activity of p21Waf1/Cip1 in thymic lymphoma. *Oncogene*, 25(29), 4128-4132.

Demetrick, D. J., Zhang, H., Beach, D. H. (1996). Chromosomal mapping of the genes for the human CDK2/cyclin A-associated proteins p19 (SKP1A and SKP1B) and p45 (SKP2). *Cytogenetics and cell genetics*, 73(1-2), 104-107.

Di Como, C. J., Gaiddon, C., Prives, C. (1999). P73 Function is Inhibited by Tumor-Derived P53 Mutants in Mammalian Cells. *Molecular and cellular biology*, 19(2), 1438-1449.

Dittmer, J. (2003). The biology of the Ets1 proto-oncogene. *Molecular cancer*, 2, 29.

Dong, J., Feldmann, G., Huang, J., Wu, S., Zhang, N., Comerford, S. A., et al. (2007). Elucidation of a universal size-control mechanism in Drosophila and mammals. *Cell*, 130(6), 1120-1133.

Dupont, S., Morsut, L., Aragona, M., Enzo, E., Giulitti, S., Cordenonsi, M., et al. (2011). Role of YAP/TAZ in mechanotransduction. *Nature*, 474(7350), 179-183.

Edgar, B. A. (2006). From cell structure to transcription: Hippo forges a new path. *Cell*, 124(2), 267-273.

Evan, G. I. & Vousden, K. H. (2001). Proliferation, cell cycle and apoptosis in cancer. *Nature*, 411(6835), 342-348.

Evans, D. G., Sainio, M., Baser, M. E. (2000). Neurofibromatosis type 2. *Journal of medical genetics*, 37(12), 897-904.

Fernandez-L, A., Northcott, P. A., Dalton, J., Fraga, C., Ellison, D., Angers, S., et al. (2009). YAP1 is amplified and up-regulated in hedgehog-associated medulloblastomas and mediates Sonic hedgehog-driven neural precursor proliferation. *Genes & development*, 23(23), 2729-2741.

Ferrigno, O., Lallemand, F., Verrecchia, F., L'Hoste, S., Camonis, J., Atfi, A., et al. (2002). Yes-associated protein (YAP65) interacts with Smad7 and potentiates its inhibitory activity against TGF-beta/Smad signaling. *Oncogene*, 21(32), 4879-4884.

Gadkar-Sable, S., Shah, C., Rosario, G., Sachdeva, G., Puri, C. (2005). Progesterone receptors: various forms and functions in reproductive tissues. *Frontiers in bioscience : a journal and virtual library*, 10, 2118-2130.

Gaffney, C. J., Oka, T., Mazack, V., Hilman, D., Gat, U., Muramatsu, T., et al. (2012). Identification, basic characterization and evolutionary analysis of differentially spliced mRNA isoforms of human YAP1 gene. *Gene*, 509(2), 215-222.

Genevet, A., Polesello, C., Blight, K., Robertson, F., Collinson, L. M., Pichaud, F., et al. (2009). The Hippo pathway regulates apical-domain size independently of its growth-control function. *Journal of cell science*, 122(Pt 14), 2360-2370.

Genevet, A., Wehr, M. C., Brain, R., Thompson, B. J., Tapon, N. (2010). Kibra is a regulator of the Salvador/Warts/Hippo signaling network. *Developmental cell*, 18(2), 300-308.

Goulev, Y., Fauny, J. D., Gonzalez-Marti, B., Flagiello, D., Silber, J., Zider, A. (2008). SCALLOPED interacts with YORKIE, the nuclear effector of the hippo tumor-suppressor pathway in Drosophila. *Current biology : CB*, 18(6), 435-441.

Guadamillas, M. C., Cerezo, A., Del Pozo, M. A. (2011). Overcoming anoikis--pathways to anchorage-independent growth in cancer. *Journal of cell science*, 124(Pt 19), 3189-3197.

Guo, X. & Wang, X. F. (2009). Signaling cross-talk between TGF-beta/BMP and other pathways. *Cell research*, 19(1), 71-88.

Halder, G. & Johnson, R. L. (2011). Hippo signaling: growth control and beyond. *Development (Cambridge, England)*, 138(1), 9-22.

Hamaratoglu, F., Willecke, M., Kango-Singh, M., Nolo, R., Hyun, E., Tao, C., et al. (2006). The tumour-suppressor genes NF2/Merlin and Expanded act through Hippo signalling to regulate cell proliferation and apoptosis. *Nature cell biology*, 8(1), 27-36.

Hao, Y., Chun, A., Cheung, K., Rashidi, B., Yang, X. (2008). Tumor suppressor LATS1 is a negative regulator of oncogene YAP. *The Journal of biological chemistry*, 283(9), 5496-5509.

Harvey, K. & Tapon, N. (2007). The Salvador-Warts-Hippo pathway - an emerging tumour-suppressor network. *Nature reviews.Cancer*, 7(3), 182-191.

Heallen, T., Zhang, M., Wang, J., Bonilla-Claudio, M., Klysik, E., Johnson, R. L., et al. (2011). Hippo pathway inhibits Wnt signaling to restrain cardiomyocyte proliferation and heart size. *Science (New York, N.Y.)*, 332(6028), 458-461.

Helias-Rodzewicz, Z., Perot, G., Chibon, F., Ferreira, C., Lagarde, P., Terrier, P., et al. (2010). YAP1 and VGLL3, encoding two cofactors of TEAD transcription factors, are

amplified and overexpressed in a subset of soft tissue sarcomas. *Genes, chromosomes & cancer*, 49(12), 1161-1171.

Hermeking, H. & Eick, D. (1994). Mediation of c-Myc-induced apoptosis by p53. *Science (New York, N.Y.)*, 265(5181), 2091-2093.

Hermsen, M., Alonso Guervos, M., Meijer, G., van Diest, P., Suarez Nieto, C., Marcos, C. A., et al. (2005). Chromosomal changes in relation to clinical outcome in larynx and pharynx squamous cell carcinoma. *Cellular oncology : the official journal of the International Society for Cellular Oncology*, 27(3), 191-198.

Hollander, M. C., Alamo, I., Jackman, J., Wang, M. G., McBride, O. W., Fornace, A. J.,Jr. (1993). Analysis of the mammalian gadd45 gene and its response to DNA damage. *The Journal of biological chemistry*, 268(32), 24385-24393.

Hong, J. H., Hwang, E. S., McManus, M. T., Amsterdam, A., Tian, Y., Kalmukova, R., et al. (2005). TAZ, a transcriptional modulator of mesenchymal stem cell differentiation. *Science (New York, N.Y.)*, 309(5737), 1074-1078.

Huang, J., Wu, S., Barrera, J., Matthews, K., Pan, D. (2005). The Hippo signaling pathway coordinately regulates cell proliferation and apoptosis by inactivating Yorkie, the Drosophila Homolog of YAP. *Cell*, 122(3), 421-434.

Imoto, I., Tsuda, H., Hirasawa, A., Miura, M., Sakamoto, M., Hirohashi, S., et al. (2002). Expression of cIAP1, a target for 11q22 amplification, correlates with resistance of cervical cancers to radiotherapy. *Cancer research*, 62(17), 4860-4866.

Imoto, I., Yang, Z. Q., Pimkhaokham, A., Tsuda, H., Shimada, Y., Imamura, M., et al. (2001). Identification of cIAP1 as a candidate target gene within an amplicon at 11q22 in esophageal squamous cell carcinomas. *Cancer research*, 61(18), 6629-6634.

Jiang, Z., Li, X., Hu, J., Zhou, W., Jiang, Y., Li, G., et al. (2006). Promoter hypermethylation-mediated down-regulation of LATS1 and LATS2 in human astrocytoma. *Neuroscience research*, 56(4), 450-458.

Kanai, F., Marignani, P. A., Sarbassova, D., Yagi, R., Hall, R. A., Donowitz, M., et al. (2000). TAZ: a novel transcriptional co-activator regulated by interactions with 14-3-3 and PDZ domain proteins. *The EMBO journal*, 19(24), 6778-6791.

Kaneko, K. J. & DePamphilis, M. L. (1998). Regulation of gene expression at the beginning of mammalian development and the TEAD family of transcription factors. *Developmental genetics*, 22(1), 43-55.

Karpowicz, P., Perez, J., Perrimon, N. (2010). The Hippo tumor suppressor pathway regulates intestinal stem cell regeneration. *Development (Cambridge, England)*, 137(24), 4135-4145.

Kuzmin, I., Gillespie, J. W., Protopopov, A., Geil, L., Dreijerink, K., Yang, Y., et al. (2002). The RASSF1A tumor suppressor gene is inactivated in prostate tumors and suppresses growth of prostate carcinoma cells. *Cancer research*, 62(12), 3498-3502.

LaCasse, E. C., Baird, S., Korneluk, R. G., MacKenzie, A. E. (1998). The inhibitors of apoptosis (IAPs) and their emerging role in cancer. *Oncogene*, 17(25), 3247-3259.

Lai, D., Ho, K. C., Hao, Y., Yang, X. (2011). Taxol resistance in breast cancer cells is mediated by the hippo pathway component TAZ and its downstream transcriptional targets Cyr61 and CTGF. *Cancer research*, 71(7), 2728-2738.

Lambros, M. B., Fiegler, H., Jones, A., Gorman, P., Roylance, R. R., Carter, N. P., et al. (2005). Analysis of ovarian cancer cell lines using array-based comparative genomic hybridization. *The Journal of pathology*, 205(1), 29-40.

Lapi, E., Di Agostino, S., Donzelli, S., Gal, H., Domany, E., Rechavi, G., et al. (2008). PML, YAP, and p73 are components of a proapoptotic autoregulatory feedback loop. *Molecular cell*, 32(6), 803-814.

Lei, Q. Y., Zhang, H., Zhao, B., Zha, Z. Y., Bai, F., Pei, X. H., et al. (2008). TAZ promotes cell proliferation and epithelial-mesenchymal transition and is inhibited by the hippo pathway. *Molecular and cellular biology*, 28(7), 2426-2436.

Levy, D., Adamovich, Y., Reuven, N., Shaul, Y. (2007). The Yes-associated protein 1 stabilizes p73 by preventing Itch-mediated ubiquitination of p73. *Cell death and differentiation*, 14(4), 743-751.

Levy, D., Reuven, N., Shaul, Y. (2008). A regulatory circuit controlling Itch-mediated p73 degradation by Runx. *The Journal of biological chemistry*, 283(41), 27462-27468.

Lewis-Tuffin, L. J., Rodriguez, F., Giannini, C., Scheithauer, B., Necela, B. M., Sarkaria, J. N., et al. (2010). Misregulated E-cadherin expression associated with an aggressive brain tumor phenotype. *PloS one*, 5(10), e13665.

Li, Y., Hibbs, M. A., Gard, A. L., Shylo, N. A., Yun, K. (2012). Genome-wide analysis of N1ICD/RBPJ targets in vivo reveals direct transcriptional regulation of Wnt, SHH, and hippo pathway effectors by Notch1. *Stem cells (Dayton, Ohio)*, 30(4), 741-752.

Lian, I., Kim, J., Okazawa, H., Zhao, J., Zhao, B., Yu, J., et al. (2010). The role of YAP transcription coactivator in regulating stem cell self-renewal and differentiation. *Genes & development*, 24(11), 1106-1118.

Lin, Y. T., Ding, J. Y., Li, M. Y., Yeh, T. S., Wang, T. W., Yu, J. Y. (2012). YAP regulates neuronal differentiation through Sonic hedgehog signaling pathway. *Experimental cell research*, 318(15), 1877-1888.

Liu, A. M., Wong, K. F., Jiang, X., Qiao, Y., Luk, J. M. (2012). Regulators of mammalian Hippo pathway in cancer. *Biochimica et biophysica acta*, 1826(2), 357-364.

Lobry, C., Oh, P., Aifantis, I. (2011). Oncogenic and tumor suppressor functions of Notch in cancer: it's NOTCH what you think. *The Journal of experimental medicine*, 208(10), 1931-1935.

Lockwood, W. W., Coe, B. P., Williams, A. C., MacAulay, C., Lam, W. L. (2007). Whole genome tiling path array CGH analysis of segmental copy number alterations in cervical cancer cell lines. *International journal of cancer.Journal international du cancer*, 120(2), 436-443.

Lowe, S. W., Jacks, T., Housman, D. E., Ruley, H. E. (1994). Abrogation of oncogene-associated apoptosis allows transformation of p53-deficient cells. *Proceedings of the National Academy of Sciences of the United States of America*, 91(6), 2026-2030.

Lowe, S. W. & Ruley, H. E. (1993). Stabilization of the p53 tumor suppressor is induced by adenovirus 5 E1A and accompanies apoptosis. *Genes & development*, 7(4), 535-545.

Malumbres, M. & Carnero, A. (2003). Cell cycle deregulation: a common motif in cancer. *Progress in cell cycle research*, 5, 5-18.

Mao, Y., Kucuk, B., Irvine, K. D. (2009). Drosophila lowfat, a novel modulator of Fat signaling. *Development (Cambridge, England)*, 136(19), 3223-3233.

Matakatsu, H. & Blair, S. S. (2006). Separating the adhesive and signaling functions of the Fat and Dachsous protocadherins. *Development (Cambridge, England)*, 133(12), 2315-2324.

Matallanas, D., Romano, D., Yee, K., Meissl, K., Kucerova, L., Piazzolla, D., et al. (2007). RASSF1A elicits apoptosis through an MST2 pathway directing proapoptotic transcription by the p73 tumor suppressor protein. *Molecular cell*, 27(6), 962-975.

Mattei, M. G., Borg, J. P., Rosnet, O., Marme, D., Birnbaum, D. (1996). Assignment of vascular endothelial growth factor (VEGF) and placenta growth factor (PLGF) genes to human chromosome 6p12-p21 and 14q24-q31 regions, respectively. *Genomics*, 32(1), 168-169.

Miller, B. W., Lau, G., Grouios, C., Mollica, E., Barrios-Rodiles, M., Liu, Y., et al. (2009). Application of an integrated physical and functional screening approach to identify inhibitors of the Wnt pathway. *Molecular systems biology*, 5, 315.

Minoo, P., Zlobec, I., Baker, K., Tornillo, L., Terracciano, L., Jass, J. R., et al. (2007). Prognostic significance of mammalian sterile20-like kinase 1 in colorectal cancer. *Modern pathology : an official journal of the United States and Canadian Academy of Pathology, Inc*, 20(3), 331-338.

Modena, P., Lualdi, E., Facchinetti, F., Veltman, J., Reid, J. F., Minardi, S., et al. (2006). Identification of tumor-specific molecular signatures in intracranial ependymoma and association with clinical characteristics. *Journal of clinical oncology : official journal of the American Society of Clinical Oncology*, 24(33), 5223-5233.

Murakami, H., Mizuno, T., Taniguchi, T., Fujii, M., Ishiguro, F., Fukui, T., et al. (2011). LATS2 is a tumor suppressor gene of malignant mesothelioma. *Cancer research*, 71(3), 873-883.

Murakami, M., Tominaga, J., Makita, R., Uchijima, Y., Kurihara, Y., Nakagawa, O., et al. (2006). Transcriptional activity of Pax3 is co-activated by TAZ. *Biochemical and biophysical research communications*, 339(2), 533-539.

Nakaya, K., Yamagata, H. D., Arita, N., Nakashiro, K. I., Nose, M., Miki, T., et al. (2007). Identification of homozygous deletions of tumor suppressor gene FAT in oral cancer using CGH-array. *Oncogene*, 26(36), 5300-5308.

Nolo, R., Morrison, C. M., Tao, C., Zhang, X., Halder, G. (2006). The bantam microRNA is a target of the hippo tumor-suppressor pathway. *Current biology : CB*, 16(19), 1895-1904.

Nusse, R. (2005). Wnt signaling in disease and in development. *Cell research*, 15(1), 28-32.

Oh, H. & Irvine, K. D. (2008). In vivo regulation of Yorkie phosphorylation and localization. *Development (Cambridge, England)*, 135(6), 1081-1088.

Oh, H., Reddy, B. V., Irvine, K. D. (2009). Phosphorylation-independent repression of Yorkie in Fat-Hippo signaling. *Developmental biology*, 335(1), 188-197.

Oh, H. J., Lee, K. K., Song, S. J., Jin, M. S., Song, M. S., Lee, J. H., et al. (2006). Role of the tumor suppressor RASSF1A in Mst1-mediated apoptosis. *Cancer research*, 66(5), 2562-2569.

Ota, M. & Sasaki, H. (2008). Mammalian Tead proteins regulate cell proliferation and contact inhibition as transcriptional mediators of Hippo signaling. *Development (Cambridge, England)*, 135(24), 4059-4069.

Overholtzer, M., Zhang, J., Smolen, G. A., Muir, B., Li, W., Sgroi, D. C., et al. (2006). Transforming properties of YAP, a candidate oncogene on the chromosome 11q22 amplicon. *Proceedings of the National Academy of Sciences of the United States of America*, 103(33), 12405-12410.

Pagano, M., Pepperkok, R., Verde, F., Ansorge, W., Draetta, G. (1992). Cyclin A is required at two points in the human cell cycle. *The EMBO journal*, 11(3), 961-971.

Page-McCaw, A., Ewald, A. J., Werb, Z. (2007). Matrix metalloproteinases and the regulation of tissue remodelling. *Nature reviews.Molecular cell biology*, 8(3), 221-233.

Pan, D. (2010). The hippo signaling pathway in development and cancer. *Developmental cell*, 19(4), 491-505.

Park, K. S., Whitsett, J. A., Di Palma, T., Hong, J. H., Yaffe, M. B., Zannini, M. (2004). TAZ interacts with TTF-1 and regulates expression of surfactant protein-C. *The Journal of biological chemistry*, 279(17), 17384-17390.

Peng, H. W., Slattery, M., Mann, R. S. (2009). Transcription factor choice in the Hippo signaling pathway: homothorax and yorkie regulation of the microRNA bantam in the

progenitor domain of the Drosophila eye imaginal disc. *Genes & development*, 23(19), 2307-2319.

Polesello, C., Huelsmann, S., Brown, N. H., Tapon, N. (2006). The Drosophila RASSF homolog antagonizes the hippo pathway. *Current biology : CB*, 16(24), 2459-2465.

Praskova, M., Xia, F., Avruch, J. (2008). MOBKL1A/MOBKL1B phosphorylation by MST1 and MST2 inhibits cell proliferation. *Current biology : CB*, 18(5), 311-321.

Qi, C., Zhu, Y. T., Hu, L., Zhu, Y. J. (2009). Identification of Fat4 as a candidate tumor suppressor gene in breast cancers. *International journal of cancer.Journal international du cancer*, 124(4), 793-798.

Reardon, D. A., Michalkiewicz, E., Boyett, J. M., Sublett, J. E., Entrekin, R. E., Ragsdale, S. T., et al. (1997). Extensive genomic abnormalities in childhood medulloblastoma by comparative genomic hybridization. *Cancer research*, 57(18), 4042-4047.

Ren, F., Wang, B., Yue, T., Yun, E. Y., Ip, Y. T., Jiang, J. (2010). Hippo signaling regulates Drosophila intestine stem cell proliferation through multiple pathways. *Proceedings of the National Academy of Sciences of the United States of America*, 107(49), 21064-21069.

Ribeiro, P. S., Josue, F., Wepf, A., Wehr, M. C., Rinner, O., Kelly, G., et al. (2010). Combined functional genomic and proteomic approaches identify a PP2A complex as a negative regulator of Hippo signaling. *Molecular cell*, 39(4), 521-534.

Roman, E., Meza-Zepeda, L. A., Kresse, S. H., Myklebost, O., Vasstrand, E. N., Ibrahim, S. O. (2008). Chromosomal aberrations in head and neck squamous cell carcinomas in Norwegian and Sudanese populations by array comparative genomic hybridization. *Oncology reports*, 20(4), 825-843.

Rosenbluh, J., Nijhawan, D., Cox, A. G., Li, X., Neal, J. T., Schafer, E. J., et al. (2012). beta-Catenin-Driven Cancers Require a YAP1 Transcriptional Complex for Survival and Tumorigenesis. *Cell*, 151(7), 1457-1473.

Sasaki, H., Kawano, O., Endo, K., Suzuki, E., Yukiue, H., Kobayashi, Y., et al. (2007). Human MOB1 expression in non-small-cell lung cancer. *Clinical lung cancer*, 8(4), 273-276.

Schlegelmilch, K., Mohseni, M., Kirak, O., Pruszak, J., Rodriguez, J. R., Zhou, D., et al. (2011). Yap1 acts downstream of alpha-catenin to control epidermal proliferation. *Cell*, 144(5), 782-795.

Scotto, L., Narayan, G., Nandula, S. V., Arias-Pulido, H., Subramaniyam, S., Schneider, A., et al. (2008). Identification of copy number gain and overexpressed genes on chromosome arm 20q by an integrative genomic approach in cervical cancer: potential role in progression. *Genes, chromosomes & cancer*, 47(9), 755-765.

Seidel, C., Schagdarsurengin, U., Blumke, K., Wurl, P., Pfeifer, G. P., Hauptmann, S., et al. (2007). Frequent hypermethylation of MST1 and MST2 in soft tissue sarcoma. *Molecular carcinogenesis*, 46(10), 865-871.

Serrano, M., Lin, A. W., McCurrach, M. E., Beach, D., Lowe, S. W. (1997). Oncogenic ras provokes premature cell senescence associated with accumulation of p53 and p16INK4a. *Cell*, 88(5), 593-602.

Silva, E., Tsatskis, Y., Gardano, L., Tapon, N., McNeill, H. (2006). The tumor-suppressor gene fat controls tissue growth upstream of expanded in the hippo signaling pathway. *Current biology : CB*, 16(21), 2081-2089.

Silvis, M. R., Kreger, B. T., Lien, W. H., Klezovitch, O., Rudakova, G. M., Camargo, F. D., et al. (2011). alpha-catenin is a tumor suppressor that controls cell accumulation by regulating the localization and activity of the transcriptional coactivator Yap1. *Science signaling*, 4(174), ra33.

Smith, M. A., Freidlin, B., Ries, L. A., Simon, R. (2000). Increased incidence rates but no space-time clustering of childhood astrocytoma in Sweden, 1973-1992: a population-based study of pediatric brain tumors. *Cancer*, 88(6), 1492-1493.

Snijders, A. M., Schmidt, B. L., Fridlyand, J., Dekker, N., Pinkel, D., Jordan, R. C., et al. (2005). Rare amplicons implicate frequent deregulation of cell fate specification pathways in oral squamous cell carcinoma. *Oncogene*, 24(26), 4232-4242.

Song, M., Cheong, J. H., Kim, H., Noh, S. H., Kim, H. (2012). Nuclear expression of Yes-associated protein 1 correlates with poor prognosis in intestinal type gastric cancer. *Anticancer Research*, 32(9), 3827-3834.

Sopko, R., Silva, E., Clayton, L., Gardano, L., Barrios-Rodiles, M., Wrana, J., et al. (2009). Phosphorylation of the tumor suppressor fat is regulated by its ligand Dachsous and the kinase discs overgrown. *Current biology : CB*, 19(13), 1112-1117.

Stavridi, E. S., Harris, K. G., Huyen, Y., Bothos, J., Verwoerd, P. M., Stayrook, S. E., et al. (2003). Crystal structure of a human Mob1 protein: toward understanding Mob-regulated cell cycle pathways. *Structure (London, England : 1993)*, 11(9), 1163-1170.

Steinhardt, A. A., Gayyed, M. F., Klein, A. P., Dong, J., Maitra, A., Pan, D., et al. (2008). Expression of Yes-associated protein in common solid tumors. *Human pathology*, 39(11), 1582-1589.

Strano, S., Monti, O., Pediconi, N., Baccarini, A., Fontemaggi, G., Lapi, E., et al. (2005). The transcriptional coactivator Yes-associated protein drives p73 gene-target specificity in response to DNA Damage. *Molecular cell*, 18(4), 447-459.

Strano, S., Munarriz, E., Rossi, M., Castagnoli, L., Shaul, Y., Sacchi, A., et al. (2001). Physical interaction with Yes-associated protein enhances p73 transcriptional activity. *The Journal of biological chemistry*, 276(18), 15164-15173.

Sudol, M. (1994). Yes-associated protein (YAP65) is a proline-rich phosphoprotein that binds to the SH3 domain of the Yes proto-oncogene product. *Oncogene*, 9(8), 2145-2152.

Sudol, M., Bork, P., Einbond, A., Kastury, K., Druck, T., Negrini, M., et al. (1995). Characterization of the mammalian YAP (Yes-associated protein) gene and its role in defining a novel protein module, the WW domain. *The Journal of biological chemistry*, 270(24), 14733-14741.

Takahashi, Y., Miyoshi, Y., Takahata, C., Irahara, N., Taguchi, T., Tamaki, Y., et al. (2005). Down-regulation of LATS1 and LATS2 mRNA expression by promoter hypermethylation and its association with biologically aggressive phenotype in human breast cancers. *Clinical cancer research : an official journal of the American Association for Cancer Research*, 11(4), 1380-1385.

Tao, W., Zhang, S., Turenchalk, G. S., Stewart, R. A., St John, M. A., Chen, W., et al. (1999). Human homologue of the Drosophila melanogaster lats tumour suppressor modulates CDC2 activity. *Nature genetics*, 21(2), 177-181.

Tapon, N., Harvey, K. F., Bell, D. W., Wahrer, D. C., Schiripo, T. A., Haber, D., et al. (2002). salvador Promotes both cell cycle exit and apoptosis in Drosophila and is mutated in human cancer cell lines. *Cell*, 110(4), 467-478.

Thiery, J. P., Acloque, H., Huang, R. Y., Nieto, M. A. (2009). Epithelial-mesenchymal transitions in development and disease. *Cell*, 139(5), 871-890.

Tian, Y., Kolb, R., Hong, J. H., Carroll, J., Li, D., You, J., et al. (2007). TAZ promotes PC2 degradation through a SCFbeta-Trcp E3 ligase complex. *Molecular and cellular biology*, 27(18), 6383-6395.

Tsai, L. H., Harlow, E., Meyerson, M. (1991). Isolation of the human cdk2 gene that encodes the cyclin A- and adenovirus E1A-associated p33 kinase. *Nature*, 353(6340), 174-177.

Varelas, X., Sakuma, R., Samavarchi-Tehrani, P., Peerani, R., Rao, B. M., Dembowy, J., et al. (2008). TAZ controls Smad nucleocytoplasmic shuttling and regulates human embryonic stem-cell self-renewal. *Nature cell biology*, 10(7), 837-848.

Varelas, X., Samavarchi-Tehrani, P., Narimatsu, M., Weiss, A., Cockburn, K., Larsen, B. G., et al. (2010). The Crumbs complex couples cell density sensing to Hippo-dependent control of the TGF-beta-SMAD pathway. *Developmental cell*, 19(6), 831-844.

Vichai, V. & Kirtikara, K. (2006). Sulforhodamine B colorimetric assay for cytotoxicity screening. *Nature protocols*, 1(3), 1112-1116.

Virtanen, I., Korhonen, M., Kariniemi, A. L., Gould, V. E., Laitinen, L., Ylanne, J. (1990). Integrins in human cells and tumors. *Cell differentiation and development : the official journal of the International Society of Developmental Biologists*, 32(3), 215-227.

Wada, K., Itoga, K., Okano, T., Yonemura, S., Sasaki, H. (2011). Hippo pathway regulation by cell morphology and stress fibers. *Development (Cambridge, England)*, 138(18), 3907-3914.

Wang, C., Zhang, L., He, Q., Feng, X., Zhu, J., Xu, Z., et al. (2012). Differences in Yes-associated protein and mRNA levels in regenerating liver and hepatocellular carcinoma. *Molecular medicine reports*, 5(2), 410-414.

Wang, D., Zhou, Y., Lei, W., Zhang, K., Shi, J., Hu, Y., et al. (2009). Signal transducer and activator of transcription 3 (STAT3) regulates adipocyte differentiation via peroxisome-proliferator-activated receptor gamma (PPARgamma). *Biology of the cell / under the auspices of the European Cell Biology Organization*, 102(1), 1-12.

Wu, S., Huang, J., Dong, J., Pan, D. (2003). hippo encodes a Ste-20 family protein kinase that restricts cell proliferation and promotes apoptosis in conjunction with salvador and warts. *Cell*, 114(4), 445-456.

Wu, S., Liu, Y., Zheng, Y., Dong, J., Pan, D. (2008). The TEAD/TEF family protein Scalloped mediates transcriptional output of the Hippo growth-regulatory pathway. *Developmental cell*, 14(3), 388-398.

Xu, M. Z., Yao, T. J., Lee, N. P., Ng, I. O., Chan, Y. T., Zender, L., et al. (2009). Yes-associated protein is an independent prognostic marker in hepatocellular carcinoma. *Cancer*, 115(19), 4576-4585.

Yabuta, N., Fujii, T., Copeland, N. G., Gilbert, D. J., Jenkins, N. A., Nishiguchi, H., et al. (2000). Structure, expression, and chromosome mapping of LATS2, a mammalian homologue of the Drosophila tumor suppressor gene lats/warts. *Genomics*, 63(2), 263-270.

Yagi, R., Chen, L. F., Shigesada, K., Murakami, Y., Ito, Y. (1999). A WW domain-containing yes-associated protein (YAP) is a novel transcriptional co-activator. *The EMBO journal*, 18(9), 2551-2562.

Yamaguchi, H., Wyckoff, J., Condeelis, J. (2005). Cell migration in tumors. *Current opinion in cell biology*, 17(5), 559-564.

Yokoyama, T., Osada, H., Murakami, H., Tatematsu, Y., Taniguchi, T., Kondo, Y., et al. (2008). YAP1 is involved in mesothelioma development and negatively regulated by Merlin through phosphorylation. *Carcinogenesis*, 29(11), 2139-2146.

Yu, J., Zheng, Y., Dong, J., Klusza, S., Deng, W. M., Pan, D. (2010). Kibra functions as a tumor suppressor protein that regulates Hippo signaling in conjunction with Merlin and Expanded. *Developmental cell*, 18(2), 288-299.

Yuan, M., Tomlinson, V., Lara, R., Holliday, D., Chelala, C., Harada, T., et al. (2008). Yes-associated protein (YAP) functions as a tumor suppressor in breast. *Cell death and differentiation*, 15(11), 1752-1759.

Zender, L., Spector, M. S., Xue, W., Flemming, P., Cordon-Cardo, C., Silke, J., et al. (2006). Identification and validation of oncogenes in liver cancer using an integrative oncogenomic approach. *Cell*, 125(7), 1253-1267.

Zhang, H., Liu, C. Y., Zha, Z. Y., Zhao, B., Yao, J., Zhao, S., et al. (2009). TEAD transcription factors mediate the function of TAZ in cell growth and epithelial-mesenchymal transition. *The Journal of biological chemistry*, 284(20), 13355-13362.

Zhang, H., Pasolli, H. A., Fuchs, E. (2011). Yes-associated protein (YAP) transcriptional coactivator functions in balancing growth and differentiation in skin. *Proceedings of the National Academy of Sciences of the United States of America*, 108(6), 2270-2275.

Zhang, J., Ji, J. Y., Yu, M., Overholtzer, M., Smolen, G. A., Wang, R., et al. (2009). YAP-dependent induction of amphiregulin identifies a non-cell-autonomous component of the Hippo pathway. *Nature cell biology*, 11(12), 1444-1450.

Zhang, J., Smolen, G. A., Haber, D. A. (2008). Negative regulation of YAP by LATS1 underscores evolutionary conservation of the Drosophila Hippo pathway. *Cancer research*, 68(8), 2789-2794.

Zhang, L., Ren, F., Zhang, Q., Chen, Y., Wang, B., Jiang, J. (2008). The TEAD/TEF family of transcription factor Scalloped mediates Hippo signaling in organ size control. *Developmental cell*, 14(3), 377-387.

Zhang, X., George, J., Deb, S., Degoutin, J. L., Takano, E. A., Fox, S. B., et al. (2011). The Hippo pathway transcriptional co-activator, YAP, is an ovarian cancer oncogene. *Oncogene*, 30(25), 2810-2822.

Zhang, Y. J., Jiang, W., Chen, C. J., Lee, C. S., Kahn, S. M., Santella, R. M., et al. (1993). Amplification and overexpression of cyclin D1 in human hepatocellular carcinoma. *Biochemical and biophysical research communications*, 196(2), 1010-1016.

Zhao, B., Li, L., Lu, Q., Wang, L. H., Liu, C. Y., Lei, Q., et al. (2011)a. Angiomotin is a novel Hippo pathway component that inhibits YAP oncoprotein. *Genes & development*, 25(1), 51-63.

Zhao, B., Li, L., Tumaneng, K., Wang, C. Y., Guan, K. L. (2010). A coordinated phosphorylation by Lats and CK1 regulates YAP stability through SCF(beta-TRCP). *Genes & development*, 24(1), 72-85.

Zhao, B., Tumaneng, K., Guan, K. L. (2011)b. The Hippo pathway in organ size control, tissue regeneration and stem cell self-renewal. *Nature cell biology*, 13(8), 877-883.

Zhao, B., Wei, X., Li, W., Udan, R. S., Yang, Q., Kim, J., et al. (2007). Inactivation of YAP oncoprotein by the Hippo pathway is involved in cell contact inhibition and tissue growth control. *Genes & development*, 21(21), 2747-2761.

Zhao, B., Ye, X., Yu, J., Li, L., Li, W., Li, S., et al. (2008). TEAD mediates YAP-dependent gene induction and growth control. *Genes & development*, 22(14), 1962-1971.

Ziosi, M., Baena-Lopez, L. A., Grifoni, D., Froldi, F., Pession, A., Garoia, F., et al. (2010). dMyc functions downstream of Yorkie to promote the supercompetitive behavior of hippo pathway mutant cells. *PLoS genetics*, 6(9), 10.1371/journal.pgen.1001140.

ACKNOWLEDGMENTS

First of all I would like to thank Dr.Piergiorgio Modena for providing me the opportunity to work on this topic. I am grateful to him for all that he taught me, for his helpfulness and great humanity and also for the time spent together thinking and discussing about the experiments.

I would like to thank Dr.Roberta Maestro for giving me the possibility to attend the Experimental Oncology 1 laboratories and learn much from her large biological knowledge.

I would like to express my thanks to all the past and present members of Experimental Oncology 1.
In particular, special thanks to my dear colleagues and great friends Elena and Monica, mostly for their kind support during these years and during the writing of this manuscript. Their companionship in the laboratory made our working together pleasant. A great thanks to Sara, my "travel companion" of these years, for all the things we shared together, for the good days and the difficult ones.

In addition I wish to thank my PhD external reviewer Dr.Daniele Bergamaschi for his valuable advice, suggestions and for his availability.

My great thanks to my precious family, my reference point: to my mum, my dad, my brother Alessandro and my sister in law Michela who have supported me for all these years and to my beloved nephews, Matteo and Nicola, who always fill me with joy and fill me in a good humor. A special thanks to my very dear grandmother because we spend together is a great gift.

I cannot forget all my friends and in particular my childhood friends, Ivana, Andrea, Walter, Luigi and Shara that always have an encouraging word and a joke ready to laugh at and my “triestine” friends Nelly, Elisa, Francesca, Erika and Chiara with who, even if there are not many opportunities to be together, always have “time” for me.

PUBLISHED ARTICLES

During my PhD studies I participated to another project resulting in the writing of two papers: one published in *Eur J Cancer, 2011* and the second submitted to *Molecular Cancer Terapeutics* is now under review.

The paper, regarding my PhD thesis topic, is under preparation.

Gasparini P, Facchinetti F, **Lorenzetto E**, Livio A, Gronchi A, Ferrari A, Massimino M, Spreafico F, Giangaspero F, Forni M, Maestro R, Alaggio R, Pilotti S, Collini P, Modena P, Sozzi G.
"*Prognostic determinants in epithelioid sarcoma"*
Eur J Cancer. 2011 Jan;47(2):287-95.

Brenca M, Rossi S, **Lorenzetto E**, Piccinin E, Piccinin S, Giuliano A, Dei Tos A.P, Maestro R, Modena P.
"SMARCB1/INI1 genetic inactivation is responsible for tumorigenic properties of epithelioid sarcoma cell line VAESBJ"
Submiteed to Molecular Cancer Terapeutics

Lorenzetto E, Boeri M, Rossi S, Brenca M, Piccinin E, Maestro R, Modena P.
"Defining the role of YAP1 in 11q22-amplified cancer cell lines"
Article under preparation.

EUROPEAN JOURNAL OF CANCER 47 (2011) 287–295

available at www.sciencedirect.com

ScienceDirect

journal homepage: www.ejconline.com

Prognostic determinants in epithelioid sarcoma

Patrizia Gasparini [a], *Federica Facchinetti* [a], *Mattia Boeri* [a], *Erica Lorenzetto* [b], *Anna Livio* [a], *Alessandro Gronchi* [c], *Andrea Ferrari* [d], *Maura Massimino* [d], *Filippo Spreafico* [d], *Felice Giangaspero* [e,f], *Marco Forni* [g], *Roberta Maestro* [b], *Rita Alaggio* [h], *Silvana Pilotti* [i], *Paola Collini* [i,*], *Piergiorgio Modena* [b,j,*], *Gabriella Sozzi* [a,j]

[a] *Unit of Molecular Cytogenetics, Fondazione IRCCS Istituto Nazionale Tumori, Milano, Italy*
[b] *Unit of Experimental Oncology 1, Centro di Riferimento Oncologico, Aviano, Italy*
[c] *Unit of Melanoma and Sarcoma Surgery, Fondazione IRCCS Istituto Nazionale Tumori, Milano, Italy*
[d] *Unit of Pediatric Oncology, Fondazione IRCCS Istituto Nazionale Tumori, Milano, Italy*
[e] *Department of Experimental Medicine and Pathology, Università La Sapienza, Roma, Italy*
[f] *Istituto Mediterraneo Neuromed, Pozzilli, Italy*
[g] *Department of Pathology, Ospedale Infantile Regina Margherita, Torino, Italy*
[h] *Unit of Pathology, University of Padova, Italy*
[i] *Unit of Pathology, Fondazione IRCCS Istituto Nazionale Tumori, Milano, Italy*

ARTICLE INFO

Article history:
Received 25 May 2010
Received in revised form 19 August 2010
Accepted 2 September 2010

Keywords:
Sarcoma
SMARCB1
INI1
Epithelioid sarcoma
Malignant rhabdoid tumour

ABSTRACT

Background: Epithelioid sarcoma (ES) is a rare soft tissue neoplasm that usually arises in the distal extremities of young adults, presents a high rate of recurrences and metastases and frequently poses diagnostic dilemmas. In order to identify markers useful for patient stratification purposes, we investigated the prognostic impact of clinical and molecular patient characteristics, including the status of *SMARCB1* tumour suppressor gene, in a consecutive series of ES cases.

Methods: Kaplan–Meier survival curves were compared by the log-rank test. Immunophenotyping and SMARCB1 protein expression were analysed by immunohistochemistry or western blotting in 40 ES patients for which tumour material was available. Cases lacking SMARCB1 protein expression were investigated for the presence of gene mutations and gene deletions by exon sequencing, fluorescent *in situ* hybridization and quantitative PCR.

Results: FNCLCC tumour grade 3 and proximal-type histology significantly correlated with shorter overall survival (log-rank $p = 0.0046$ and $p = 0.0001$, respectively). We identified loss of SMARCB1 protein expression in the majority of ES cases (25/40, 62.5%), including 24/34 (71%) adult cases but only 1/6 (17%) paediatric/adolescent cases ($p = 0.02$, two-tailed Fisher's exact test). The absence of protein is strongly correlated with *SMARCB1* gene deletion ($p = 0.003$, two-tailed Fisher's exact test). We observed a trend towards the correlation between *SMARCB1* inactivation and both higher tumour grading and a clinical course of the disease characterised by the occurrence of multiple relapses/metastasis.

Conclusion: These data show that both tumour grading and subtype are prognostic factors in ES. Loss of SMARCB1 protein expression in ES is a frequent occurrence mediated by gene deletion events, thus pointing to a crucial role of *SMARCB1* in ES genesis. Analysis of

* *Corresponding authors*: Addresses: Unit of Pathology, Fondazione IRCCS Istituto Nazionale Tumori, via Venezian 1, 20133 Milano, Italy (P. Collini), Unit of Experimental Oncology 1, Centro di Riferimento Oncologico, via F. Gallini 2, 33081 Aviano, PN, Italy (P. Modena).
E-mail addresses: paola.collini@istitutotumori.mi.it (P. Collini), pmodena@cro.it (P. Modena).
[j] Senior co-authorship.

doi:10.1016/j.ejca.2010.09.003

SMARCB1 status in ES warrants prospective investigation as a prognostic marker and therapeutic target.

1. Introduction

Epithelioid sarcoma (ES, International Classification of Diseases for Oncology Code Number 8804/3) is a rare mesenchymal neoplasm that displays variable epithelioid morphology, presents a high rate of recurrences and metastases and frequently poses diagnostic dilemmas.[1] It usually affects young adults and arises in the distal extremities (classic-type ES) or, more rarely, in proximal sites of the trunk (proximal-type ES). Proximal-type ES is more frequently associated with epithelioid or rhabdoid morphology and higher mitotic activity,[2] but the prognostic impact of ES subtype is still unclear.

Similarly, grading schemes in ES are disputed and have been discouraged by some Authors who considered ES a high-grade soft tissue sarcoma,[1] although recently the FNCLCC grading system demonstrated prognostic value in a cohort of ES in children and adolescents.[3]

We previously reported evidence of *SMARCB1* inactivation in 6/11 ES cases.[4] The *SMARCB1* gene, located at the 22q11 chromosomal region, encodes for an invariant subunit of SWI/SNF chromatin remodelling complex and has been reported to act as a tumour suppressor gene in infantile malignant rhabdoid tumour (MRT),[5,6] a highly aggressive neoplasm affecting renal or extrarenal soft tissue and cerebral tissue in paediatric patients. Previous studies indicate that the analysis of the status of *SMARCB1* may be an informative predictor for rational targeted interventions directed against the Cdk/Cyclin pathway, such as 4-HPR[7] and flavopiridol[8] Cdk/Cyclin inhibitors.

We therefore investigated the prognostic value of relevant clinico-pathologic variables as well as the frequency and the mechanism of *SMARCB1* inactivation in a consecutive series of ES and examined potential associations with clinical parameters. Our results show that FNCLCC tumour grade 3 and proximal-type histology significantly correlated with shorter overall survival and that the loss of SMARCB1 protein expression by means of gene deletion events is a frequent occurrence, thus pointing to a crucial role of *SMARCB1* in ES genesis.

2. Materials and methods

2.1. Patient samples

Fifty-six Bouin's- or formalin-fixed, paraffin-embedded (FFPE) tumour samples were retrieved from the Department of Pathology of the Istituto Nazionale Tumori of Milan archives. Slides were reviewed and diagnoses confirmed applying updated criteria.[1,9] The case series was formed by 40 ESs, 10 high-risk gastro-intestinal stromal tumours (GISTs) and 6 MRTs (3 renal, 1 extrarenal and 2 ATRT). ESs were subdivided into classic and proximal-type and the FNCLCC system[1,10] for ES grading was applied, in order to investigate its potential prognostic value. This system is based on a final grading which combines the scores for differentiation, mitotic index, and necrosis. Clinical features of ES patients were in part previously published.[3,11] Six cases aged 10–18 years were admitted and treated at the Paediatric Oncology Department. Thirty-two adult patients aged above 18 were admitted and treated at the Unit of Melanoma and Sarcoma Surgery. In selected cases frozen tumour tissue samples, collected following institutional review board guidelines, were available. DNA was extracted from 10 μm frozen or FFPE tissue sections using Qiagen DNA Mini kit (Qiagen, Italy, Milano I), following manufacturer's recommendations. Haematoxylin–eosin staining was performed prior to extraction to verify for the presence of more then 60% tumour cells in frozen samples. FFPE normal tissues microarray was purchased from AccuMax array (Petagen Inc., Seoul Korea).

2.2. Protein expression

Immunophenotyping with CD34, cytokeratins, epithelial membrane antigen and CD31 antibodies was performed for uniform pathologic re-examination. Protein expression of SMARCB1 was investigated by immunohistochemistry using anti-BAF47/SNF5 antibody 1:100 (BD Transduction Laboratories, Buccinasco I). Endogenous peroxidise was blocked with 0.3% hydrogen peroxide in methanol for 30 min. For antigen retrieval the slides were immersed in citrate buffer solution 5 mM pH 6 and heated in autoclave at 95 °C for 15 min. Immunohistochemistry analysis was done using Ultra vision detection system (LabVision, Fremont, CA). As controls, sarcoma samples from different subtypes were analysed concomitantly. Loss of SMARCB1 protein expression as detected by immunohistochemistry was not observed in GIST tumours, including high-risk cases (0/10) that frequently suffer of chromosome 22 losses, whilst the paediatric malignant rhabdoid tumours investigated invariably displayed SMARCB1-negative immunostaining. For Western blot analysis, protein lysates were prepared in RIPA buffer (Sigma–Aldrich S.r.l., Milano I), 40 μg of cell lysate were loaded on 4–15% gradient polyacrylamide gels (Biorad Lab, Segrate I) and electro-blotted on to polyvinylidene difluoride membranes (Amersham, GE Healthcare, Milano I). Subsequently, membranes were incubated 1 h at room temperature in a solution of phosphate-buffered saline supplemented with 5% nonfat dry milk. For immunodetection, the anti-BAF47/SNF5 (1:250, BD Transduction Laboratories) and anti-CyclinD1 (1:1000, DCS6 Santa Cruz Biotechnology, CA) antibodies were used. After overnight incubation at 4 °C with the primary antibody, membranes were washed in TBST [10 mmol/l Tris–HCl (pH 8.0), 0.15 mol/l NaCl, and 0.05% Tween 20], followed by AlexaFluor680- or IRDye800CW-conjugated antibodies (from Invitrogen Life Technologies, San Giuliano Milanese I and Li-Cor Biosciences, Lincoln US, respectively). Odyssey infrared imaging system (Li-Cor Biosciences) was used for detection. Protein loading equivalence was assessed using an anti-Gapdh antibody (Sigma–Aldrich).

2.3. Fish

Gross gene deletions were analysed by fluorescent *in situ* hybridization (FISH) with BAC (Bacterial Artificial Chromosome) probes, using BAC RP11-71g19 encompassing *SMARCB1* gene at 22q11 and control BAC RP11-262a13 located at 22q13.3 (probes kindly provided by Resources for Molecular Cytogenetics, Bari I). FISH analysis was performed on FFPE or frozen tumour samples as previously described.[4] A minimum of 100 nuclei were counted, the expected number of nuclei showing 0, 1 and 2 signals was calculated on control, normal FFPE samples or on patient's epidermis in sub-cutaneous tumours where it was part of the same tissue block. Deviation from the expected number of signals in the tumour tissue analysed was evaluated by Chi-square test. Control probe provided a technical control of the labelling and hybridization procedures.

2.4. Mutational and deletion analysis

Mutational analysis was performed by exon amplification and sequencing as previously described.[4] Intragenic deletions were detected by quantitative genomic PCR using primer pairs spanning *SMARCB1* exon 4. As control loci, 2 loci located in a separate chromosome (chr11:98891904–98891994 and chr11:100863268–100863358) that we previously validated for proper amplification efficiency and ability to reveal copy-number changes (Fig. S1) were also analysed by genomic q-PCR. Primers (see Fig. S1) were designed uniformly in relation to Tm, GC content, primer and amplicon length using Primer-Express software (Applied Biosystems Foster City, CA, USA). Quantitative PCR assays were performed in 20 μl volume of 1× SybrGreen PCR master mix (Applied Biosystems), using 100 nM of primers and 10 ng of genomic DNA, with the thermal profile 52° 2 min, then 40 cycles of 92° 15 s, 60° 1 min. Data were analysed with the ddCt method for relative quantification, using the 11q22 locus amplicons as endogenous controls and the normal, donor-derived genomic DNA as calibrator. We preliminarily validated the relative quantification method by calculating the amplification efficiency of each primer pair at different DNA concentrations ranging from 1 to 100 ng. We subsequently verified the sensitivity of the assay using G401 rhabdoid sarcoma cell line, which carries a homozygous deletion of *SMARCB1* gene. Dilution of G401 genomic DNA with donor-derived normal DNA titrated at different ratios (0%, 25%, 50%, 75%, 90% and 100%) showed that under the conditions applied a 50% mixture (corresponding to a uniform hemizygous deletion or a homozygous deletion in 50% of cells analysed) was consistently measurable (Fig. S1). Four paediatric malignant rhabdoid tumours could be analysed concomitantly at the molecular level (Fig. S3) and revealed *SMARCB1* gene deletion in two cases (1 extrarenal soft tissue and 1 cerebral atypical theratoid–rhabdoid tumour) and point mutations in two other cases (1 renal and 1 cerebral atypical theratoid–rhabdoid tumour).

2.5. Cell cultures

G401 malignant rhabdoid tumour cancer cell line (American Type Culture Collection, Manassas, VA) was maintained in RMPI + 10% foetal bovine serum medium, in conventional 5% CO_2 atmosphere and 100% humidity incubators. Short-term cell cultures were established from fresh tumour material by mechanical and collagenase II enzymatic dissociation, followed by culturing in Amniomax-C100 medium (Gibco Life Technologies, San Giuliano Milanese I). Conventional and Spectral Karyotyping (Applied Spectral Imaging, Vista, CA) was performed as previously described.[12]

2.6. Statistics

All statistical analyses were carried out using GraphPad software (GraphPad Inc., La Jolla, CA). Comparisons between two classes have been performed by two-tailed Fisher's exact test. Kaplan–Meier survival curves were plotted and compared by the log-rank test. $p < 0.05$ was considered statistically significant.

3. Results

3.1. Clinical variables analyses

Fifty-two ES cases were treated at the Istituto Nazionale Tumori of Milan in the period 1986–2006. Pathologic re-examination was preformed in 40 cases for which suitable tumour material was available (Table 1). Median age was 31 years (range 10–66), histology was classic-type in 27 (67.5%) and proximal-type in 13 (32.5%), FNCLCC grading was 2 in 15 (37.5%) and 3 in 25 (62.5%). Six were paediatric/adolescent cases aged 10–18 years and 34 were adult patients above 18 years. In 14 patients, a neoadjuvant chemo- or radiotherapy regimen was administered prior to surgery. Ten cases presented multiple nodules or metastasis at the time of first surgery. Twenty patients experienced pulmonary or extrapulmonary metastasis during the disease course and 18 of them died of disease. In total, 26 patients relapsed, 19 patients died of their disease and two patients presented relapsing disease at last follow-up. Average and median follow-up time for patients alive were 51 and 50 months, respectively. Event-free survival and overall survival at 5 years were 21% and 60%, respectively.

As shown by Kaplan–Meier survival curves in Fig. 1, both tumour grade 3 and proximal-type histology were significantly correlated with shorter overall survival (log-rank test $p = 0.0046$ and $p = 0.0001$, respectively). The risk ratio (HR) conferred by grade 3 was 8.6 (95% confidence interval (CI) 1.9–38) and by proximal-type histology was 5.6 (95% CI 2.4–13.2). There was no significant correlation between occurrence of patient relapse and FNCLCC grading ($p = 0.50$) or ES histological subtype ($p = 0.15$).

3.2. SMARCB1 protein expression analysis

Immunohistochemistry revealed the absence of SMARCB1 protein expression (Fig. 2) in 25/40 (62.5%). SMARCB1 loss was predominant in the adult cases (24/34, 71%) compared to the paediatric/adolescent ones (1/6, 17%) ($p = 0.02$). The difference was still significant when the cut-off was set at 25 years of age ($p = 0.04$, Table 2), suggesting that SMARCB1 inactivation is likely to play a minor role in the juvenile form of ES compared to the adult form. No correlation was found between SMARCB1 expression and staging, location, subtype

Table 1 – Characteristics of epithelioid sarcoma patients.

ES no.	Age	Gender	Site	Size (cm)	ES subtype	FNCLCC grading	SMARCB1 IHC	*SMARCB1* status	Relapses	Metastasis	Follow-up	Status
1	29	M	Forearm	10	C	2	neg	HD	4	No	46	NED
2	36	M	Forearm	4	C	2	neg	na	No	No	4	NED
3	29	M	Hand	6	C	3	neg	na	No	Y	14	DOD
4	33	M	Hand	5	C	3	neg	HD	4	No	42	AWD
5	25	M	Hand	1	C	2	neg	na	1	No	4	NED
6	66	F	Trunk	6	P	3	neg	HD	4	No	9	DOD
7	31	M	Hand	2	C	3	pos	wt	1	Y	41	DOD
8	26	F	Hand	1	C	2	neg	HD	3	No	50	NED
9	36	M	Hand	4	C	3	neg	HD	1	Y	82	DOD
10	31	F	Thigh	9	P	3	neg	HD	No	Y	43	DOD
11	47	F	Thigh	4	P	3	pos	wt	No	No	50	NED
12	25	M	Hand	3	C	3	neg	wt	2	Y	77	DOD
13	55	F	Foot	3	C	2	pos	wt	1	Y	11	DOD
14	40	M	Forearm	2	C	3	neg	HD	3	No	56	AWD
15	30	M	Hand	1	C	3	neg	wt	3	No	55	NED
16	25	M	Leg	5	C	2	neg	wt	2	No	121	NED
17	34	M	Hand	1	C	2	neg	wt	1	Y	74	NED
18	25	M	Proximal arm	8	C	3	pos	wt	1	Y	10	DOD
19	34	F	Trunk	12	P	3	neg	na	No	Y	7	DOD
20	21	M	Hand	2.5	C	2	pos	wt	4	Y	58	DOD
21	25	F	Thigh	1	C	3	pos	wt	No	No	53	NED
22	32	F	Trunk	4	P	3	neg	HD	No	No	13	NED
23	66	M	Thigh	19	P	3	pos	na	No	Y	2	DOD
24	65	M	Trunk	6	P	3	neg	na	1	No	11	NED
25	27	M	Leg	1	C	3	neg	wt	No	Y	24	DOD
26	34	M	Forearm	0.5	C	3	neg	HD	2	Y	96	DOD
27	71	M	Trunk	5	P	3	pos	wt	1	Y	9	DOD
28	47	F	Trunk	3	P	3	neg	HD	2	Y	13	DOD
29	48	F	Trunk	3	P	3	neg	na	1	Y	2	NED
30	22	M	Hand	1	C	3	neg	HD	5	Y	24	DOD
31	36	F	Trunk	4	P	3	neg	wt	No	Y	9	DOD
32	27	M	Proximal arm	5	C	2	neg	wt	No	No	88	NED
33	64	M	Trunk	8	P	3	pos	na	No	Y	2	DOD
34	45	M	Thigh	2	C	2	pos	na	No	No	12	NED
35	16	F	Leg	3	C	2	pos	na	1	No	124	NED
36	17	M	Proximal arm	8	C	3	neg	wt	1	Y	54	DOD
37	10	M	Forearm	6	C	2	pos	wt	2	No	126	NED
38	16	F	Hand	3	C	2	pos	na	1	No	66	NED
39	13	M	Neck	4	P	2	pos	na	1	No	20	NED
40	18	F	Proximal arm	3	C	2	pos	na	No	No	20	NED

Abbreviations: ES = epithelioid sarcoma; age in years; C = classic-type; P = proximal-type; HD = homozygous deletion; na = not available; wt = normal; Y = yes; NED = no evidence of disease; DOD = dead of disease; and AWD = alive with disease.

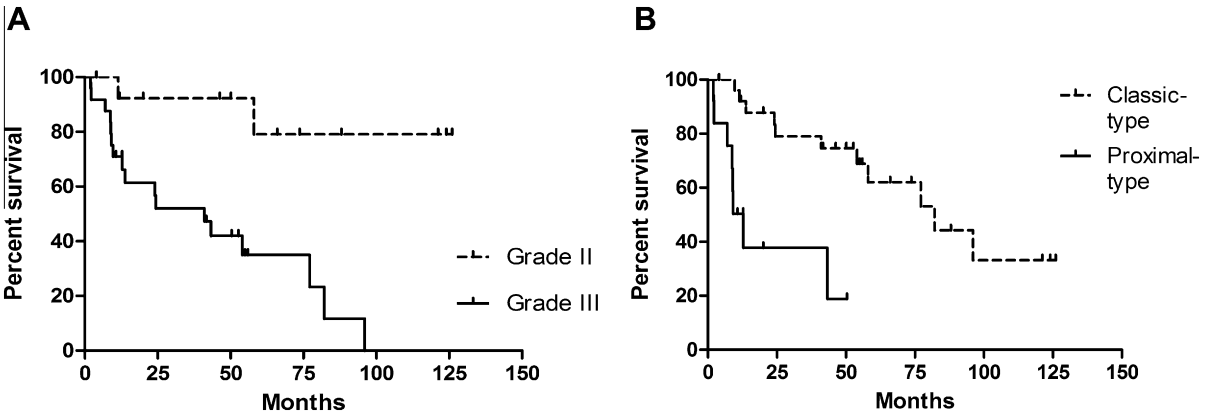

Fig. 1 – Kaplan–Meier survival curves of epithelioid sarcoma patients according to (A) grading II versus III ($p = 0.0046$ by log-rank test) and (B) classic versus proximal-type histology ($p = 0.0001$ by log-rank test).

or other clinical characteristics investigated (Table 2), including overall survival (HR = 2.1, 95% CI 0.7–6.1, log-rank $p = 0.16$ for adult cases only; HR = 1.2 95% CI 0.4–3.4, log-rank $p = 0.69$ for all patients). Interestingly, loss of SMARCB1 expression was prevalent in tumours that tended to evolve to metastatic/highly recurrent disease (more then two consecutive relapses): 19/25 IHC-negative cases (76%), in contrast to only 7/15 IHC-positive cases (47%), developed metastatic disease or more then two relapse events ($p = 0.09$). Neoadjuvant chemo- or radiotherapy regimen administered prior to surgery had no effect on SMARCB1 expression: the fraction of SMARCB1-positive and -negative tumours was the same in pre-treated versus naive cases (9/14 pre-treated cases were SMARCB1-negative compared to 16/26 of non pre-treated cases, $p = 1.00$).

The CD34 marker, which is used in routine diagnostics and is reported consistently negative in malignant rhabdoid tumours, was expressed in 14/34 (41%) cases analysed, including 10/24 (42%) SMARCB1-negative cases and 4/10 (40%) SMARCB1-positive cases, indicating that negative staining for SMARCB1 in ES did not correlate with lack of CD34 expression (Table 2).

3.3. *SMARCB1 gene status*

FISH analysis was performed successfully in 27/40 cases (Fig. 2), the main cause for FISH failure being fixation in Bouin's reagent. A strong correlation between SMARCB1 expression and gene status was observed: the SMARCB1 locus was retained in all 9/9 IHC-positive cases tested and lost in 9/18 IHC-negative cases analysed ($p = 0.01$). Similar to IHC analyses, no association between *SMARCB1* gene status and ES subtype, staging or location was detected. Instead, there was a significant correlation between tumour grading and SMARCB1 gene deletion as detected by FISH: all the 9 cases showing *SMARCB1* deletion by FISH were grade 3 compared to only 10/18 cases without deletion ($p = 0.03$).

Mutational analysis by exon amplification and sequencing in 18 cases, for which frozen or adequate FFPE tissue was available, did not reveal mutations. These cases included 7/9 IHC-negative cases that displayed normal gene copy-number as detected by FISH.

Since the BAC probe used for FISH analysis spans 148,000 bp, encompassing 9 genes (7 completely and 2 partially contained within the BAC probe), to investigate the presence of subtle *SMARCB1* gene deletions that may have escaped the FISH analysis, we applied a gene dosage assay by quantitative PCR in 13 IHC-negative cases for which frozen or adequate FFPE tissue was available (Figs. 3 and S1). In addition to confirming the presence of gene deletion previously detected by FISH, quantitative PCR uncovered significant loss of *SMARCB1* signal in two additional cases for which FISH signal was normal. These data suggest the presence of more subtle deletion events in a fraction of ES cases. Therefore, combining FISH and q-PCR results, we detected retention of *SMARCB1* in all 9/9 IHC-positive cases tested and loss of the entire *SMARCB1* gene in 11/18 IHC-negative cases tested ($p = 0.003$). Correlation between tumour grading and the occurrence of gene deletion was no more statistically significant, whilst a trend for an association with older age, already observed with IHC analysis, was present ($p = 0.09$, Table 2). There was no significant association between administration of neoadjuvant chemo- or radiotherapy regimen prior to surgery and *SMARCB1* gene status, suggesting that the deletion events identified are not caused by the treatment received in the short time preceding surgery ($p = 0.67$).

3.4. *Additional tissues and sarcoma samples analysed*

In addition to the previously reported cases,[4] we analysed a further short-term cell culture from one of the ES samples, which displayed the absence of SMARCB1 protein expression and gene deletion. Interestingly, this tumour sample showed weak SMARCB1 expression by western blotting and the absence of nuclear staining by immunocytochemistry, whilst presenting high CCND1 protein expression (Fig. S2), a phenomenon linked to *SMARCB1* ablation in paediatric MRTs.

Loss of SMARCB1 protein expression as detected by immunohistochemistry was not observed in GIST tumours, including high-risk cases (0/10) that frequently suffer of chromosome 22 losses, whilst the paediatric malignant rhabdoid tumours investigated displayed SMARCB1-negative immunostaining associated with the presence of gene mutations (Fig. S3).

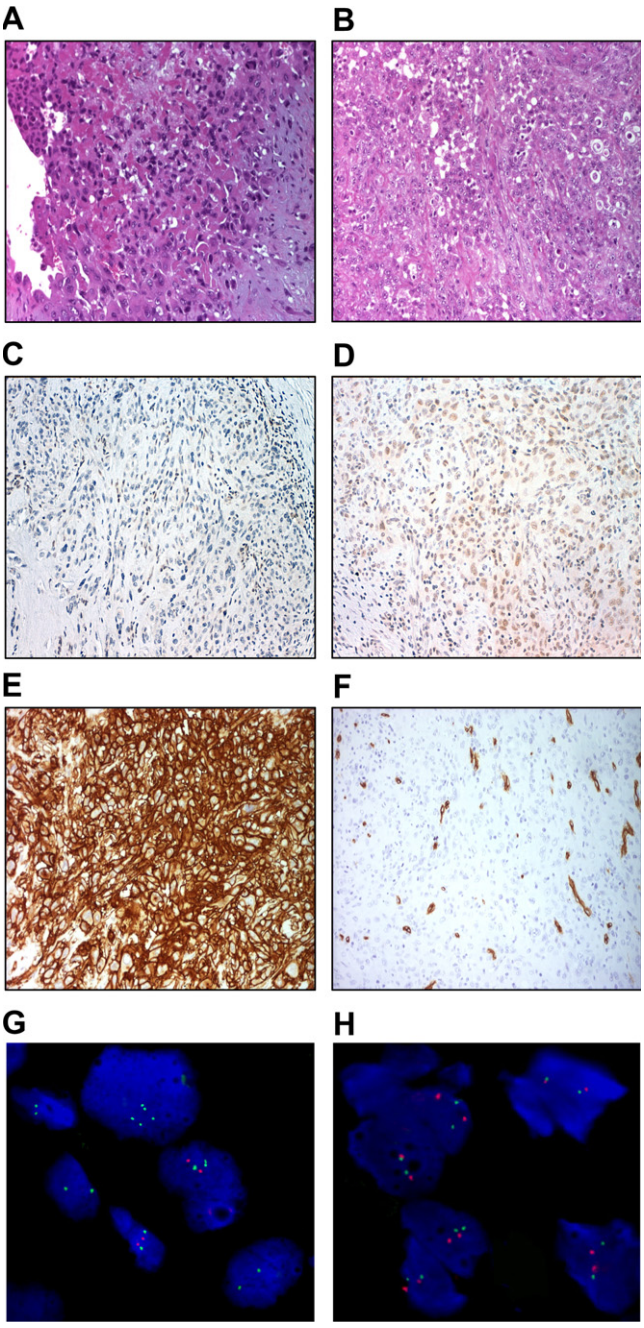

Fig. 2 – Immunohistochemistry and FISH analysis of epithelioid sarcoma samples. Representative IHC and FISH results from a SMARCB1-negative, FISH-deleted case (A–D) and a SMARCB1-positive, FISH wild-type case (E–H). Panels represent: haematoxylin–eosin staining (A and E); immunohistochemistry analysis for SMARCB1 (B and F) and CD34 (C and G) markers; FISH analysis (D and H) of *SMARCB1* (red signal) and control locus (green signal).

SMARCB1 is considered an invariant subunit of SWI-SNF chromatin remodelling complex and is predicted to be expressed ubiquitously. Nevertheless, scanty information are actually available on the actual pattern of expression of SMARCB1 in non-cancerous tissues. Therefore, we investigated SMARCB1 expression by IHC analysis in different normal tissues and established that the expression at the protein level is not ubiquitous (Fig. S2). The highest expression levels were detected in lymphoid tissue, followed by epithelial tissues. Kidney, the site of classic malignant rhabdoid tumour, showed strong staining at tubular structures. In addition, epithelial linings of colon and ovary displayed intense staining, whilst brain compartments showed only moderate to weak protein expression. Staining was invariably nuclear.

4. Discussion

In an attempt to define prognostic factors that may provide useful information for the management of ES, we analysed a consecutive series of 40 ES surgically treated at the INT National Cancer Institute in Milan. In our case series, histological subtype and FNCLCC grading represent strong prognostic indicators of poor prognosis. We also found suggestive evidence of correlation at the univariate analysis between tumour grading or aggressive evolution (metastasis/multiple relapse events) and *SMARCB1* gene and protein loss, respectively. Intrinsic limitations related to disease rarity and heterogeneity in treatment approach over long periods of time, even within a single Institution, hamper further statistical analyses. Therefore, only prospective investigation in the frame of multicentric clinical trials will have the potential to ascertain the prognostic value of *SMARCB1* in ES.

We previously reported evidence of *SMARCB1* alteration in 6/11 ES cases.[4] In the present report, we confirm in a larger patient series the frequent inactivation of *SMARCB1* tumour suppressor in ES, a tumour entity distinct from MRTs previously known to be caused by *SMARCB1* mutation. Very recently, additional studies concordantly reported SMARCB1 protein silencing in ES,[13,14] but the gene status was rarely investigated at the molecular level.[15,16] Herein we provide evidence that SMARCB1 protein loss in ES is associated with homozygous gene deletion in over 60% of the cases. We failed to detect gene point mutations in our series and the causative genetic or epigenetic event leading to *SMARCB1* inactivation remains elusive in 39% of the IHC-negative cases, which retain an apparently normal gene copy-number. However, by a genomic q-PCR approach we were able to unveil two additional cases of gene deletion that were missed by FISH. It should be emphasised that our q-PCR approach was performed by focusing on a small region spanning exon 4. Thus, it is likely that other small deletions, involving genomic regions other then exon 4, may account for IHC negativity in ES. More refined deletion–detection techniques, such as multiplex ligation-dependent probe amplification (MLPA)[18] may further improve the sensitivity of the assessment of *SMARCB1* intragenic deletions. Unfortunately, also for these approaches the use of old FFPE tissue samples may represent a limitation. Moreover, other mechanisms of gene silencing operating at the transcriptional or post-transcriptional level cannot be ruled out. Notably, consistent with our results, the other reports of ES cases investigated for *SMARCB1* gene status reported the occurrence of deletions[4,15,16] and so far, only one case of ES carrying a 1-bp substitution has been reported,[17] showing

Table 2 – Association between SMARCB1 status and clinical characteristics.

	SMARCB1 IHC		*p*-Value	SMARCB1gene status		*p*-Value
	neg	pos		HD	wt	
ES subtype						
C	17	10	1.00	7	13	0.39
P	8	5		4	3	
FNCLCC grading						
2	7	8	0.18	2	6	0.40[b]
3	18	7		9	10	
Tumour site						
extremity	15	6	0.33	7	9	1.00
other	10	9		4	7	
TNM staging						
T1N0M0	12	10	0.33	5	10	0.45
higher	13	5		6	6	
Metastasis or multiple relapses[a]						
yes	19	6	0.09	10	10	0.18
no	7	8		1	6	
Age						
>25	20	7	0.04[c]	10	9	0.09
⩽25	5	8		1	7	
CD34 stain						
neg	14	6	1.00	5	10	0.44
pos	10	4		5	5	
SMARCB1 status						
HD	11	0	0.003			
wt	7	9				

Abbreviations: ES = epithelioid sarcoma; C = classic-type; P = proximal-type; and HD = homozygous deletion as assessed by FISH and/or q-PCR.
[a] Patients were distinct based on the occurrence of metastatic disease or more than two consecutive recurrence events.
[b] The *p*-value = 0.03 if considering SMARCB1 gene status by FISH only.
[c] The *p*-value = 0.02 if considering the 18 years cut-off age.

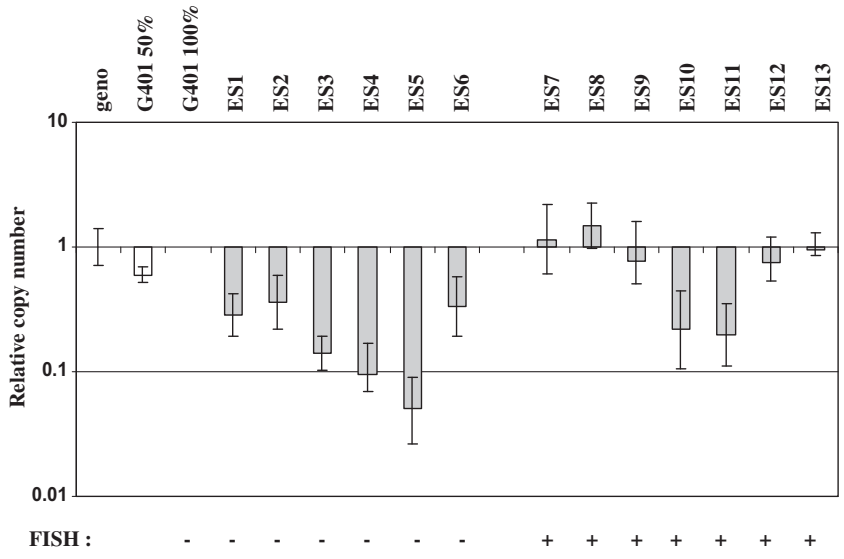

Fig. 3 – Quantitative PCR analysis of *SMARCB1* exon 4 copy-number in immunohistochemistry-negative epithelioid sarcoma cases. Normal genomic DNA (geno) was used as calibrator, genomic DNA from G401 cell line (carrying a homozygous deletion of *SMARCB1* gene) and a 1:1 mixture of the two DNAs were used as controls. Amplification of an unrelated genomic locus was used as endogenous control. Data show evidence of gene deletion in FISH-deleted epithelioid sarcoma cases, and also in two additional FISH-positive cases, suggesting the presence of an intragenic deletion.

that, although rarely, even point mutations can contribute to the malignant transformation of epithelioid sarcoma.

Soft tissue sarcomas encompass the paediatric and adult age groups and so far it is not established whether the distinct sarcoma subtypes have the same clinical behaviour when arising in adults or in children. In addition, to our knowledge no published data clearly showed the presence of alternative molecular features in the different age groups affected by the same sarcoma subtype. Notably, in our case series *SMARCB1* inactivation was more frequent in patients older than 25 years, suggesting that juvenile ES are only rarely associated with *SMARCB1* inactivation. Investigation of a larger cohort of ES will be necessary to establish whether different molecular alterations affect paediatric versus adult patients.

Several issues raise the possibility that ES and MRT may actually represent distinct manifestations of a unique tumour entity, and that the age-window in which *SMARCB1* inactivation occurs does influence the different clinical course observed between ES and MRT. Nevertheless, a number of facts are still difficult to reconcile with this hypothesis and rather support an independent origin of the two entities. In fact, to the best of our knowledge, no ES occurrences have been reported so far in the spectrum of the rhabdoid predisposition syndrome, despite the existence of adult mutation-carriers; a different mutational spectrum has been observed in ES and MRT; morphologic and immunophenotyping analyses are reported to distinguish between ES and MRT tumours.[19,20] Thus far, the issue remains unresolved.

A number of different neoplasms are characterised by the loss of genetic material at the chromosome region 22q11. Indeed, in addition to *SMARCB1*, several other known or candidate tumour suppressor genes lie on this chromosome arm including CHEK2, EP300 and NF2, which may explain the importance of 22q loss in tumours retaining *SMARCB1* expression, such as the high-risk GISTs samples we analysed. Interestingly, SAGE data show a significant reduction of *SMARCB1* expression in lymphomas compared to non-cancerous lymph nodes (http://cgap.nci.nih.gov/SAGE), which is the tissue holding the highest expression of SMARCB1 protein, as we determined by immunohistochemistry. In addition, very recently SMARCB1 protein loss of expression has been reported as a prognostic marker in melanoma, but no genetic investigations have been performed so far.[21] Due to the subtle nature of *SMARCB1* gene alterations, particularly small homozygous deletions, and to the difficulty in detecting downregulation at the RNA level, which is greatly masked by infiltration of normal cells expressing high level of SMARCB1 transcript, we propose that a broader involvement of *SMARCB1* inactivation in cancer is worth to be investigated by combined analyses at the genomic DNA level by FISH and/or q-PCR and at the protein level by immunohistochemistry.

Previously published studies indicate that *SMARCB1/INI1* gene is involved in the control of genomic stability and in the regulation of cell cycle progression.[22] SMARCB1 stimulates the p16/Rb tumour suppressor pathway by activation of CDKN2A and inhibition of Cdk/CyclinD.[23] As a result, in MRT cell lines it has been demonstrated that *SMARCB1* loss is associated with responsiveness to Cdk/Cyclin inhibitors, such as 4-HPR[7] and flavopiridol.[8] In addition, the *in vivo* spontaneous tumourigenesis in *SMARCB1* knock-out mice is prevented by CCND1 ablation.[24] These results suggest that the analysis of the status of *SMARCB1* may be an informative predictor for rational targeted interventions directed against the Cdk/Cyclin pathway. Our results provide a rationale for the investigation of the therapeutic potential of such molecules in any type of *SMARCB1*-negative neoplasm. In this regard, the availability of *in vitro* models to test this hypothesis remains mandatory.

Conflict of interest statement

None declared.

Acknowledgements

This work was supported by the Italian Ministry of Research and Health (MIUR-Fondo per gli Investimenti della Ricerca di Base; Ricerca Finalizzata, 5X1000 funding), the Italian Association for Cancer Research (AIRC) and Fondazione Italiana per la lotta al neuroblastoma. E. Lorenzetto is a recipient of Alleanza contro il Cancro fellowship. The funding agencies had no role in the study.

Appendix A. Supplementary data

Supplementary data associated with this article can be found, in the online version, at doi:10.1016/j.ejca.2010.09.003.

REFERENCES

1. Fletcher CCD, Unni KK, Mertens F, editors. *Pathology and genetics of tumors of soft tissue and bone*. Lyon: IARC Press; 2002.
2. Dei Tos AP, Wagner AJ, Modena P, Comandone A, Leyvraz S. Epithelioid soft tissue tumors. *Semin Oncol* 2009;**36**(4):347–57.
3. Casanova M, Ferrari A, Collini P, et al. Epithelioid sarcoma in children and adolescents: a report from the Italian Soft Tissue Sarcoma Committee. *Cancer* 2006;**106**(3):708–17.
4. Modena P, Lualdi E, Facchinetti F, et al. SMARCB1/INI1 tumor suppressor gene is frequently inactivated in epithelioid sarcomas. *Cancer Res* 2005;**65**(10):4012–9.
5. Versteege I, Sevenet N, Lange J, et al. Truncating mutations of hSNF5/INI1 in aggressive paediatric cancer. *Nature* 1998;**394**(6689):203–6.
6. Biegel JA, Zhou JY, Rorke LB, et al. Germ-line and acquired mutations of INI1 in atypical teratoid and rhabdoid tumors. *Cancer Res* 1999;**59**(1):74–9.
7. Alarcon-Vargas D, Zhang Z, Agarwal B, et al. Targeting Cyclin D1, a downstream effector of INI1/hSNF5, in rhabdoid tumors. *Oncogene* 2006;**25**(5):722–34.
8. Smith ME, Cimica V, Chinni S, et al. Rhabdoid tumor growth is inhibited by flavopiridol. *Clin Cancer Res* 2008;**14**(2):523–32.
9. Biegel JA, Zhou JY, Rorke LB, et al. Germ-line and acquired mutations of INI1 in atypical teratoid and rhabdoid tumors. *Cancer Res* 1999;**59**(1):74–9.
10. Guillou L, Coindre JM, Bonichon F, et al. Comparative study of the National Cancer Institute and French Federation of Cancer Centers Sarcoma Group grading systems in a population of 410 adult patients with soft tissue sarcoma. *J Clin Oncol* 1997;**15**(1):350–62.

11. Baratti D, Pennacchioli E, Casali PG, et al. Epithelioid sarcoma: prognostic factors and survival in a series of patients treated at a single institution. *Ann Surg Oncol* 2007;**14**(12):3542–51.
12. Lualdi E, Modena P, Debiec-Rychter M, et al. Molecular cytogenetic characterization of proximal-type epithelioid sarcoma. *Genes Chromosomes Cancer* 2004;**41**(3):283–90.
13. Chbani L, Guillou L, Terrier P, et al. Epithelioid sarcoma: a clinicopathologic and immunohistochemical analysis of 106 cases from the French sarcoma group. *Am J Clin Pathol* 2009;**131**(2):222–7.
14. Hornick JL, Dal Cin P, Fletcher CD. Loss of INI1 expression is characteristic of both conventional and proximal-type epithelioid sarcoma. *Am J Surg Pathol* 2009;**33**(4):542–50.
15. Raoux D, Peoc'h M, Pedeutour F, et al. Primary epithelioid sarcoma of bone: report of a unique case, with immunohistochemical and fluorescent in situ hybridization confirmation of INI1 deletion. *Am J Surg Pathol* 2009;**33**(6):954–8.
16. Kohashi K, Izumi T, Oda Y, et al. Infrequent SMARCB1/INI1 gene alteration in epithelioid sarcoma: a useful tool in distinguishing epithelioid sarcoma from malignant rhabdoid tumor. *Human Pathol* 2009;**40**(3):349–55.
17. Flucke U, Slootweg PJ, Mentzel T, Pauwels P, Hulsebos TJ. Re: Infrequent SMARCB1/INI1 gene alteration in epithelioid sarcoma: a useful tool in distinguishing epithelioid sarcoma from malignant rhabdoid tumor: direct evidence of mutational inactivation of SMARCB1/INI1 in epithelioid sarcoma. *Human Pathol* 2009;**40**(9):1361–2.
18. Schouten JP, McElgunn CJ, Waaijer R, et al. Relative quantification of 40 nucleic acid sequences by multiplex ligation-dependent probe amplification. *Nucleic Acids Res* 2002;**30**(12):e57.
19. Fisher C. Epithelioid sarcoma of Enzinger. *Adv Anat Pathol* 2006;**13**(3):114–21.
20. Izumi T, Oda Y, Hasegawa T, et al. Prognostic significance of dysadherin expression in epithelioid sarcoma and its diagnostic utility in distinguishing epithelioid sarcoma from malignant rhabdoid tumor. *Mod Pathol* 2006;**19**(6):820–31.
21. Lin H, Wong RP, Martinka M, Li G. Loss of SNF5 expression correlates with poor patient survival in melanoma. *Clin Cancer Res* 2009;**15**(20):6404–11.
22. Vries RG, Bezrookove V, Zuijderduijn LM, et al. Cancer-associated mutations in chromatin remodeler hSNF5 promote chromosomal instability by compromising the mitotic checkpoint. *Genes Dev* 2005;**19**(6):665–70.
23. Imbalzano AN, Jones SN. Snf5 tumor suppressor couples chromatin remodeling, checkpoint control, and chromosomal stability. *Cancer Cell* 2005;**7**(4):294–5.
24. Tsikitis M, Zhang Z, Edelman W, Zagzag D, Kalpana GV. Genetic ablation of Cyclin D1 abrogates genesis of rhabdoid tumors resulting from Ini1 loss. *Proc Natl Acad Sci USA* 2005;**102**(34):12129–34.

Supplemental Figure legends.

Fig. S1. Validation experiments for quantitative PCR measurement of *SMARCB1* gene copy-number. (A) Primers used for quantitative PCR assay. (B, C) Sensitivity assay. Genomic DNA from G401 cell line (carrying a homozygous deletion of *SMARCB1* gene) and normal, donor-derived DNA were mixed at various ratios and used as template for the q-PCR assay. Normal genomic DNA 100% (geno) was used as calibrator. The 11q locus B primer set was used as endogenous control. An independent control locus (11q locus A) displayed a uniform normal copy-number in all samples. (D) Amplification efficiency plot of the q-PCR assay for *SMARCB1* and endogenous control (11q locus B) primer sets.

Fig. S2. *SMARCB1* alteration in an epithelioid sarcoma short-term cell culture. Immunocytochemistry analysis of SMARCB1 protein expression in (A) *SMARCB1* wild-type MDA-435 breast cancer cell line, in (B) *SMARCB1*-negative G401 malignant rhabdoid tumour cell line, and in (C) *SMARCB1*-negative SEP1 short-term cell culture, which displayed an abnormal karyotype by Spectral Karyotyping analysis. Red circles indicate a reciprocal t(1;9) translocation. (D) Western blot analysis of epithelioid sarcoma samples displaying increased expression of CCND1 in SMARCB1-negative SEP1. (E) SMARCB1 protein immunohistochemistry from formalin-fixed, paraffin-embedded tumour sample of SEP1 case.

Fig. S3. *SMARCB1* gene alterations identified in malignant rhabdoid tumour samples by exon amplification and sequencing (a) or quantitative PCR (b).

Fig. S4. Immunohistochemical analysis of *SMARCB1* protein expression in a normal tissues microarray.

Suppl. Figure 1. Validation experiments of quantitative PCR analysis of SMARCB1 gene copy number

A

Primers used for quantitative PCR assay:

11q-locusA-F	5'-AGGAACCGCTCTCTCTGAACTG-3'
11q-locusA-R	5'-GATGCCAGACTCCACTGTCCTT-3'
11q-locusB-F	5'-TGTCTCCTGTTGATTCGCAGAT-3'
11q-locusB-R	5'-CGGTGACAATGAGGGATACAGTG-3'
SMARCB1-ex4F	5'-CAAGAGGAACAGCCAGTGGGTA-3'
SMARCB1-ex4R	5'-GCGGTTCCTGTTGATGGTTGT-3'

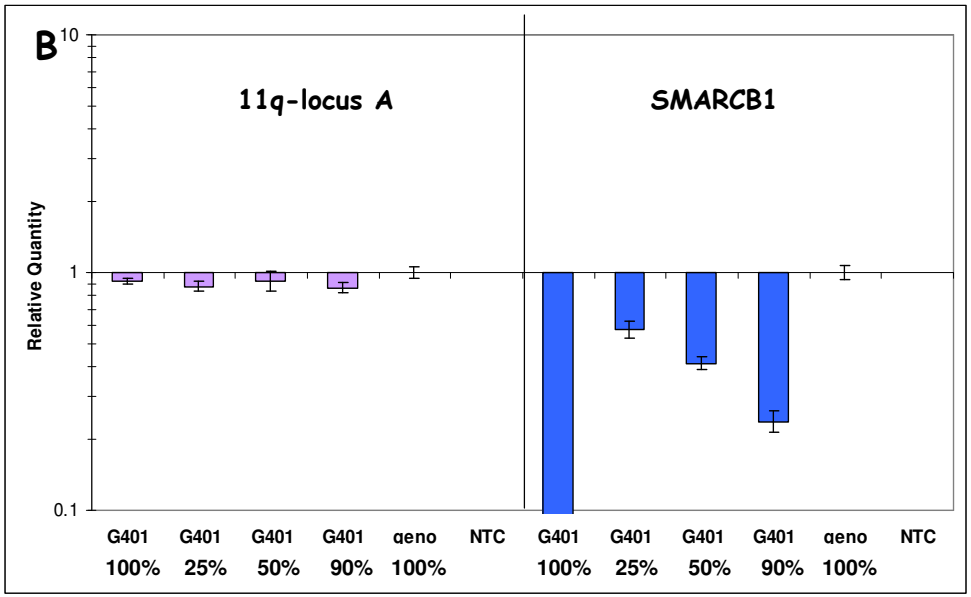

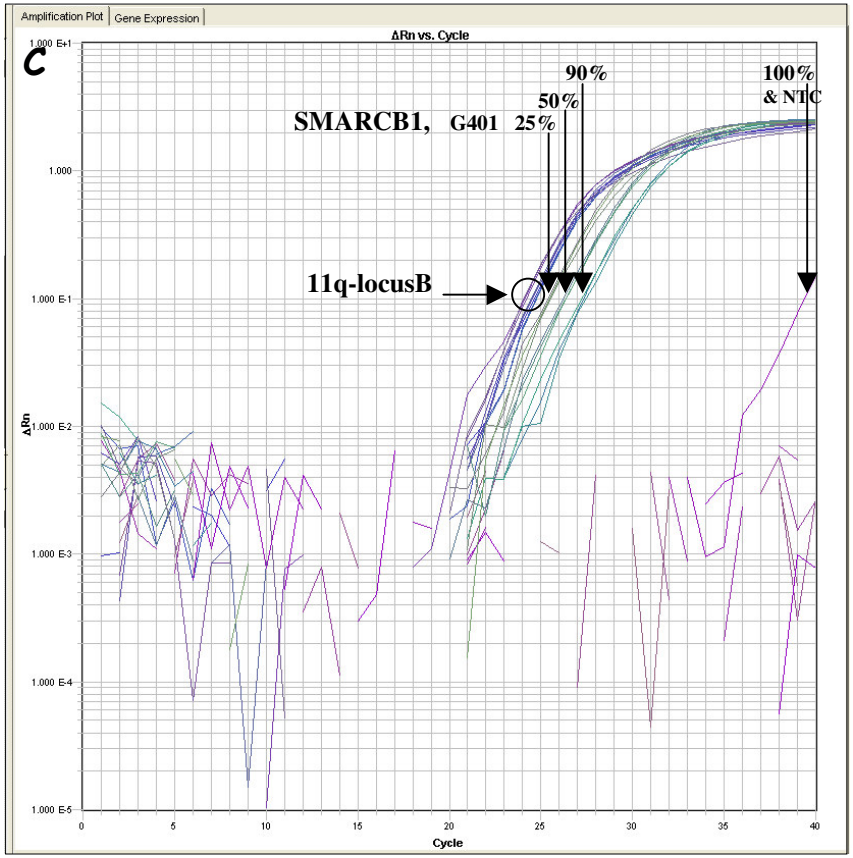

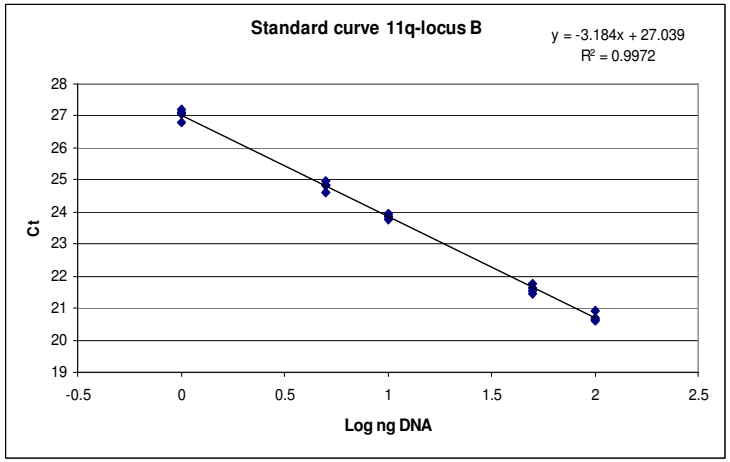

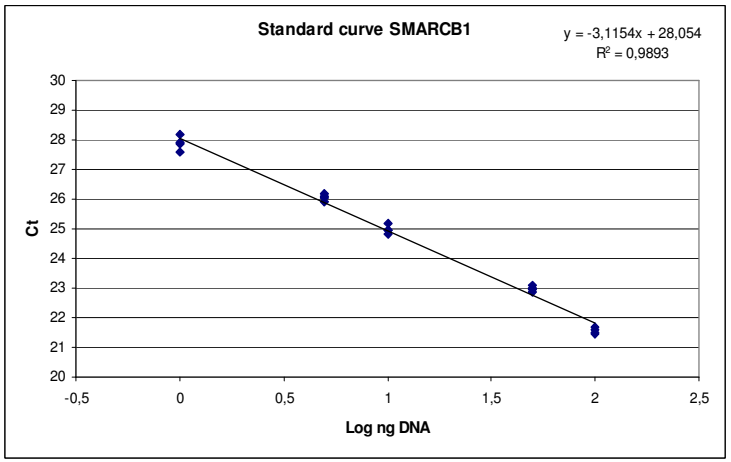

Supplemental Figure 2

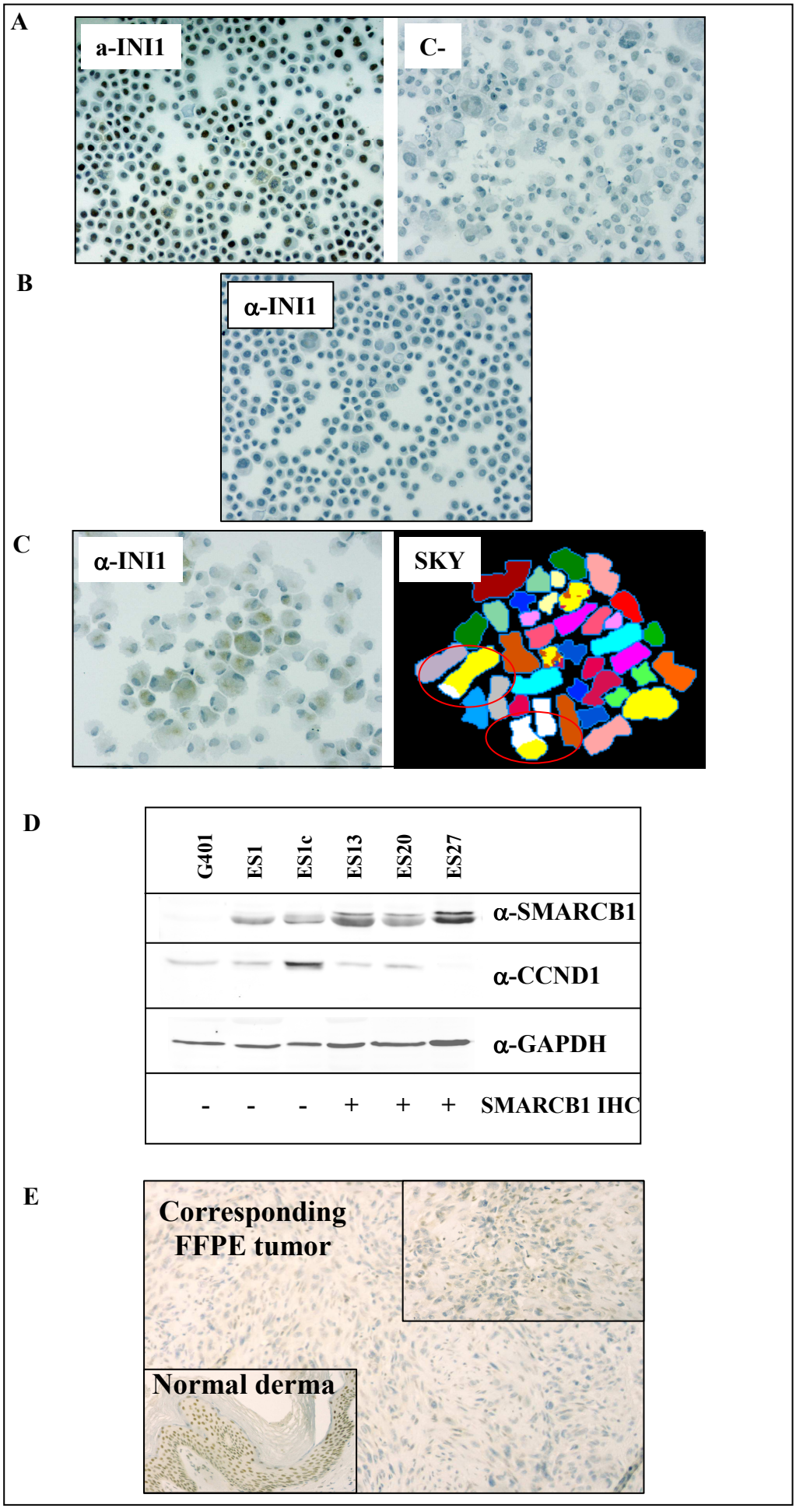

Suppl. Figure 3. SMARCB1 gene alterations identified in pediatric malignant rhabdoid tumor samples (MRTs)

a) Detection of homozygous T to C transition mutation in intron 5 donor splice site in a renal MRT.

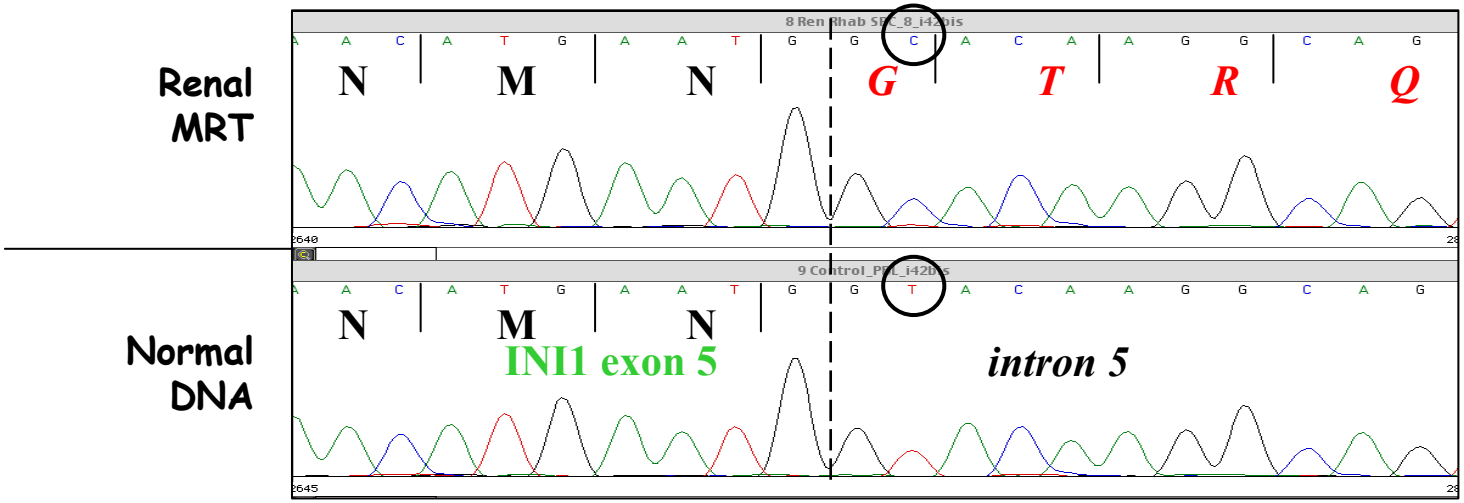

b) Quantitative-PCR analysis of INI1 deletion on genomic DNA.

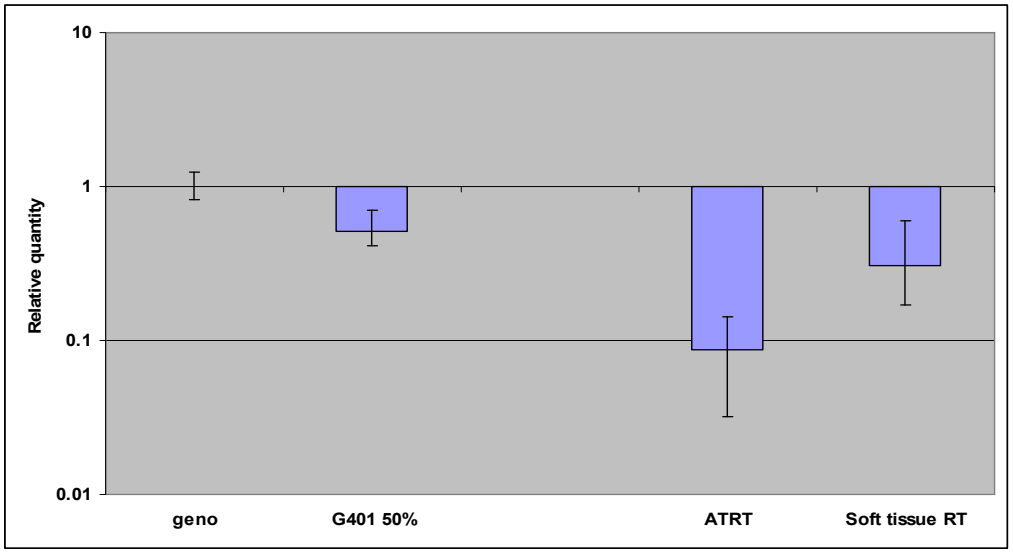

Suppl. Figure 4. IHC analysis of SMARCB1/INI1 in Normal Tissues

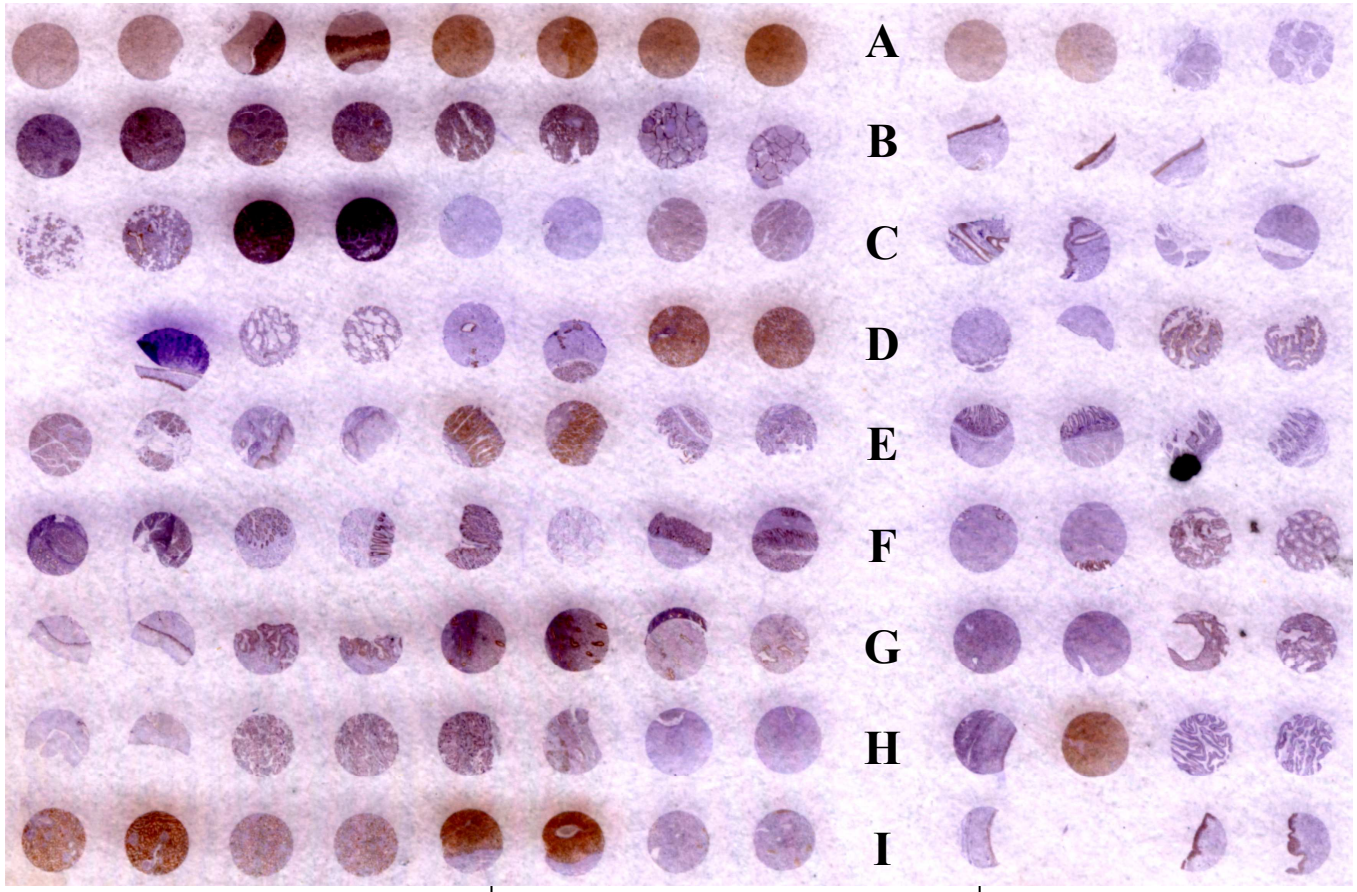

A	1,2	cerebral cortex
A	3,4	cerebellum
A	5,6	basal ganglia
A	7,8	hipocampus
A	9,10	spinal cord
A	11,12	peripheral nerve
B	1,2	spleen
B	3,4	tonsil
B	5,6	parathyroid
B	7,8	thyroid gland
B	9,10	larynx
B	11,12	hypopharynx
C	1,2	salivery gland
C	3,4	lymph node
C	5,6	blood vessel
C	7,8	heart
C	9,10	skin
C	11,12	skeletal muscle
D	2	bronchus
D	3,4	lung
D	5,6	breast
D	7,8	liver
D	9,10	bile duct
D	11,12	gall bladder
E	1,2	pancreas
E	3,4	esophagus
E	5,6	stomach
E	7,8	duodenum
E	9,10	jejuni
E	11,12	ileum
F	1,2	appendix
F	3,4	cecum
F	5,6	colon
F	7,8	rectum
F	9,10	prostate
F	11,12	testis
G	1,2	exocervix
G	3,4	endocervix
G	5,6	pro-endometrium
G	7,8	decidua
G	9,10	myometrium
G	11,12	sec-endometrium
H	1,2	placenta amnion
H	3,4	plac. chorionvilli
H	5,6	plac. basal plate
H	7,8	umbilical cord
H	9,10	ovary
H	11,12	fallopian tube
I	1,2	kidney cortex
I	3,4	kidney medulla
I	5,6	adrenal cortex
I	7,8	adrenal medulla
I	10	ureter
I	11,12	urinary bladder